AEROSOL TRACE METAL CONCENTRATION AND DISSOLUTION CHARACTERISTICS FROM KNOWN DUST EMITTERS IN SOUTHERN AFRICA

KAUKURAUEE ISMAEL KANGUEEHI (BSC HONS EARTH SCIENCE)

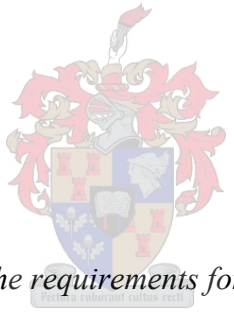

Thesis submitted in fulfilment of the requirements for the degree Master of Science (in Geology) at Stellenbosch University.

SUPERVISOR: Dr Susanne Fietz
CO-SUPERVISOR: Prof Frank Eckardt

December 2017

DEPARTMENT OF EARTH SCIENCES

DECLARATION

By submitting this report electronically, I declare that the entirety of the work contained therein is my own, original work, that I am the sole author thereof (save to the extent explicitly otherwise stated), that reproduction and publication thereof by Stellenbosch University will not infringe any third-party rights and that I have not previously in its entirety or in part submitted it for obtaining any qualification.

Signature:

Date: December 2017

ACKNOWLEDGEMENTS

First of all, I would like to thank my supervisor, Dr Susanne Fietz and my co-supervisor Prof Frank Eckardt for all the guidance, comments and suggestions during this project. I couldn't have wished for better supervisors. In the same breath, I also want to thank Prof Roy, your comments and insight in this project is highly appreciated. Thank you for all the suggestions and discussions we had over the course of the project.

I would also like to thank Johanna von Holdt for providing me with the samples used for the analytical experiments.

I would also like to thank the NRF and NSFAF for financial assistance during this project, without this institutions, this project wouldn't have been possible.

To all my family and friends, whose names will probably fill up another thesis. Thank you so much, I am here today because of all your motivations, encouragements, support, love, kindness and prayers.

To my parents: I will forever be indebted to you guys, thank you for all the support through all these years.

To my mentor, my dad, Mr Godwin Murangi and Cynthia Kandorozu, words cannot explain how much you guys have done for me all these years, my achievements will always be yours as well. I am blessed to have you guys as part of my life, your prayers definitely pulled me through it all.

Special shout out goes to Athina Kenned, Peter Iikondja, and Shelley Haupt for proof reading through my thesis besides your busy schedules.

Lastly but not least, I want to thank the Almighty Lord for everything, for being with me through thick and thin. Thank you for directing my steps daily and I couldn't have done this without your love, mercy and grace.

I dedicate this thesis to my late brother Uaisapo Kangueehi, you might be gone but I miss you every day and my joy is your joy.

TABLE OF CONTENTS

LIST OF FIGURES

LIST OF TABLES

ABSTRACT

Dust can be a source of micronutrients to surrounding areas such as oceans and terrestrial regions. The deposition of dust can provide trace elements to the open oceans, which can increase primary production and ultimately remove carbon dioxide from the atmosphere, therefore reducing global warming. Previous remote sensing studies have shown that southern African is a prominent dust emitting region and can potentially provide micronutrients to oceanic regions which might be depleted in some bioactive trace elements. Hysplit modeling software was used to estimate the long distance transport of dust emissions observed in southern Africa between January 2005 and December 2008. The observations revealed that most of the dust emissions occur during spring and winter seasons, with very little emissions in autumn. Most of the dust emissions tend to travel off the Namibian coastline towards the north-west Africa regions and are mainly influenced by strong south easterly trade winds. A strong air mass migrates towards the Indian Ocean and as far as the Australian continent due to the effects of the westerlies. Fewer air masses travel towards the nutrient-limited regions of the Atlantic Southern Ocean and central eastern Indian Ocean. The locations further north of the southern Africa preferentially travel towards the north west Atlantic Ocean, because the westerlies are not strong enough to transport air-masses towards the southern oceanic regions. This study also revealed that the prominent dust emitting sites in southern Africa are two ephemeral rivers, Kuiseb and Omaruru River as well as two ephemeral pans, the Etosha Pan in Namibia and Makgadikgadi Pan in Botswana. Emissions from these sources tend to travel towards north west Atlantic Ocean and south east Indian Ocean, with the exception of the Etosha Pan, which has emissions that travel towards the northern regions.

These emitters were investigated for particle size distribution, mineralogical characteristics and trace elemental concentrations. The role of ephemeral rivers in southern Africa as potential sources of micronutrients to marine environments has not been previously investigated extensively. Most previous studies focussed on the ephemeral pans. Particle sizes can be an indicator of how far the sediments can potentially travel and of the trace elemental solubility. Etosha Pan has the finest grain sizes, while the Makgadikgadi had the coarsest grain size. Omaruru and Kuiseb River showed medium grain size variation. Our dissolution experiments showed, however, that the dissolution of the sediments is mostly influenced by the mineralogy rather than the particle sizes. The two pans appeared to be enriched in calcite, silica oxide and quartz, while the two rivers were more enriched in kaolinite, quartz, illite and muscovite. High trace element solubility in the Etosha Pan is most probably attributed to the high calcite content, which is highly soluble. A continuous flow through method proved to be effective and inexpensive. This study is one of the few in southern Africa which aimed at modelling the air mass pathways from dust emissions that have been observed instead of just creating simulations. Our findings highlight the importance of additional studies to prove the dissolution and quality of dust in dry regions as potential contributors to marine primary production.

UITTREKSEL

Stof kan 'n bron van mikrovoedingstowwe wees vir omliggende gebiede soos oseane en landstreke. Die afsetting van stof kan spoorelemente aan die oop oseane verskaf, wat primêre produksie kan verhoog en uiteindelik koolstofdioksied uit die atmosfeer verwyder, wat sodoende globale verwarming verminder. Vorige afstand waarnemings studies het getoon dat suidelike Afrika 'n prominente stof vrystellende streek is en moontlik mikronutriënte kan verskaf aan oseaanstreke wat in sommige bioaktiewe spoorelemente uitgeput is. Hysplit-modelleringsagteware is gebruik om die langafstand vervoer te beraam van stofvrystellings wat in suidelike Afrika waargeneem is tussen Januarie 2005 en Desember 2008. Hierdie waarnemings het getoon dat die meeste stofvrystellings gedurende die lente- en winterseisoene plaasvind, met baie min vrystelling tydens herfs. Die meeste van die stofvrystellings is geneig om van die Namibiese kus na die noordwestelike Afrika-gebiede te reis en word hoofsaaklik deur sterk Suid-Oosterse handelswinde beïnvloed. ‘n Sterk lugmassa migreer na die Indiese Oseaan en so vêr as die Australiese vasteland as gevolg van die uitwerking van die westewinde. Minder lugmassas reis na die voedingsarm gebied van die Suidelike Oseaan en Sentraal-Oos-Indiese Oseaan. Die stof van areas verder noord van die suidelike Afrika streek reis verkieslik na die noordwestelike Atlantiese Oseaan, want die westewinde is nie sterk genoeg om lugmassas na die suidelike oseaanstreke te vervoer nie. Hierdie studie het ook aan die lig gebring dat die prominente stof vrystellers in suider-Afrika twee kortstondige riviere, die Kuiseb en Omaruru-rivier sowel as twee kortstondige panne, die Etosha Pan in Namibië en Makgadikgadi Pan in Botswana is. Stof vrystelling van hierdie bronne is geneig om te reis na die Noordwes-Atlantiese Oseaan en Suid-Oos Indiese Oseaan, met die uitsondering van die Etosha Pan, wat vrystelling het wat na die noordelike streke reis. Hierdie stof vrystellers is ondersoek vir deeltjiegrootteverdeling, mineralogiese eienskappe en spoorelement-konsentrasies. Die rol van kortstondige riviere in Suider-Afrika as potensiële bronne van mikrovoedingstowwe in mariene omgewings is nie voorheen breedvoerig ondersoek nie. Die meeste vorige studies het gefokus op die kortstondige panne.

Partikelgroottes kan 'n aanduiding wees van hoe vêr die sedimente potensieel kan beweeg en elementêre oplosbaarheid van die verskillende stof vrystellingsbronne kan opspoor. Etosha Pan het die fynste korrel groottes, terwyl die Makgadikgadi die grofste korrel grootte gehad het. Omaruru- en Kuisebrivier het 'n middlematige korrelgrootte variasie getoon. Die twee panne was verryk in kalsiet, silikaoksied en kwarts, terwyl die twee riviere meer kaoliet, kwarts, illiet en muskoviet ryk was. Hoë oplosbaarheid in die Etosha Pan word waarskynlik toegeskryf aan die hoë kalsiet inhoud, wat hoogs oplosbaar is. Ons resultate het getoon dat die dissolusie van die sedimente meestal deur die mineralogie eerder as die deeltjiegroottes beïnvloed word. 'n Deurlopende vloei metode was effektief en goedkoop. Hierdie studie is een van die min in suider Afrika wat daarop gemik was om die lugmassas te modelleer van stofvrystellings wat in ag geneem is, in plaas van om net simulasies te skep. Ons bevindings beklemtoon die belangrikheid van bykomende studies om die dissolusie en kwaliteit van stof in droë streke te bewys as moontlike bydraers tot primêre produksie in mariene stelsels.

CHAPTER 1:

GENERAL INTRODUCTION

1.1 INTRODUCTION

Some of the major oceanic regions are typically characterized by continually high macronutrient levels yet low and persistent levels of phytoplankton stocks, which has been a contradiction long documented by oceanographers (Gran, 1931), commonly known as High Nutrient Low Chlorophyll (HNLC) regions. The subarctic north Pacific, the east equatorial Pacific and the Southern Ocean are widely regarded as the three major HNLC regions. One of the well-studied trace elements that is limited in the HNLC regions is iron. The atmospheric deposition of mineral dust is one of the likely corridors for the impact of trace elements to the surface waters of the open ocean regions such as for example the Southern Ocean (Johnson et al. 2011). Dust depositions from South America, Australia and southern Africa contribute 58%, 36% and 2% of dust deposition respectively, into the Southern Ocean (south of 50° S) (Li et al. 2008). The McMurdo Dry Valleys, which are ice-free in Antarctica have also been proposed as a new probable supplier of bioactive trace metal via atmospheric deposition to the Southern Ocean (Bhattachan et al. 2015).

Fluvial river inputs and groundwater sources (Poulton & Canfield 2005), volcanoes, continental upwelling zones (Elrod et al. 2004; Lam et al. 2006; Compton et al. 2009; Chever et al. 2010), remineralisation of descending material, dissemination from pore waters and discharge of bioavailable trace elements from glaciers (Bhattachan et al. 2015), and hydrothermal inputs (Tagliabue et al. 2010) are some of the other major sources of macro- and micronutrients to oceans. However, such sources tend to have a lower dispersion rate than atmospheric inputs (Boye et al. 2006; Raiswell et al. 2008b). Sceptics over these sources argue that most emissions are likely localized (Jickells 2005; Jickells 1995). Atmospheric deposition is therefore essential as it can potentially alter the biogeochemistry of open oceans and it brings vital sources of trace elements, including Fe to the oceanic biota (Martin et al. 1990). There is a positive correlation between mineral dust emissions from Patagonia and southern Australia with the Southern Ocean primary productivity and phytoplankton abundance in surface waters

(Gabric et al. 2002), while studies in southern Africa on the role of dust on productivity are still missing.

Evidence for significance of the link between dust-ocean-climate feedback processes is still incomplete, especially in the Southern Hemisphere. In order to understand the influence of bioactive trace elements like Fe, Zn, Cu, Cd and Mn when deposited in the Southern Ocean and South Atlantic, it is important to investigate and characterise initial compositions at sources such as Patagonian Desert (South America) (Johnson et al. 2011), Australia and southern Africa. An important objective in atmospheric research is to better understand the role of physical and chemical processes influences on the formation of dissolved bioactive trace elements in mineral dust during atmospheric transport from the source regions to the oceans (Johnson & Meskhidze 2013) and after deposition. These processes ultimately control the likelihood of dust emissions becoming a potential source of both macro and micronutrients in terrestrial and marine environments. However, not all mineral dust containing iron can be bioavailable to the phytoplankton communities but only the soluble forms of iron in the surface ocean is considered bioavailable (Martin et al. 1990; Boyd et al. 2010). The solubility of aerosol mineral dust iron is still an uncertainty in our knowledge of the marine cycle of iron and through the correlation between bioactive trace elements role, phytoplankton nutrient requirements and the global carbon cycle (Baker et al. 2006). Research on the biogeochemistry of dust emitting sources in southern Africa is still very limited to studies on salt/clay pan and desiccated lacustrine emission areas such as the Etosha and Makgadikgadi Pan and the Kalahari Desert (Bhattachan et al. 2015), while other sources such as ephemeral rivers have been overlooked until a recent study by Dansie et al. (2017) that investigated three ephemeral rivers along the Namibian coastline. This is despite extensive remote sensing studies having shown the importance of ephemeral rivers as prominent dust emitters (Eckardt & Kuring 2005; Vickery & Eckardt 2013; Vickery et al. 2013)

Dust sources commonly include desert and semi-arid desert areas, ephemeral dry lake or riverbeds, and anthropological induced land surfaces (Prospero et al. 2002; Mahowald 2003; Ginoux et al. 2012). These areas provide necessary conditions for dust emissions as soil surfaces are predominantly dry and sparsely vegetated. In southern Africa, numerous small dust plumes were observed along the Namibian coastline which is dominated by the arid Namib Desert, with a north south extent of 1 500 km (Vickery 2010). Since most of the dynamic dust emissions occur as ‘hot spots’ within dry regions, which is a regular phenomenon in prominent

global dust emitters, rather than being huge uniform dust emissions regions, most dust investigations should be conducted at correspondingly fine scales. Prospero et al. (2002) identified various environments ranging from dry playa lakes and dry pans which are highly influenced by occasional flooding and drying as important mineral dust sources.

Numerous dust emitting sources observations in southern Africa have been investigated especially along the Namibian coastline, although there remains a mystery in the long-range transport of these plumes. Recently, the United States based National Oceanic and Atmospheric Administration (NOAA) has provided a research platform, the Hybrid Single-Particle Lagrangian Integrated Trajectory (Hysplit; http://www.arl.noaa.gov/HYSPLIT_info.php) for the modelling of "single or multiple air mass trajectories from sources during transport, dispersion, chemical alteration, and deposition models" (Stein et al. 2015). Hysplit has been widely applied in simulations describing the long-range atmospheric transport in the Northern Hemisphere (Ashrafi et al. 2014), South America (Gasso & Stein 2007) and Australia (McGowan & Clark 2008), but similar simulation studies southern Africa are missing. All major dust emitting sources depend on the interaction between sediments types (physical characteristics), soil compaction, abundance of vegetation and groundwater level (Ginoux et al. 2012). Although there is a growing realization that dust from southern Africa can potentially contribute to surrounding ocean productivity, little is known about the correlation of southern African dust and global climatic changes (Bryant 2013; Mahowald et al. 2014).

1.2 AIMS AND OBJECTIVES

The aim of this study is to understand effects of southern African dust on the biogeochemistry of the proximal oceans in the region. This study will characterize dust pathways from these dusts emitting regions. In order to achieve this, the following key objectives and questions have been set up:

Key Objective 1: To determine air-mases pathways from the dust emitting sources

1. What is the preferential air mass pathways from southern Africa dust emitting sources?
2. How do the air masses pathways differ based on the location of the source area?
3. How do the different seasons influence the air mass pathways directions?

Key Objective 2: To determine how the particle sizes, mineralogy and trace elemental composition influence the dissolution of sediments (soil) from southern Africa

1. What is the particle size distribution of the surface soil samples?
2. What is the mineralogical composition of the surface soil samples?
3. What is the overall trace elemental composition and dissolution rates of the surface soil samples?
4. Which dust emitting region is most suitable to stimulate phytoplankton growth in oceans?

1.3 STRUCTURE OF THE THESIS

Chapter 1 introduced the thesis, and then its aims and objectives.

Chapter 2 will provide a detailed literature review of the study.

Chapter 3 presents a study and interpretation of the different pathways for the air masses from southern Africa influenced by seasonality and source locations.

Chapter 4 presents a detailed study on the trace elemental chemistry of the soils from the dust emitting sites and how the mineralogy and particle sizes can influence the solubility (bioavailability).

Chapter 5 will present the overall conclusions and recommendations for further studies based on our research questions.

CHAPTER 2:

LITERATURE REVIEW

2.1 SIGNIFICANCE OF DUST RESEARCH

Dust plumes and aerosol atmospheric processes have appealed to society and towards the science research community for millennia (Knippertz & Stuut 2014). Scientific observation on dust transport and deposition over long distances has been known for the past two centuries in history since the times of Charles Darwin and the *Beagle* Expeditions across the world (Pye 1987). Dobson in 1781 in one account indicated of the Harmattan wind between Cape Verde and Cape Lopez, reporting conditions of poor visibility which he attributed to the dust of the air (Pye 1987). Darwin in (1846) famously summarised earlier reports of dust falls on vessels off the West Coast of Africa and described a fall observed at first hand during the voyage of the Beagle:

> *"On the 16th of January (1833), when the Beagle was ten miles off the N.W. end of St. Fago (Cape Verde Islands), some very fine dust was found adhering to the underside of the horizontal wind-vane at the mast head… During our stay of three weeks at St. Fago (to February 8th) the wind was N.E., as is always the case at this time of the year; the atmosphere was often hazy, and very fine dust was almost constantly falling, so that the astronomical instruments were roughened and a little injured. The dust collected on the Beagle was excessively fine-grained, and of a reddish brown colour; it does not effervesce with acids; it easily fuses under the blowpipe into a black or grey bead".*
>
> ***(Darwin, 1889:26)***

The focus of dust research changed over the past decades. Earlier work predominantly studied radiation, transportation and deflation of dust in the atmosphere (Ravi et al. 2011). In 1941 though, Bagnold presented a major breakthrough towards process orientated dust studies in his book "The physics of blown sand and desert dunes", which for many decades served as the primary reference textbook for mineral dust transport (Knippertz & Stuut 2014). More than

twenty years later, Pitty (1968) investigated the characteristics of dust travelling thousands of kilometres from sources to deposition (Knippertz & Stuut 2014). In the meantime, Policard and Collet (1952) had published on the role of Saharan dust particles in transporting harmful diseases (Knippertz & Stuut 2014). Over time, research has evolved into observations of mineral aerosols of dust fall downwind of the major source regions. For example, the role of mineral dust as a significant source of trace elements and nutrients to the open ocean was soon established, while questions remain unresolved until nowadays about the functioning of the relevant processes such as uplift, transport and deposition (Patey et al. 2015).

Possibly one of the most documented and famous dust occurrence in the last century is the 1930s Dust Bowl event, which has been referred to as the Black Sunday (storm) which occurred in the American Great Plains, United States of America (USA) and it was very devastating to agricultural farmers. Some experts regard it to be as one of the most disturbing environmental catastrophes in the agricultural sector history of the USA (Romm 2009). Dust Bowl was partly caused by consecutive years where conditions were very dry and there was low vegetation cover leading to surface soils being vulnerable to wind erosion (Goudie & Middleton 2006). An estimated 300 million tons of topsoil displaced from the prairie area in the USA (Romm 2009). The emissions were mainly a result of poor land management practices and drought, which lead to poor vegetation cover (Bennet 1938 as quoted from Romm 2009). Agricultural practices such as overgrazing was one of the key factors in producing the dust bowl effect (Cook et al. 2009). Mineral dust aerosols have a variety of adverse effects from human health, air pollution, atmospheric chemistry, most biogeochemical cycles to radiative budgets (Mahowald et al. 2009).

In recent decades, there was an increasing consciousness on the significance of aerosols on the Earth`s physical system and biosphere. Atmospheric dust research is a science that can be interdisciplinary across the field of geology, biology, chemistry and atmospheric sciences, and even incorporating work from the terrestrial scientific community (Muhs 2013). Over the past decades, North Africa has been the region where most interest in mineral dust research since it is the world`s major consistent dust emitting regions (namely the Sahara desert), contributing more than two-third of entire global dust emissions (Huneeus et al. 1993). It is only in recent years that more efforts were made for long-range transport studies of dust from southern Africa

(Fishman et al. 1990; Washington et al. 2003; Vickery et al. 2013). More dust studies need to be conducted in the Southern Hemisphere and particularly in southern Africa as dust can provide macro- and micronutrients to the both terrestrial and ocean ecosystems. There is evidence that mineral dust from southern Africa provides nutrients to proximal oceanic regions and Cape Floristic region of south-western South Africa (Soderberg & Compton 2007; Dansie et al. 2017).

Dust can be defined as the fine grains in suspension or deposition of such fine particles (Pye 1981). "Dust is the fine particle materials that is picked up from the continental surfaces by physical weathering processes and is tiny enough (having diameters of less than 0.08 mm) to stay in suspension in the atmosphere" (Bagnold 1941 as quoted from Pye 1981). McTainsh and Strong (2007) defined dust as mineral sediments broken down during weathering processes, sized <100 µm which can be transported in suspension. Grains larger than about 20 µm settle back to the surface quite quickly when the turbulence associated with strong winds decreases, but smaller particles remain in suspension for days or even weeks unless washed out by rain (Pye 1987). Although all dry and exposed sediments that are found in suspension can qualify to be classified as dust but most studies mainly focus on sediments observed in dry and semi to arid regions (Bullard et al. 2011; Vickery 2010).

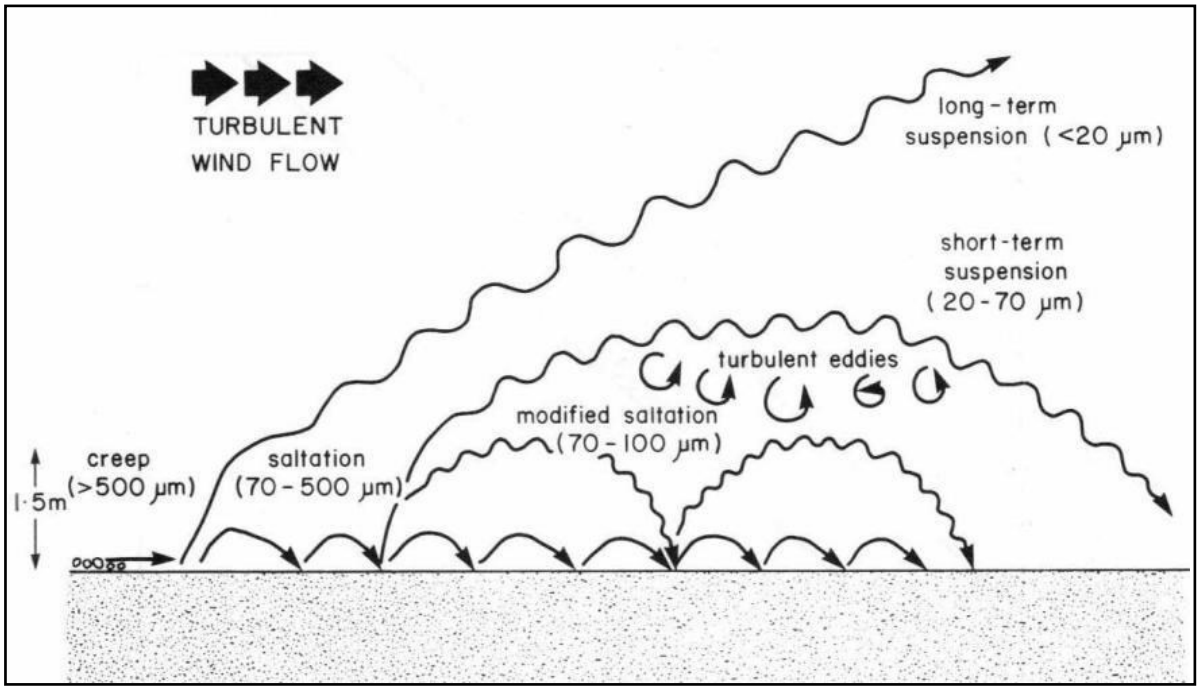

Figure 2-1 Different mineral dust particles size distribution transported by wind (Pye 1987).

Material which get to travel long distances in the Earth's atmosphere is usually smaller than 10 µm and can be much smaller than 2 µm (Figure 2-1) (Pye 1987). In locations remote from the main areas of natural and industrial particulate emission, such as Antarctica, the Artic and the Central Pacific, a high proportion of the deposited dust is sub-micron in size mainly due to the travelling distance (Pye 1987). However, there have been studies which reported gigantic aeolian crystals of weathering resistant mineral grains (>62.5 µm) to arise more frequently than formerly assumed, besides the fact that the mechanisms that enable such long-range, large-sized grain transport are not still understood (Dulac et al. 1992; Scheuvens et al. 2011). Continental loess deposits are composed mainly of particles in the 10 - 50 µm size range which usually do not get transported great distances (Pye 1987). Dust can change nutrient dynamics, biogeochemical cycles of ecosystems which can influence soil characteristics, ocean productivity and air chemistry. The particle size distribution decreases with the proximity from dust emitting source regions (Pye 1987), with most fine particles found furthest away from the source. Fine grain size is used as a reference for particle sizes ranging between 4 - 63 µm and < 4 µm in size which usually have a clay to silt texture (Wentworth, 1992).

Table 2-1 Maximum mean aerosol index (AI) values for major global dust sources determined using the Total Ozone Mapping Spectrometer Satellite (TOMS) (Goudie & Middleton 2001).

Location	AI value	Average annual rainfall (mm)
Bodélé Depression of south central Sahara	>30	17
West Sahara in Mali and Mauritania	>24	5–100
Arabia (Southern Oman/Saudi border)	>21	<100
Eastern Sahara (Libya)	>15	22
Southwest Asia (Makran coast)	>12	98
Taklamakan/Tarim Basin	>11	<25
Etosha Pan (Namibia)	>11	435–530
Lake Eyre Basin (Australia)	>11	150–200
Mkgadikgadi Basin (Botswana)	>8	460
Salar de Uyuni (Bolivia)	>7	178
Great Basin of the USA	>5	400

Largest dust emissions in the world occur in the Northern Hemisphere in locations such as North Africa, Middle East, Asia and North America (famously known as the 'dust belt') with the Sahara Desert being biggest source on earth (Goudie & Middleton 2006; Prospero et al. 2002) with the highest aerosol index (AI) (Table 2-1). Up to 80% of all global emissions are associated with the Northern Hemisphere sources while the Southern Hemisphere counterparts contribute about 10% to the total emissions based on the current model estimations (Ginoux et al. 2004; Li et al. 2008). The AI represents the radiative effect of aerosols calculated as:

"$AI= -100\log_{10}[(I_{340}/I_{380})_{meas}-(I_{340}/I_{380})_{calc}]$,

where I_{meas} is the measured backscattered radiance at a given wavelength and I_{calc} is the radiance calculated at the wavelength using an atmospheric model that assumes a pure gaseous atmosphere. The difference between the measured and calculated radiances is attributed to aerosols."(Prospero et al. 2002) Currently major active dust emitting sources in the Southern Hemisphere are the Lake Eyre Basin in Australia, the Makgadikgadi and Etosha salt pans in southern Africa (

Table 2-1) (Prospero et al., 2002), the Salar De Uyuni in Bolivia and the Patagonian Desert in South America (Bozlaker et al. 2013; Ginoux et al. 2012). In the Southern Hemisphere, and to a lesser extent in the Northern Hemisphere, mineral aerosols can potentially influence the

climatological and biogeochemical processes, although how specific sources role in open oceans is not yet well known (Mahowald & Luo 2003).

2.2 DUST AND CLIMATE

It is widely recognised that dust emissions are linked to climate while the production and transport of it is extremely susceptible to climatic changes (Figure 2-2). There is a considerable correlation of dust when examining climate indicators found in the paleo-records such as ice cores (Schultz 1980). Paleo-records show that if there is an increase glacial mineral dust deposition logged in Antarctic ice cores, these enhanced supplies of iron stimulated marine productivity, stimulating carbon depletion in the deep ocean and resulting in a decline in atmospheric CO_2 levels (Martin et al. 1990). Glacial-interglacial cycles of the Pleistocene were paced by variations in insolation, but largely driven by ice-albedo feedbacks and variations in atmospheric CO_2 (Shackleton 2000). Mineral dust and aerosol impurities found in ice cores in Antarctic ice point to roughly 25 times greater glacial dust fluxes likened to interglacial (Lambert et al. 2008). There is significant correlation between the CO_2 content of the atmosphere and climate over the past 400,000 years (Petit et al. 1999), which has increased widespread investigation and interest on the processes responsible for controlling the CO_2 content of the atmosphere. It has been shown in ice core records that mineral dust input in the oceans may have removed atmospheric CO_2 by 10-20 ppm in glacial versus interglacial periods (Wang et al. 2015). Although there are other sources of trace elements into oceans, atmospheric inputs (mainly via dust) are widely considered to be the most significant and dominant source mainly because of its ability to disperse over a larger area to remote ocean regions.

In the late eighties John H Martin and co-authors reported evidence there is a deficiency of iron in the Southern Ocean that limits the growth of phytoplankton communities (Martin & Fitzwater 1988; Martin et al. 1990). Martin et al. (1990), recognized that one important significance of this finding was that with increasing bioavailable iron in HNLC regions could have positively effect on marine primary productivity and organic carbon sinking to the bottom of the ocean, and therefore could impact the efficiency of the global biological pump in removing atmospheric CO_2 (Martin & Fitzwater 1988). After this discovery (famously known as the “Iron Hypothesis”), more experiments were developed and conducted to test the iron deficiency in the Southern Ocean HNCL regions (Figure 2-2). Preceding experiments conducted during the subsequent two decades have confirmed and accepted this hypothesis

which shows that addition of trace elements to remote marine surface waters does stimulate phytoplankton blooms and hence primary productivity (Boyd et al. 2007). Since there are low dust emitting regions in the Southern Hemisphere (region contributing approximately 10% of the global emissions), there is low deposition rates of important nutrients such as iron and phosphorous, and the overall primary productivity of the Southern Ocean is lower in comparison to other oceans (Ridgwell 2002).

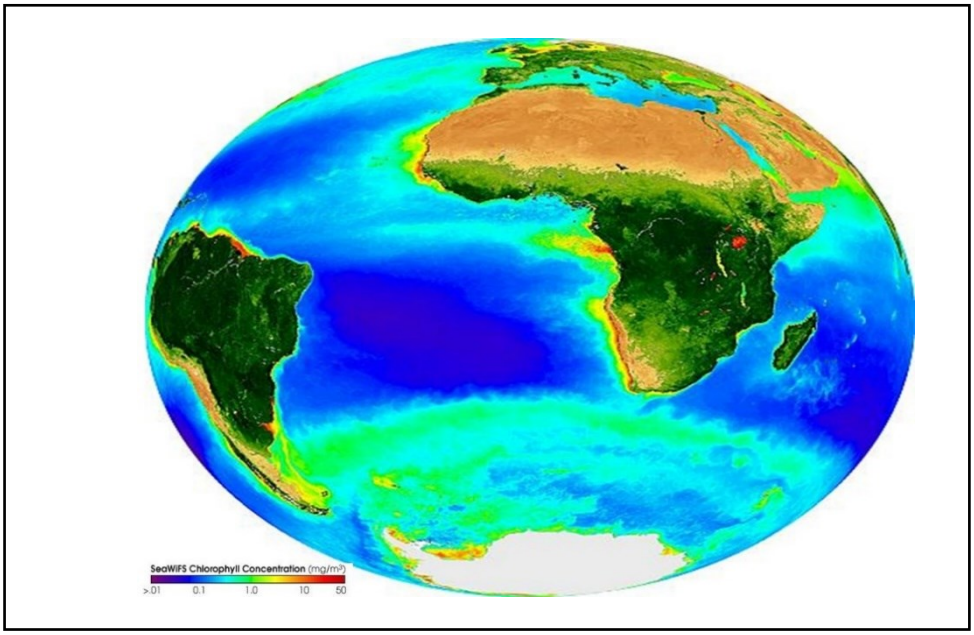

Figure 2-2 Global oceanic and terrestrial photoautotroph abundance from three years of data from the Sea-viewing Wide Field-of-view Sensor (SeaWiFS). This is a rough indicator of primary production potential, and not an actual estimate of it. Colours show marine deserts with low chlorophyll (blue) in warm water, a bounty of life (light green) in cool water, and abundant life (red) near the coasts (credit. SeaWiFS Project, NASA/Goddard Space Flight Centre).

2.3 SOUTHERN HEMISPHERE DUST SOURCES

Although it is widely recognized that finer particles (<2.5 µm) tend to travel thousands of kilometres from sources, numerous new studies have revealed that larger particles (greater than 10-20 µm) have also been observed significant distances away from sources (Bhattachan et al. 2015). From the total of 910 M ton of aerosols transported yearly to the ocean surfaces, about 50% is deposited in the North Atlantic Ocean, supplied predominantly by the Sahara Desert (Figure 2-3), while less than 3% tend to reach the South Atlantic Ocean (Duce & Tindale 1991),

where there the annual mean deposition rate is about 0.47 g m^{-2} (Prospero 1996). The Northern Hemisphere dust long distance transport has been long documented with emissions from North Africa to Europe, the United States, the Caribbean, Asia and North Pacific transport of Asian dust (Schultz 1980; Bozlaker et al. 2013; D'Almeida 1986; Van Der Does et al. 2016). Despite the known effects of dust on climates, there has been considerably fewer studies which focused on the long transport of mineral dust emissions in the Southern Hemisphere (Table 2-2) (Tyson & D'Abreton 1998; Tyson & Gatebe 2001a).

Table 2-2 Illustrations of long-distance dust transport (Knippertz & Stuut 2014)

Approximate Distance (km)	Traced from	Traced to	Reference
6500	Sahara	Barbados	Delany et al. (1967)
8000	Sahara	Miami	Prospero (1981)
>1000	Sahara	Cape Verde Islands	Jaenicke and Schütz (1978)
2000	Sahara	Gulf of Guinea	Schütz (1980)
6500	Sahara	French Guiana	Prospero et al. (1981)
4000	Sahara	Berlin	MWR (1980)
7000	Sahara	Illinois	Gatz and Prospero (1996)
4000	Sahara	Hungary	Borbérly-Kiss et al. (2004)
7000	Sahara	Fennoscandia	Franzen et al. (1994)
10 000	Sahara	China	Tanaka et al. (2005)
750	Interior Morocco	Gibraltar	Ward (1950)
4000	Western Sahara	Cyprus	Gordon and Murray (1964)
2000	Libya and Egypt	Negev, Israel	Yaalon and Ganor (1975)
3500	Algeria	Denmark and USSR	VDL (1902)
700	Mkgadikdadi	Johannesburg	Resane et al. (2004)
10 000	Central Asia	Barrow, Alaska	Rahn et al. (1977), Andrews et al. (2003)
11 000	Central Asia	Tropical North Pacific (Eniwetok and Hawaii)	Turekian and Cochran (1981), Duce et al. (1980)
2000	West Kazakhstan	Baltic Sea	Hongisto and Sofiev (2004)
4000	China	Japan	Willis et al. (1980)
4000	China	Pacific Ocean (2500 km from coast)	Ing (1972)
>16 000	China	USA and Canada	Husar et al. (2001), McKendry et al. (2001)
>20 000	China	French Alps	Grousset et al. (2003)
>16 000	China	Greenland	Drab et al. (2002)
1500	Middle East	Southern USSR	Balakirev (1968)
3500	Caucasus	Rumania, Bulgaria and Czechoslovakia	Lisitzin (1972)
3500	Australia	New Zealand	Kidson and Gregory (1930)
3500	Australia	Singapore	Durst (1935)
2500	Canadian prairies	Illinois, USA	Van Heuklon (1977)
2500	Nebraska and Dakotas	Washington, D.C.	Hand (1934)
6000	Patagonia	Antarctica	Smith et al. (2003)
>7000	USA	Greenland	Smith et al. (2003)

One of the most effective ways of studying and monitoring this long range transport is through the use of satellites when combined with ground based atmospheric observations and distribution modelling (Gasso et al. 2007). In the Southern Hemisphere, using the Total Ozone Mapping Spectrometer Satellite (TOMS) researchers identified that there are two fairly minor but visibly well-established dust emitting regions in southern Africa with numerous other smaller ones (Washington et al. 2003). Southern Africa has two of the major dust emitting

sources in the Southern Hemisphere: the most intense being the Etosha Pan of Namibia and the other is the centre of the Makgadikgadi Depressions of Botswana (Prospero et al. 2002). TOMS data and observations have illustrated most of the world`s key dust sources are areas of hyper aridity, usually associated with average yearly rainfall of under 100 mm (Goudie & Middleton 2001). However, the drawback of using TOMS is the fact that it does not identify dust transport beneath 1000 m, which means it does not capture numerous smaller plumes (Eckardt & Kuring 2005).

In Southern Hemisphere, Patagonia, Australia and southern Africa are the three continental regions supplying mineral dust deposited to the Southern Ocean (Figure 2-3 (b, c, d)) (Li et al. 2008). In South America, similar studies have identified the Patagonian Desert as a significant dust emitter and contributing dust to Antarctica (Gaiero et al. 2003), although counter arguments have proven that the Lake Eyre, Australia is also one of the most significant contributors (Mcgowan & Clark 2008). Recent modelling studies by Albani et al. (2012) and Li et al. (2012) revealed that more than 80% of recent dust deposition in the western and central Pacific Southern Ocean originates from Australia. Dust emissions from southern Africa tend to effect predominantly the Indian Ocean and lower latitudes areas in the South Atlantic close to the continent (Li et al. 2008; Qu 2016).

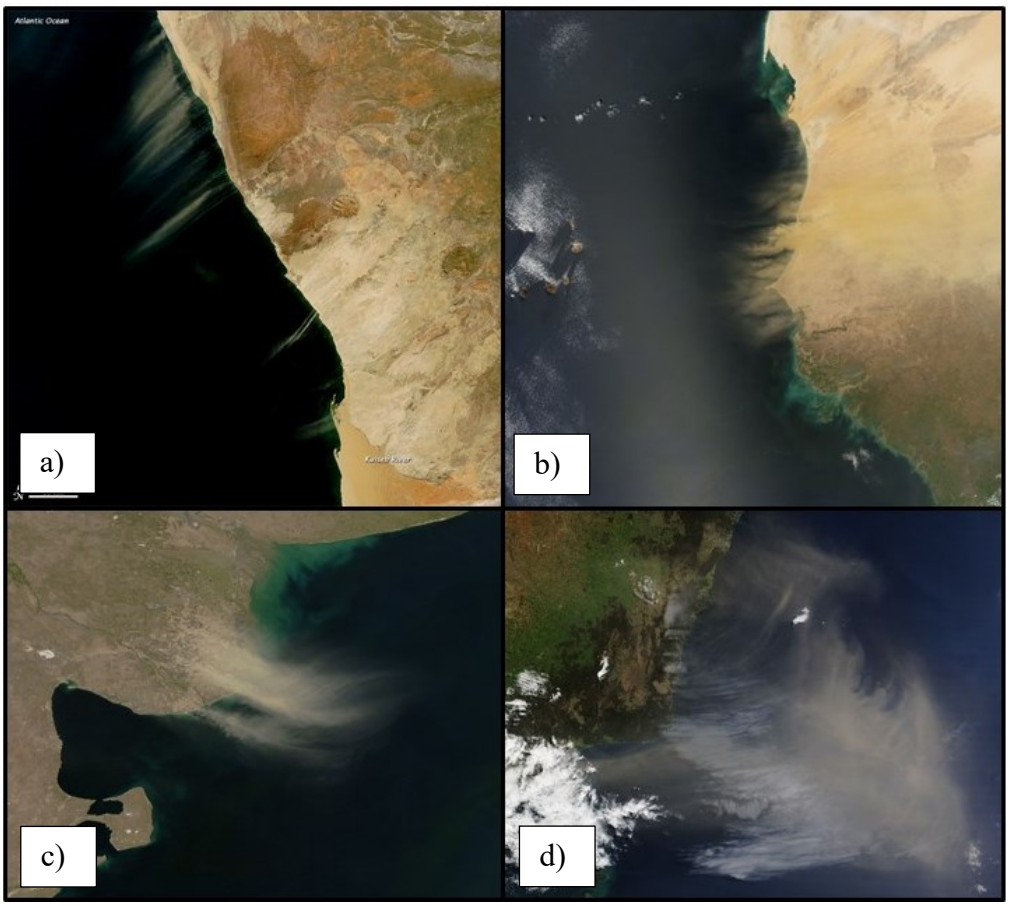

Figure 2-3 Dust emissions off the major dust sources namely: (a) Namibian coastline on June 17, 2010 with the use of MODIS on NASA's Terra satellite, (b) Sahara Desert on February 26, 2015 with the use of MODIS on NASA's Aqua Satellite on a trans-Atlantic journey from Senegal, Mauritania, and Gambia, (c) Patagonian Desert (South American continent) acquired on September 11, 2009 on NASA's Aqua satellite, and (d) Australian continent on September 12, 2009 on NASA's Terra satellite. (Credit: NASA). The dust plumes are the thickest near their points of origin and dissipate as they travel away from sources.

Although most of the sources are associated with dry areas, the action of flowing fluvial inputs plays a significant role, as the existence of ephemeral streams, rivers, lakes, and playas lakes (ephemeral or desiccated lakes which contain deposits of clay, silt, and salts). The major dust sources in southern Africa are occasionally flooded and dry quickly, which leads to the development of new sediment deposits (Li et al. 2008). The Namib Desert dust sources are mainly linked with either dry saline pans (for example Etosha and Makgadikgadi salt pans) or occasionally flooding river beds, and major dust supply is preserved by fluvial landforms and hydrogeological processes (Eckardt & Kuring 2005) and these regions are the emitting hotspots. Major dust sources are not homogenous but are located in arid regions (Goudie &

Middleton 2006) and regions where there is frequent flooding and drying accumulating substantial sediments (Prospero et al. 2002).

2.4 MAJOR CIRCULATION SYSTEMS AROUND SOUTHERN AFRICA

Due to the importance for the subsequent data interpretation, I briefly give a description of the climatology of the atmospheric transport over the southern African continent. There are four major circulations of the atmosphere in southern Africa revised in detail by Tyson (1986) and Preston-Whyte and Tyson (1989). These circulations vary in frequency based on different periods during the year, ranging from primary, semi-permanent subtropical anticyclones which are a typical of the large-scale subsidence region found between the Hadley and Ferrell cells of the Southern Hemisphere (Newell et al. 1972 as quoted from Preston-Whyte & Tyson 2000). In southern Africa, there is a continental high pressure system that is most intense in winter (from June to July), occurring frequently up to 70% of days. In the summer months (from December to January), their occurrence subsidises to less than 20%.

Southern Africa is in a region were common circulation of the atmosphere is dominated for much of the year by subsidence of the descending limb of the Hadley cell (Newell et al. 1972 as quoted from Preston-Whyte & Tyson 2000). Most of the dust emissions are influenced by the development of low level easterly circulations over the interior in southern Africa (Washington et al. 2003). Short-lived eddies, in the form of west-to-east migrating anticyclones travelling to the west of a Rossby wave-trough axis, are confined to the oceanic areas closely to the south of the subcontinent causing into the unbroken escarpment (Tyson & Preston-White 2000). The movement of air masses in these systems leads to an improved east-west gradient and the equivalent unusual easterlies, which, over the western half of the subcontinent, are related with dust storms and plumes over the subtropical southeast Atlantic (Goudie & Middleton 2006).

For long periods of the year, atmospheric states under such anticyclone conditions are typically free, or nearly free, of clouds, maximizing daytime insolation (Swap et al. 1996). This pattern of circulation results in the “River of Smoke” (Swap et al. 2003) and is estimated to transport

75% of aerosols off towards the Indian Ocean from southern Africa. There is strong re-circulation in the region which is a direct response to the stable discontinuity at 500 hPa (Tyson & Preston-Whyte 2000) which traps a pall of aerosols beneath its surface at an altitude of between 4 and 6 km, this stable layer "blankets the whole subcontinent" (Tyson & Preston-Whyte 2000). This phenomenon occurs throughout the year, most characteristically on rain-free days as are experienced over the subcontinent in the austral spring and summer (Tyson & Gatebe 2001b). The model simulations by Li et al. (2008) showed that dust from southern Africa characterizes a comparatively minor amount of dust deposition to the Southern Ocean and mainly dominates the lower latitudes areas of the Indian and South Atlantic Ocean.

Hysplit is a computing calculating system that uses complicated transportation, scattering, advection and deposition models to predict the transport of air parcels pathways (Stein et al. 2015). Hysplit has been widely applied in simulations describing the transport of suspended materials and deposition of contaminants and harmful materials. Simulations can be calculated for both forward and backward trajectories to predict the transport pathways for potential sources or deposition sites. Some long distance dust forward trajectories simulations examples include: the dust storm simulation over Iran (Ashrafi et al. 2014), mineral aerosols transport dispersion models from Lake Eyre, Australia (McGowan & Clark 2008), dust transport from Patagonia to sub-Antarctic Atlantic Ocean (Gasso & Stein 2007; Johnson et al. 2011). Some backward-trajectories examples: the tracking dust sources from northwest Pacific Ocean cruises (Buck et al. 2006), from south-east Atlantic (Chance et al. 2015), from the equatorial North Atlantic (Van Der Does et al. 2016) and Kerguelen Islands (South Indian Ocean) (Heimburger et al. 2013). Most of the simulations for both forward and backward trajectories are run for 5 to 10 days at heights ranging from 10 m to 5000 m above sea level (Ashrafi et al. 2014; McGowan & Clark 2008: Chance et al. 2015; Buck et al. 2006). Hysplit model applications have consistently been evolving since its inception 30 years ago, from calculating single trajectories based on radiosonde observation to predicting multiple interacting air masses migrating, dispersed and suspended in the atmosphere from sources, at local to global scales (Stein et al. 2015).

2.5 LONG RANGE DUST TRANSPORT IN SOUTHERN AFRICA

A notable in-depth study of trace elemental long range transport specifically for southern Africa was conducted during the year 2000 and 2001 field campaign: The Southern African Fire Atmosphere Research Initiative (SAFARI 2000), which studied transfers of aerosols constituents from southern Africa into proximal oceans (Swap et al. 2003) and Transport and Atmospheric Chemistry near the Equator-Atlantic (TRACE-A) (Fishman et al. 1996). Work conducted during the SAFARI, according to Swap et al. (2003), proved that aerosols from southern Africa where biogeochemically significant to the Indian Ocean and South Atlantic. Furthermore, SAFARI project revealed that large plumes of aerosols were transported off to the Indian Ocean than previously thought, and much more in comparison to transport towards the south Atlantic Ocean. SAFARI 2000 project then laid the foundation for aerosol and trace metal observations at various locations around southern Africa (Swap et al. 2003). The SAFARI project also revealed that atmospheric circulation around southern Africa are influenced by the existence of a consistent stable stratification atmospheric levels in the lower and middle troposphere (Cosijn & Tyson 1996). During most winter months there is a anticyclone circulation due to the subtropical high-pressure belt which is found in southern Africa (Tyson & Gatebe 2001b; Tyson et al. 1996). The total flux to the south-eastern Indian Ocean at 35 °S is significantly higher than towards the Atlantic Ocean at 10 °E (Tyson et al. 1996). Prospero et al. (2002) revealed with remote sensing techniques that southern African aerosols are carried north westward mainly due to the presence of south trade winds that transport mineral dust from the Namibian and Angolan coastlines.

Investigation of satellite images in southern Africa has shown occurrence of mineral dust emissions driven off westwards from the Namib by berg winds (Figure 2-3). There are two moderately minor, but evidently prominent dust emitting regions in southern Africa (Washington et al. 2003). The most strongest of these is the central part of Etosha Pan in northern Namibia (Bryant 2013). The other centre is in the Makgadikgadi Depression in northern Botswana. Etosha Pan`s location is not favourable enough for the occurrence of berg winds which are needed to allow large deposits in oceans (Tllhalerwa et al. 2005). Berg winds are strong but occur occasionally by transporting large amount of sand and dust from inland and deposit into the ocean, extending up to 100 km from the coastline (Vickery & Eckardt 2013). Although southern Africa is not a main region for dust production, the few arid terrains inland such as the many scattered pans can cause a few isolated dust storms as observed by

numerous satellite images. Satellite images have shown dust plumes migrating westerly to the South Atlantic (Eckardt & Kuring 2005; Washington et al. 2003). The interior part of southern Africa is characterised by low level easterly circulations which effects most dust emissions (Washington et al. 2003). The geographical location (low topography) of the two ephemeral pans prevents strong winds from accelerating to produce huge dust sources (when compared to the Northern Hemisphere counterparts) (Goudie & Middleton 2006).

Piketh et al. (2000) reported that iron rich southern African mineral dust that gets transported to the ocean is mainly deposited in the Indian Ocean along latitude ~35°E while predicting that small amounts enter the South Atlantic. Dust derived iron delivery to oceans in southern Africa are mainly influenced by the extent, frequency and duration of the dust events (Piketh et al. 2000). Work by Piketh et al. (2000) also stated that dust events tend to occur every eleven days or so while lasting approximately five days on each event. On an annual basis, southern African dust flux towards the Indian Ocean is approximately 45 Tg a^{-1} while another 25 Tga-1 gets deposited into the southern Atlantic (Tyson & D'Abreton 1998; Tyson et al. 1996). Besides these model estimations, Heimburger et al. (2012) used direct measurements to calculate dust flux values 20 times higher than previous estimation calculated by Wagener et al. (2008), hence highlighting the importance of direct observations. Therefore, continental aerosols travelling to the Indian Ocean are cloud processed during their long range transport in the atmosphere and over the ocean, which will ultimately dramatically increase their solubility (Heimburger et al. 2013).

2.6 TRACE ELEMENTS IN OCEANS

Atmospheric aerosols play a leading role in the transportation of trace metals and altering the biogeochemistry cycles in the atmosphere. Besides decades of research on the influence of trace metals in biogeochemical cycles (with the exception of iron), especially on oceanic productivity in the HNLC regions such as the Southern Ocean our understanding is still lacking (Boyd et al. 2010). Most trace elements such as Zn, Cu, Ni, Fe, Co and Mn have essential functions to the phytoplankton communities and may limit productivity in oceans (Brand et al. 1983). On the flipside, high concentrations of these trace elements can be toxic to the phytoplankton (Paytan et al. 2009). Various sources of trace metals to oceans such as rivers,

mineral dust, volcanoes, hydrothermal vents and atmospheric inputs is what ultimately controls the distribution of trace metals within the water column (Spokes et al. 2001).

Various trace elements tend to be in high proportions in the sediments because of the role they play in the soils, for example aluminium and manganese are mainly crustal in origin, generated from the erosion and weathering of soils (Spokes et al. 2001). Aluminium contributes for about ~8.4% of the continental crust, manganese accounts for ~0.14% (Taylor and McLennon 1985). Al has been used in most studies as a crustal indicator trace metal and standard element for aerosols in enrichment factor studies (e.g. Schultz 1980; Remenyi 2013). Another element with high abundance is iron which is mostly attributed by presence of iron oxides (e.g. hematite, magnetite) and iron hydroxides (e.g., goethite, lepidocrocite). From a geochemical point of view, many reactions in soils are kinetically controlled and cannot be described sufficiently by thermodynamic considerations (Wiederhold, 2006). Therefore, soils are highly heterogeneous systems and variable in space and time. This leads to the study of soil biogeochemistry to be a challenging task and requires multidisciplinary approaches (Wiederhold, 2006). Mineral dust chemistry can vary even in proximal regions, and this can impact the gas phase composition of the atmosphere and ultimately impact biogeochemical cycles, climate and health (Krueger et al. 2004). Besides the high abundance of trace elements such as iron in dust, most of it exists as a crystalline oxide and in aluminosilicates such as clay (Shi et al. 2012). Most of the Fe in these aluminosilicates and iron oxides rarely become bioavailable due to the low solubility of these minerals (Shi et al. 2015).

2.7 BIOAVAILABILITY OF TRACE ELEMENTS

One of the unresolved questions in atmospheric research is the quantification of trace metals deposited on oceans despite several decades of research (Chance et al. 2015). There is a high variability in the atmospheric depositions of trace elements over the ocean surface, which reflects the heterogeneity of source areas and the periodic nature of dust emitting regions. The role of aeolian dust trace metal deposition in open marine ecosystems is complicated by bioavailability (solubility) of trace elements, which controls oceanic primary productivity rather than the total amount of mineral trace metals (Jickells et al. 2005). To illustrate the complexity, the example of iron is given: The bioavailable fraction of Fe deposited in oceans is not well known, but it is usually regarded as the portion of iron in Fe (II) phase or the labile

iron fraction (e.g. Mahowald et al. 2005; Zhu et al. 1997). However, Fe (III) may also be bioavailable (Barbeau et al. 2001) and Fe (II) might not always be bioavailable (Visser et al. 2003). Therefore, many have used soluble iron as a proxy for bioavailable iron. The consensus is that depending on the biological community and timescale, almost all incoming iron may ultimately become bioavailable (Weber et al. 2005).

Dust from different dust emitting regions tend to have varied mineral compositions, in some cases even in proximity. Mineral dust iron solubility for example varies from approximately 0.1% in prominent dust areas to roughly 80% in minor dust areas depending hugely on the source. There are various factors that essentially control the solubility and understanding them is very vital for quantifying soluble bioactive trace elements responses in open oceans (Baker & Croot 2010; Baker et al. 2006; Mahowald et al. 2008). Some of these controls can be the particle size of the aerosols, the mineralogical composition, speciation of the elements and residence time of the trace elements. Most studies have suggested that smaller particles have higher solubility (Baker & Jickells 2006).

The bioavailability of Fe is highly influenced by the geochemical concentrations and physical characteristics (e.g. particle shape forms, size, surface area) of the aerosols and the amount of time the particles are in the euphotic zone (Mahowald et al. 2003). The upper limit of the aerosol bioavailability is estimated as the water soluble Fe that passes through a 0.2 or 0.45 μm aerosol-laden filter when filtered with deionized water. Despite all these efforts there is still no compromise about which method produces an accurate value for calculating iron dissolution for in-situ seawater environment. Experimental methods used to determine the bioavailability of the trace elements also creates problems, as there appears to be no standard method to calculate the bioavailability. The solubility (proxy for bioavailability) measurements are also hugely affected by the extractant/solvent used to extract the trace elements (Shi et al. 2012). Researchers tend to differ in methods of different assessments in the link between the role dust in biological productivity and assessing how trace elements are dissolved in the ocean (Baker et al. 2006).

2.8 GEOMORPHOLOGY OF SOURCES

Most of the dust emissions are primarily associated with deserts, semi-arid deserts, dry lake beds and ephemeral channels, although regions with low vegetation cover and extreme soil moisture can also be natural sources (Table 2-3) (Choobari & Sturman 2014). Most of the global sources such as Bodélé Depression, Makgadikgadi Pan and Etosha Pan are identified as dry, ephemeral lakes in arid and semi-arid regions, where deep and extensive deposits of alluvial source material accumulated via fluvial inundation during Pleistocene (Prospero et al. 2002; Mahowald et al. 2005; Bryant et al. 2007). Anthropogenic disturbances of land, such as during coal combustion, ploughing and construction work can be additional sources of dust, although these sources are relatively small (Muhs et al. 2014) besides contributing to an increase in mineral dust in the atmosphere (Prospero et al. 2002).

Table 2-3 "Types of geomorphologies in terms of influences to dust emissions", reproduced from Bullard et al. (2011).

Geomorphic type	**Typical texture**	**Importance for dust emission**
Lakes		
Wet	Sand, Silt, Clay	Low
Ephemeral	Silt, Clay	High (if sandblasting)- Medium
Dry, consolidated	Silt, Clay	Low
Dry, non-consolidated	Silt, Clay	High (if Sand Blasting)-Medium
High Relief Alluvial Deposits		
Armoured, incised	Mega-gravel, Gravel, Sand	Low
Armoured, incised	Mega-gravel, Gravel, Sand	Low
Unarmoured, incised	Gravel, Sand, Silt, Clay	Medium
Unarmoured, unincised	Sand, Silt, Clay	Medium - High
Stony Surfaces	Gravel, Sand, Silt, Clay	Low
Sand		
Sand sheet	Sand	Low to medium
Aeolian sand dunes	Sand	Low to high
Loess	Silt, Clay	Low – medium
Low emission surfaces: bedrock, rocky slopes, duricrust, snow/ice permanent cover	Mega-gravel, Gravel, Sand, Silt, clay	Low

Other known dust emissions originate from glacial loess, hydrothermal vents and volcanoes. Due to micronutrient limitations in the Southern Ocean, those regions receiving very little atmospheric deposition are expected to respond intensely and are more sensitive to variations in the atmospheric deposition (Mahowald et al. 2005). Desert dust represents the largest source of both micro and macronutrients in the atmosphere to oceans (Mahowald et al. 2003).

2.9 STUDY AREAS

The four major dust-emitting sources in southern Africa used in this study are located in Namibia and Botswana (Figure 2-4). These study areas are predominantly ephemeral rivers and ephemeral saltpans that flood during the rain seasons. These areas where chosen because they are prominent dust sources and frequent emitters in southern Africa based on the number emissions observed via satellite (Vickery et al. 2013).

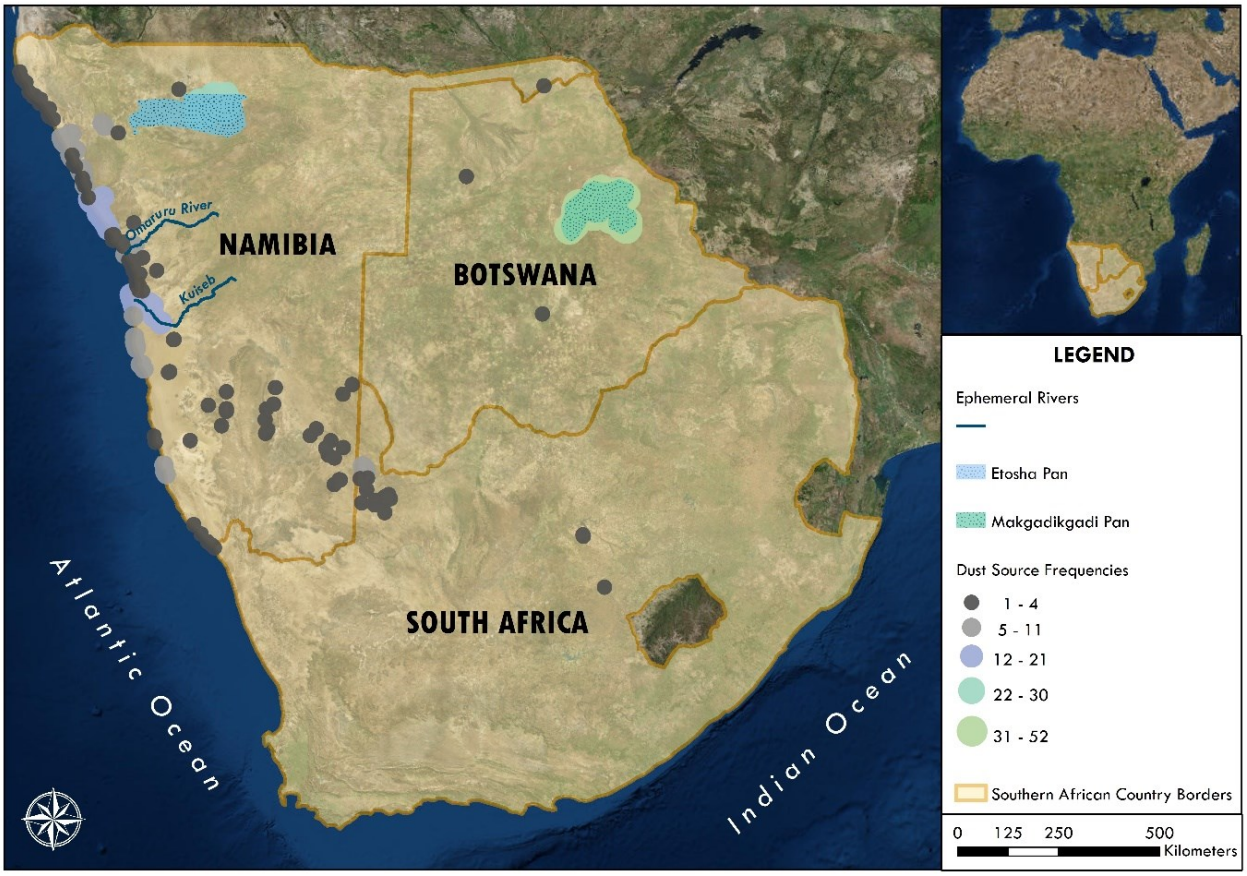

Figure 2-4 Location Map of the study area modified from Vickery et al. (2013).

The four major dust emitting sources for this study is Etosha Pan, Makgadikgadi Pan, Kuiseb river and Omaruru river. As seen in Figure 2-4 the Makgadikgadi Pan is situated in Botswana and the Etosha Pan is situated in Namibia.

2.9.1 Etosha Pan

Etosha Pan is located in the northern central part of Namibia, while the pan is situated on the far east portion of Etosha National Park in a region which is predominantly dry. Etosha Pan forms part of the Etosha basin and is situated in the southern part underlain formations and surrounded by the Kalahari Group sediments (Thomas & Shaw 1991). The Etosha Basin forms a portion of the interior depo-centre in the Kalahari Basin lying as the north-western outlier (Bryant 2003). Etosha Pan covers surface area of almost 6000 km^2 and is the centre of an ancient low lying ephemeral pan that drains sediments and water in its interior from northern Namibia and Southern Angola above the mountainous highlands (Bryant 2003).

A wide-ranging network of ephemeral waterways extent from the northern part of Namibia (commonly referred to as oshanas or omurambas) and supplies waters and sediments into the Etosha Pan. During the rainy season, this flow of water and sediments leads to shallow flooding in Etosha Pan (Bryant 2003). During the dry seasons, these deposited sediments from the northern regions can provide substantial dust material. The Etosha Pan is regarded as one of the most dynamic dust emitting regions in the Southern Hemisphere as rainfall varies largely from year to year, ranging from lower than 300 mm to above 500 mm (Bryant 2003). On average, yearly rainfall fluctuates between 400 and 450 mm (Bryant 2003). The majority of the precipitation occurs during the summer months from October to April (Bryant 2003). Therefore, most of the deflation occurs during the winter months when it is extremely dry and dust plumes frequently occur between August and October (Prospero et al. 2002).

Figure 2-5 *The dry salt pan of Etosha, which has regular dust emissions between August and December. (Credit: Alchemist-hp).*

2.9.2 Makgadikgadi Basin

The Makgadikgadi basin is located in the hot and dry central region of Botswana (20 –21.50°S and 24.5 –26.50°E), with a surface area of approximately 37,000 km^2, and comprises a range of morphological features such as fluvial, lacustrine, and aeolian (Bryant et al. 2007). The basin forms part of the larger Lake Paleo-Makgadikgadi, linked with the Makgadikgadi-Okavango-Zambezi (MOZ) rift, and is characterized as one of the major paleo-lakes in Africa (White & Eckardt 2006). Makgadikgadi basin is regarded as amongst the largest arid zone, saline, inland pan systems in the world (Eckardt et al. 2008). The Makgadikgadi pans covering 6000 km^2, lie in the north of the central part of Botswana, below a height of about 945 m (Thomas & Shaw 1991). From all sides the land slopes gently down towards them, though to the west there is a link along the Boteti river to the trough occupied by the Okavango Delta (Cooke 1979).

The Makgadikgadi Basin confines Sua Pan in the east and Ntwetwe Pan in the west but there are also numerous smaller pans as notable emitters (Figure 2-6). The Makgadikgadi Basin along with the Etosha Basin has regularly been regarded as being part of the 10 most significant global mineral dust emitters in numerous recent studies (Washington et al. 2003). The Makgadikgadi ephemeral lakes are consequently recognised as major mineral dust emitting regions in southern Africa (Vickery 2014; Prospero et al. 2002). There is quite a mystery as to what controls sediment supply and availability for dust emission in the basin, although it has

been presumed that flooding and drying processes may play an important part (Bryant et al. 2007).

Figure 2-6 *The Makgadikgadi Pan which is dry salt pan with emissions also attributed by anthropogenic activities* (Credit: Travel Butlers).

2.9.3 Kuiseb River

The Kuiseb River is located on the central Namib coastline, and has a catchment encompassing an area of 15,500 km^2 (Jacobson et al. 1995). Its drainage system, which is a component of the Namib Atlantic drainage, rising in the Khomas Highlands to flow through the central Namib Desert and extending towards the coast close to Walvis Bay (Marker 1977). This westerly flowing ephemeral river crosses the width of the Namib Desert (Jacobson et al. 1995) (Figure 2-7). The furthest point of the river lie at 2280 m above sea level with an average rainfall of 335 mm yr^{-1} (Botes et al. 2003) but only 5% of the entire catchment receives more than 300 mm yr^{-1} (illustrating how dry the river can get) and only 52% more than 100 mm yr^{-1} (Jacobson et al. 1995). The lower part of the river, close to the ocean receives less 20 mm of rainfall, an area which cuts through the central Namib Desert (Srivastava et al. 2006). Very little surface water reaches the coast, being absorbed by the deep sands of the lower river bed, adjoining dunes and the delta area (Huntley 1985).

The catchment is divided into four geomorphological units, namely being the gravel plains, delta, river channels and associated flood plains and the Namib Sand Sea (Vickery & Eckardt 2013). The sources of the Kuiseb River rise to the west of Windhoek on the Khomas Hochland. The Hochland is an extensive mica schist plateau of 800 to 2033 m with well-preserved remnants of the original planation surface (Huntley, 1985). Dust plumes in this river are usually linked with the lower part of Kuiseb River, which is extents from the end of the bedrock canyon at Natab and the Kuiseb River towards the Atlantic Ocean (Vickery & Eckardt 2013). The Kuiseb River has been recognized as the dustiest river in southern Africa, which is usually influence by summer floods and dry conditions in winter (Eckardt & Kuring 2005; Vickery et al. 2013). Van Holt (2013) pointed out that this is mainly due to recent human-induced disturbances of the surface have played a part in the production of dust, increasing tourism exhibitions (off-road driving), mining activities, communal livestock farming practices which leads to surfaces being disjointed and produce dust emissions. Most of the dust emissions recorded from 2005-2008 by Vickery et al. (2013) appeared to be originating from the delta and river channel.

Figure 2-7 *Portion of the Kuiseb River showing the different ecosystems that are cross-cut by the river* (Credit: Mporta)

2.9.4 Omaruru River

The Omaruru River is a major river that cuts through the Khomas, Otjozondjupa and Erongo regions of the western central part of Namibia extending from east to west (the western section goes into the Atlantic Ocean). The river initiates in the Etjo Mountains, and flows through the city of Omaruru and extends towards the Atlantic Ocean a few kilometres north of Henties Bay (Figure 2-8). It is one of the ephemeral rivers with low yearly run-off of approximately 40 million m^3. Its paleo-channels form an underground delta of the Namib Desert. The total catchment of the Omaruru River covers an area of 15,700 km^2 and reaches an altitude of 1450 m above sea level (asl) with a peak area at 2100 m asl (Geyh & Ploethner 1995). The mountainous region of the catchment above 100 m asl receives an average yearly rainfall of between 200 and 450 mm. The Omaruru sediments contain up to 10% palygorskite (Heine & Völkel 2010). Omaruru River mainly drains sediments of highly metamorphosed rocks from the Damara Inland Branch, which is widely exposed of granites, granitoid fragments and feldspatho-quartzose (Garzanti et al. 2014). There are frequent dust plumes observed along the river during the winter months (Figure 2-8). Dust emissions appear to have been enhanced by anthropogenic modifications along the river such as the construction of the Omaruru Dam in the area.

Figure 2-8 *The Omaruru River with dust plumes off into the Atlantic Ocean* (Credit: Kaukurauee Kangueehi).

CHAPTER 3:

DETERMINING DUST TRANSPORT PATHWAYS FROM SOUTHERN AFRICA MAJOR DUST SOURCES USING HYSPLIT

NOTE: A presentation of the prepared research paper:

This research manuscript will be prepared for a journal submission. I am the lead author on the work and Dr Susanne Fietz, Prof. Alakendra Roychoudhury and Prof Frank Eckardt are co-authors.

I was responsible for data compilation, written work and the creation of all diagrams. My co-authors mainly played a supervisory role in developing this chapter.

DETERMINING DUST TRANSPORT PATHWAYS FROM SOUTHERN AFRICA MAJOR DUST SOURCES USING HYSPLIT

K. Kangueehi [a], S. Fietz [a], A. N. Roychoudhury[a], F. D. Eckardt [b],

[a] *Earth Science Department, University of Stellenbosch, South Africa*

[b] *Environmental and Geographical Science Department, University of Cape Town, South Africa*

ABSTRACT

Southern African dust sources are known to be active, but there are few simulation studies that can be used to assess their impacts on oceans and terrestrial regions. Hysplit modelling software is used to produce seasonal pathway directions of the air masses trajectories from southern Africa`s most active dust sources for the period between January 2005 to December 2008. Trajectories were calculated forward for ten days from the four major sources: Kuiseb River, Omaruru River, Makgadikgadi Pan and Etosha Pan. The results showed that air masses originating from southern Africa could provide trace elements to open oceans, depending on the season. During winter, air masses from Makgadidkgadi dominantly travel towards the Indian Ocean, and extend all the way to Australia and Antarctica. Air mass along the Namibian coastline appear to travel towards the North West direction, potentially affecting the northern coastal areas of Angola, Gabon and extending as far as Ghana. Dust from interior sources such as Etosha Pan and to a lesser extent Makgadikgadi Pan can also affect regions such as terrestrial regions such Congo forest, Zambia, Zimbabwe and far off to Malawi. Consequently, emissions from southern African can alter geochemical, biological, atmospheric processes and a wider range of ecosystems than previously thought. However, there are additional factors which influence the impact of the dust on oceanic regions such as chemical transformations during transport, solubility, the receiving environment and particle size distribution. Most emissions occur during winter seasons when there is minimum light for photosynthesis, hence not stimulating primary productivity. Emissions in summer are much less, probably due to precipitation which can limit dust emissions. Our findings highlight the importance of additional research and more field based observations to approve the travelling of mineral dust in the regions recorded in this study.

3.1 INTRODUCTION

The need to understand and study the role of long distance transport of dust on environments is significant because dust is capable of reducing visibility, affect the air quality, soiling properties, affecting cloud formations and carry diseases (Chan & Simpson 1997; Chan et al. 1999). Some future climatic predictions show that many parts of the world will experience longer and deeper droughts seasons (particularly southern Africa) meaning dust plumes will become more prominent and hence the need to study them (Mahowald & Luo 2003). The role of mineral dust particles on ocean productivity, climate and terrestrial ecosystems is hugely influenced by the physical and chemical properties of individual particles (Prospero & Mayol-Bracero 2011).

Using remote sensing techniques such as satellites and other ground based observations has greatly increased our ability to study dust plumes and aerosols (Prospero et al. 2002). Satellite remote sensing observations provide an overview of how dust particles are distributed globally worldwide (e.g. Prospero et al. 2002; Remer 2006). Preliminary work in this project used remote sensing techniques to detect dust emissions in southern Africa. Regions which show persistent and large dust plumes have been identified and can be plotted with satellites and high-flying aircraft techniques (Washington et al. 2003; Prospero et al. 2002). The fact that satellite remote sensing tools are widely distributed across the globe gives it an advantage in terms of investigating mineral dust aerosols on a spatial and temporal distribution scale. Dust emissions are highly irregular in nature and especially in regions near to the sources (Spokes et al. 2001). The widespread study using TOMS images, provides a picture of major dust emitters, highlighting the importance of satellites in dust observations (Prospero et al. 2002). Other techniques such as a combination of aerosol ground based dimensions with MODIS and OMI makes it distinctive that it is possible to locate the presence and the type of aerosol at high spatial resolution (Gasso & Stein 2007). All these new advances in remote sensing technologies have led to an improved knowledge of modelling long range dust pathways over the oceans, which was not possible in the past. In addition to remote sensing, Hysplit has been extensively utilised in a range of models relating the transport, scattering and interaction of suspended aerosols (both natural and human induced pollutions) (Stein et al. 2015).

Most of the dust emissions in Southern Hemisphere are associated with small areas as "hot spots" rather than large uniform areas (Gillette 1999), which illustrates the importance of investigating areas at a smaller scale. Aerosol production over southern Africa particularly lies between the latitudes of approximately 15° S and 30° S and undergoes seasonality. Bhattachan et al. (2012) has highlighted the importance of the Southern Kalahari as a probable new dust emitting region in southern Africa, while Bryant et al. (2007) emphasized the potential environmental factors presently affecting dust plumes from these sources. Analysis of satellite images has recently shown that ephemeral rivers from Namibia can be potential dust plume sources (Vickery & Eckardt 2013). Westerly winds appear to predominate in the Southern Hemisphere, while mineral and volcanic dust sources in southern South America and Australia are regarded to be the leading sources of mineral dust contributions to the South Atlantic (Gaiero et al. 2003; Li et al. 2008). Similar studies in southern Africa are missing.

Between the period of January 2005 and December 2008, Vickery and Eckardt (2013) recorded a total number of 327 dust plumes (Figure 3-1). These dust plumes were recorded from 101 locations meaning some of the locations recorded multiple dust plumes during the monitored period (Table 3-1). These dust plumes were mainly derived from ephemeral lakes, dry pans, mine tailings, dry river beds and valleys around southern Africa. Previous work conducted by Vickery et al. (2013) enabled us to clearly identify dust plume sources in southern Africa. Four dust plume sources were the prominent dust emitting sources namely being Etosha Pan, Kuiseb and Omaruru River in Namibia as well as the Makgadikgadi Pan in Botswana (Figure 3-1). Hysplit modelling has been used extensively in the Patagonian desert (Gasso & Stein 2007; Johnson et al. 2011) and Lake Eyre (McGowan & Clark 2008) to understand dust long range transport from sources, but similar studies are still missing in southern Africa. Using Hysplit, this paper aims at investigating air masses, whether it can transport essential nutrients to different oceanic regions such as the Indian, Southern and West Atlantic Oceans, and in which season this would happen.

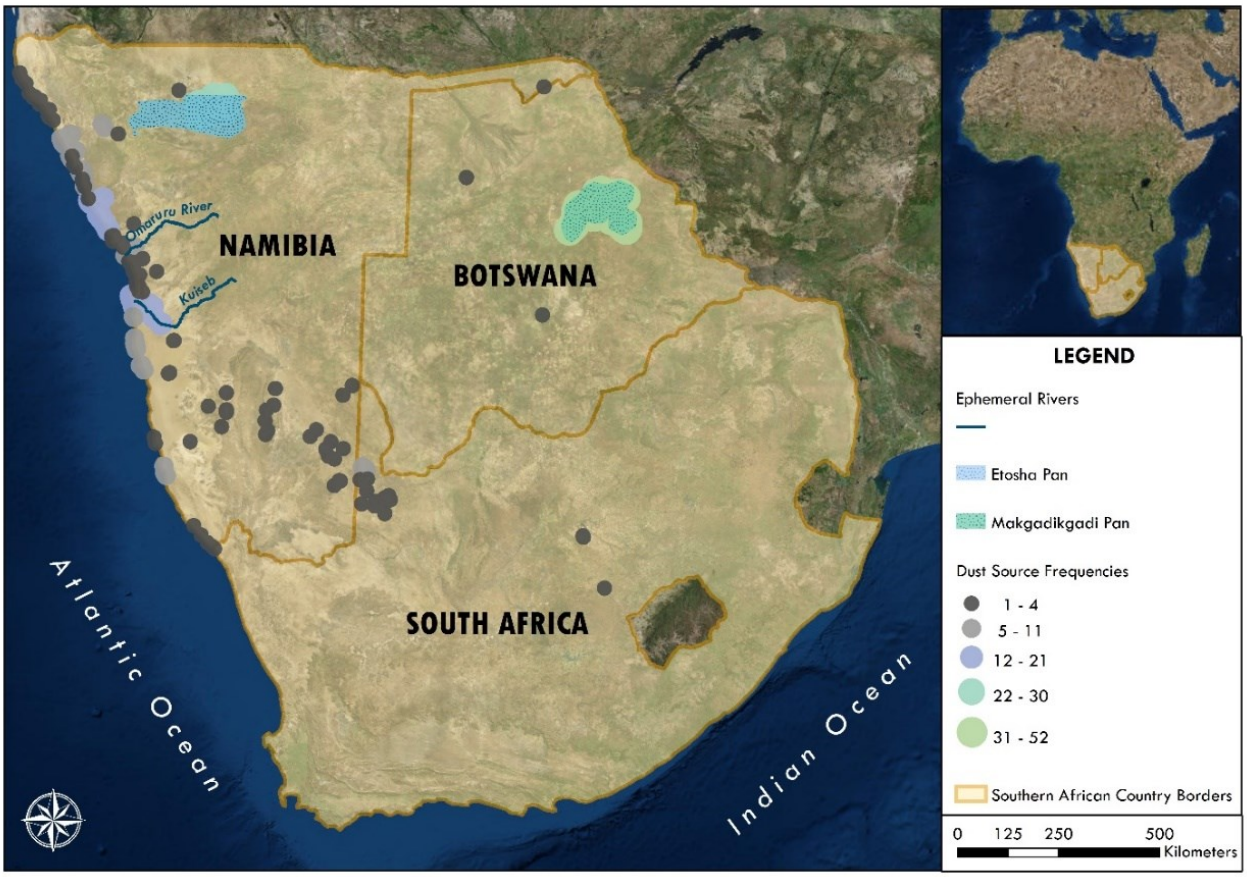

Figure 3-1 Location Map of the sampled areas with the ephemeral rivers and pans (Vickery et al. 2013).

3.2 METHODOLOGY

3.2.1 HYSPLIT

The Hysplit modelling software was used to determine forward trajectories calculations from the southern African regions. The Hysplit-web (internet-) based option was selected, with the Run Hysplit Trajectory Model (no registration required) option selected. The 'compute archive option' was selected to meet the aims of this study. The following step was to select the number of trajectory starting locations; for this study one starting location was selected, while the type of trajectory selected was 'normal'. After choosing these options, the next section was to select 'Meteorological and Starting Locations'. For meteorology, the GDAS (1 degree, global, 2006-present) option was selected. The GDAS option has previously been used in similar studies such as by Ashrafi et al. (2014), McGowan & Clark (2008) and Bhattachan et al. (2012).

The source location data that was used is provided in Table 3-1, reproduced from Vickery et al. (2013). After selecting these variables, the next option was to choose the archived meteorological file, which is the date when the dust emission was observed from Table 3-1. Once this has been selected, next step was to select the 'Model Parameters' options. Trajectory direction was forward, vertical motion option chosen was the default "Model vertical velocity" that utilises the perpendicular velocity field from the meteorological data. The starting time was selected as 12:00 for all the emissions. Total run time selected was 240 hours (10 days), with a maximum number of trajectories selected to be one. Reproductions of dust in the existing generation of dust models show large variances in their wet and deposition lifetimes that range from 56 days (Ginoux et al. 2001) to 10 days (Mahowald et al. 2002), which shows that there needs to be more work done to reduce the discrepancies. Hysplit has formerly been used widely to calculate both forward and backward trajectories extending from a few hours to up to two weeks (Stein et al. 2015; Ashrafi et al. 2014; Mcgowan & Clark 2008; Gasso & Stein 2007).

The different level heights chosen where 500 m for level 1, 1000 m for level 2 height and 1500 m for level 3 height. In terms of the display options, GIS output of contours was selected as Google Earth (kmz) and GIS shapefiles. The rest of the options were left as default settings, although no labels option was selected. Then the trajectory request option was selected in order for the trajectory to be calculated. Under the Hysplit trajectory model results section, the results can be saved in several options such as either Graphics Interchange Format (GIF), Portable

Document Format (PDF) and Keyhole Mark-up Language Zipped (KMZ) files. For this study, the files were saved as pdf and kmz files. The Hysplit modelling software steps are illustrated in more detail in Appendix A.

The created files in Hysplit where then exported as shapefiles and Keyhole Mark-up Language (KML) files which were then imported into ArcMap. All the exported shapefiles were then combined into one file based on the season and dust emitting location. New shapefiles were formed by selecting data from each location to analyse the trajectory paths. Kernel density analysis were created on different selected seasons and locations utilizing a search range of 10 km, which then created an even curved raster surface. A similar approach was conducted by McGowan & Clark (2008) on air mass from the Australian continent. The images produced displayed a raster image of the number of trajectory hits per 10 km^2. For the different seasons, all the dust emissions observations were used from Table 3-1. In terms of the density maps, the different heights were merged into a single shapefile to produce the maps for the different seasons and sources.

Table 3-1 The recorded observed dust emissions in southern Africa between Jan 2005 to December 2008 (Vickery et al. 2013)

Source Name	Source Type (PRU)	Longitude	Latitude	Year	Month	Day
18 Latitude Pan	Pan	11.8239	-17.9889	2007	5	11
18 Latitude Pan	Pan	11.8736	-18.1267	2007	7	14
Bloemfontein	Dam Margin / Agricultural	26.3763	-29.0453	2006	12	2
Cape Cross Pan	Pan	13.9486	-21.6712	2007	5	12
Cape Cross Pan	Pan	13.9610	-21.6834	2008	8	10
Cape Cross Pan	Pan	13.9767	-21.6932	2006	7	1
Cape Cross Pan	Pan	13.9856	-21.7198	2007	7	15
Cape Fria Pan	Pan	11.9627	-18.2240	2007	5	11
Cape Fria Pan	Pan	11.9658	-18.2209	2007	7	14
Cape Fria Pan	Pan	12.0351	-18.4435	2007	7	14
Conception Bay Pan	Pan	14.4873	-23.9419	2007	5	11
Conception Bay Pan	Pan	14.4890	-24.0572	2007	7	15
Conception Bay Pan	Pan	14.4925	-23.9862	2007	7	2
Conception Bay Pan	Pan	14.4946	-24.0882	2006	7	1
Conception Bay Pan	Pan	14.4969	-24.0838	2008	8	11
Conception Bay Pan	Pan	14.5070	-24.0621	2006	6	30
Conception Bay Pan	Pan	14.5262	-24.1480	2007	7	3
Conception Bay Pan	Pan	14.5307	-24.1991	2005	7	7
Conception Bay Pan	Pan	14.5364	-24.1654	2007	5	22
Donavan se Pan	Pan	20.2765	-27.2497	2005	6	23
Donavan se Pan	Pan	20.2768	-27.2556	2006	7	1
Duwisib River	River	16.2985	-25.4598	2005	9	13
Etosha	Pan	15.9747	-18.8222	2008	8	10
Etosha	Pan	16.0038	-18.7941	2006	5	22
Etosha	Pan	16.0089	-19.0265	2005	9	15
Etosha	Pan	16.0121	-18.8197	2007	5	6
Etosha	Pan	16.0288	-18.9870	2005	9	14
Etosha	Pan	16.0312	-18.6828	2007	1	1

Etosha	Pan	16.0360	-18.9642	2008	8	5
Etosha	Pan	16.0473	-18.8064	2007	9	18
Etosha	Pan	16.0524	-18.8492	2007	7	13
Etosha	Pan	16.0788	-18.9116	2007	1	1
Etosha	Pan	16.1179	-18.9901	2007	10	20
Etosha	Pan	16.1433	-18.9822	2007	6	5
Etosha	Pan	16.1681	-18.8848	2007	7	4
Etosha	Pan	16.1761	-18.8445	2007	9	18
Etosha	Pan	16.1970	-18.8562	2008	8	10
Etosha	Pan	16.2034	-18.7675	2005	11	13
Etosha	Pan	16.2451	-18.8035	2007	8	25
Etosha	Pan	16.3372	-18.8281	2007	6	27
Etosha	Pan	16.3592	-18.5345	2005	10	15
Etosha	Pan	16.3909	-18.5776	2007	6	5
Etosha	Pan	16.4958	-18.6298	2005	11	12
Etosha	Pan	16.5350	-18.7647	2005	7	6
Etosha	Pan	16.5980	-18.8665	2007	9	18
Etosha	Pan	16.6299	-18.6676	2007	6	10
Etosha	Pan	16.6300	-18.6061	2005	8	26
Etosha	Pan	16.6326	-18.6381	2005	10	15
Etosha	Pan	16.6361	-18.8770	2007	9	18
Etosha	Pan	16.6455	-18.5335	2008	5	12
Etosha	Pan	16.6512	-18.7266	2005	10	15
Etosha	Pan	16.6525	-18.6404	2005	9	14
Etosha	Pan	16.6959	-18.6709	2007	6	23
False Cape Fria	Pan	12.1360	-18.5472	2005	7	9
False Cape Fria	Pan	12.1589	-18.5541	2008	4	4
False Cape Fria	Pan	12.1708	-18.5246	2007	5	11
Fish river	River	17.7340	-25.5253	2007	5	19
Gamanas Pan	Pan	17.7223	-26.0673	2007	5	19
Gamanas Pan	Pan	17.7733	-25.9809	2007	5	19

Gannapan / Bloemhofdam	Pan	25.7197	-27.9426	2006	12	3
Gannapan / Bloemhofdam	Pan	25.7316	-27.9695	2006	12	16
Gemsbokbrak	Pan	20.4850	-27.5815	2005	6	23
Gemsbokhoorn	Pan	20.5040	-27.4804	2005	6	23
Grasheuwel Pan	Pan	18.8260	-26.0909	2007	5	19
Groot - Witpan	Pan	20.7500	-27.7485	2006	7	1
Groot - Witpan	Pan	20.7504	-27.7426	2005	6	23
Groot - Witpan	Pan	20.7509	-27.7357	2007	5	19
Grundorner	River	17.9065	-25.4129	2007	6	25
Grundorner	River	17.9403	-25.0421	2007	5	19
Gui uin	Other - marsh / vlie	12.9629	-19.3922	2008	4	22
Gui uin	Other - marsh / vlie	12.9925	-19.3930	2006	6	30
Gui uin	Marshes / Vlei	13.0081	-19.3767	2005	9	27
Gui uin	Marshes / Vlei	13.0113	-19.3761	2007	10	8
Gui uin	Other - marsh / vlie	13.0210	-19.3951	2007	8	8
Gui uin	Other - marsh / vlie	13.0349	-19.3887	2006	5	22
Hakskeenpan	Pan	20.1438	-26.7284	2005	6	23
Hakskeenpan	Pan	20.1849	-26.8422	2005	6	23
Hakskeenpan	Pan	20.1901	-26.8417	2006	7	1
Hakskeenpan	Pan	20.1993	-26.8226	2007	5	19
Hakskeenpan	Pan	20.2131	-26.7655	2007	6	25
Hakskeenpan	Pan	20.2410	-26.8529	2007	5	19
Haseweb River	River	16.7403	-25.1521	2007	5	19
Helmering River	River	16.6351	-25.9172	2005	9	13
Hoanib	River	12.7660	-19.4655	2005	7	9
Hoanib	River	13.7420	-19.1560	2007	7	13
Hoanib	River	13.8017	-19.2317	2007	7	4
Hoanib Pan	Pan	12.7952	-19.5190	2007	5	11
Hoanib Pan	Pan	12.8031	-19.5469	2007	7	14
Hoanib Pan	Pan	12.8037	-19.5587	2005	7	9

Hoanib Pan	Pan	12.8047	-19.5524	2007	5	6
Hoanib Pan	Pan	12.8446	-19.6081	2008	4	4
Hoanib Pan	Pan	12.8458	-19.5986	2005	7	9
Hoarusib	River	12.5968	-19.0549	2006	5	22
Huab Pan	Pan	13.5782	-20.9375	2007	7	31
Huab Pan	Pan	13.5787	-20.9429	2008	4	22
Huab Pan 2	Pan	13.4269	-20.8584	2005	7	9
Huab Pan 3	Pan	13.4692	-20.8563	2007	7	31
Huab Pan 3	Pan	13.4755	-20.8604	2007	5	11
Huab Pan 4	Pan	13.4348	-20.8793	2006	5	22
Huab River	River	13.4580	-20.9124	2008	4	22
Huab River	River	13.4795	-20.8971	2008	6	29
Huab River	River	13.4990	-20.8960	2008	8	10
Huab River	River	13.5148	-20.8969	2007	5	6
Huab River	River	13.5208	-20.8833	2005	7	7
Huab River	River	13.5258	-20.8931	2006	6	30
Huab River	River	13.5391	-20.8873	2007	5	7
Huab River	River	13.6294	-20.8680	2007	7	15
Huab River	River	13.7397	-20.8163	2005	7	9
Hunkab Pan	Pan	12.9744	-19.8544	2007	5	11
Hunkab Pan	Pan	12.9761	-19.8710	2008	8	10
Hunkab Pan	Pan	12.9773	-19.8618	2006	5	22
Hunkab Pan	Pan	12.9815	-19.8742	2007	7	15
Hunkab Pan	Pan	12.9882	-19.8687	2007	5	6
Hunkab Pan	Pan	13.0197	-19.9438	2007	7	14
Hunkab River	River	13.0740	-19.7893	2006	6	30
Hunkab River	River	13.1356	-19.7543	2008	4	22
Ilhea Point	Pan	14.4584	-23.4621	2007	5	11
Ilhea Point	Pan	14.4753	-23.4871	2006	6	30
Isirub River	River	15.2070	-26.8061	2006	5	24
Isirub River	River	15.2276	-26.9606	2006	6	30

Isirub River	River	15.2678	-27.0209	2007	8	8
Kanibes River	River / Perennial Pan	17.7066	-25.7649	2007	5	19
Khan River	Near River	15.0275	-22.4568	2007	9	14
Khumib	River	12.4554	-18.8356	2005	7	9
Khumib	River	12.4705	-18.8393	2007	7	14
Khumib	River	12.4907	-18.8228	2007	5	12
Khumib	River	12.5029	-18.8180	2008	4	22
Kiriis Ost Pan	Pan	19.6577	-26.3360	2007	5	19
Klein - Aarpan	Pan	20.7283	-27.3982	2005	6	23
Koeipan	Pan	20.8736	-27.4298	2005	6	23
Koemkoep Pan	Pan	19.6004	-25.1452	2007	9	11
Koichab	River	15.8587	-26.2532	2005	9	13
Koigab Pan 1	Pan	13.3067	-20.5376	2007	7	15
Koigab Pan 1	Pan	13.3155	-20.3824	2007	5	7
Koigab Pan 1	Pan	13.3271	-20.5636	2007	5	11
Koigab Pan 1	Pan	13.3316	-20.5679	2005	7	9
Koigab Pan 1	Pan	13.3367	-20.5804	2007	5	12
Kongapan	Pan	20.7027	-27.4843	2006	7	1
Konkiep	River	16.7442	-25.5331	2007	5	19
Konkiep River	River	16.7471	-25.5941	2007	6	25
Koppieskraalpan	Pan	20.2847	-26.9954	2006	7	1
Kuiseb River	River	14.6233	-23.1678	2007	7	3
Kuiseb River	River	14.7960	-23.3424	2008	8	11
Kuiseb River	River	14.8214	-23.2073	2007	5	12
Kuiseb River	River	14.8529	-23.2031	2006	6	30
Kuiseb River	River	14.8657	-23.3576	2007	5	12
Kuiseb River	River	14.8660	-23.3509	2008	8	11
Kuiseb River	River	14.9197	-23.2528	2008	8	9
Kuiseb River	River	14.9531	-23.4728	2008	8	9
Kuiseb River	River	15.1315	-23.6238	2005	7	9
Kuiseb River Delta	Other - Delta	14.4045	-23.0023	2007	7	2

Kuiseb River Delta	Other - Delta	14.4256	-23.0702	2008	4	21
Kuiseb River Delta	Other - Delta	14.4733	-23.1509	2008	6	16
Kuiseb River Delta	Other - Delta	14.4758	-23.1997	2006	7	1
Kuiseb River Delta	Other - Delta	14.4761	-23.0776	2007	7	15
Kuiseb River Delta	Other - Delta	14.4831	-23.1629	2006	6	30
Kuiseb River Delta	Other - Delta	14.4946	-23.0944	2007	7	2
Kuiseb River Delta	Other - Delta	14.4963	-23.1107	2008	4	21
Kuiseb River Delta	Other - Delta	14.5126	-23.3073	2007	5	23
Kuiseb River Delta	Other - Delta	14.5191	-23.1123	2007	5	7
Kuiseb River Delta	Other - Delta	14.5217	-23.1090	2007	6	17
Kuiseb River Delta	Other - Delta	14.5381	-23.1186	2008	4	22
Kuiseb River Delta	Other - Delta	14.5742	-23.1297	2005	7	9
Kuubmaansvlie	Pan	19.2181	-26.3619	2005	6	23
Lake Ngoni	Lake Margin	22.3484	-20.1964	2005	9	27
Langer Werner	River	14.2221	-21.9059	2005	7	9
Linyandi Marshlands	Marshes / Vlei	24.0557	-18.1099	2005	10	7
Magkadikgadi	Pan	24.9953	-20.8986	2005	8	4
Magkadikgadi	Pan	25.0057	-20.6928	2007	11	13
Magkadikgadi	Pan	25.0463	-20.7840	2007	9	21
Magkadikgadi	Pan	25.0463	-20.9155	2007	9	25
Magkadikgadi	Pan	25.1064	-20.9125	2007	11	13
Magkadikgadi	Pan	25.1153	-20.7123	2005	10	6
Magkadikgadi	Pan	25.3866	-20.8558	2007	11	14
Magkadikgadi	Pan	25.4272	-20.3866	2005	10	7
Magkadikgadi	Pan	25.5241	-20.3318	2005	10	10
Magkadikgadi	Pan	25.5284	-20.3896	2007	9	21
Magkadikgadi	Pan	25.9066	-20.4802	2005	9	14
Magkadikgadi	Pan	25.9123	-20.5336	2005	10	10
Magkadikgadi	Pan	25.9305	-20.4351	2007	9	11
Magkadikgadi	Pan	25.9783	-20.5532	2005	10	7
Magkadikgadi	Pan	25.9809	-20.4772	2005	10	6

Magkadikgadi	Pan	25.9881	-20.5507	2005	8	26
Magkadikgadi	Pan	26.0279	-20.4314	2007	7	2
Magkadikgadi	Pan	26.0337	-20.4013	2005	9	29
Magkadikgadi	Pan	26.0612	-20.4479	2005	7	9
Magkadikgadi	Pan	26.0761	-21.0887	2005	9	14
Magkadikgadi	Pan	26.1117	-21.1131	2007	8	8
Magkadikgadi	Pan	26.1789	-20.9990	2007	7	2
Makgadikgadi Pan	Pan	24.8352	-21.2393	2008	8	12
Makgadikgadi Pan	Pan	24.8824	-21.1936	2008	6	10
Makgadikgadi Pan	Pan	24.9379	-21.0902	2008	6	19
Makgadikgadi Pan	Pan	24.9487	-21.1159	2008	7	18
Makgadikgadi Pan	Pan	24.9725	-20.8251	2006	8	27
Makgadikgadi Pan	Pan	25.0085	-20.9393	2008	8	12
Makgadikgadi Pan	Pan	25.0287	-20.9158	2006	7	13
Makgadikgadi Pan	Pan	25.0352	-20.8459	2008	8	11
Makgadikgadi Pan	Pan	25.0552	-20.8693	2008	8	5
Makgadikgadi Pan	Pan	25.0626	-20.8782	2008	6	10
Makgadikgadi Pan	Pan	25.0639	-20.9244	2008	6	19
Makgadikgadi Pan	Pan	25.0695	-20.9035	2008	7	18
Makgadikgadi Pan	Pan	25.0884	-20.9152	2006	7	16
Makgadikgadi Pan	Pan	25.1870	-20.6734	2006	6	26
Makgadikgadi Pan	Pan	25.2420	-20.6794	2008	10	7
Makgadikgadi Pan	Pan	25.2750	-20.7093	2007	6	5
Makgadikgadi Pan	Pan	25.3898	-20.9108	2006	6	26
Makgadikgadi Pan	Pan	25.4745	-20.5870	2007	6	14
Makgadikgadi Pan	Pan	25.6096	-20.6256	2007	6	14
Makgadikgadi Pan	Pan	25.6354	-20.5339	2007	11	13
Makgadikgadi Pan	Pan	25.8027	-20.9555	2008	5	19
Makgadikgadi Pan	Pan	25.8606	-20.7350	2007	5	11
Makgadikgadi Pan	Pan	25.9507	-20.3554	2007	5	11
Makgadikgadi Pan	Pan	25.9958	-20.4969	2007	4	14

Makgadikgadi Pan	Pan	26.0151	-20.4342	2007	10	25
Makgadikgadi Pan	Pan	26.0987	-20.4455	2007	7	2
Makgadikgadi Pan	Pan	26.1116	-21.0455	2007	8	8
Makgadikgadi Pan	Pan	26.1685	-21.1293	2008	8	5
Makgadikgadi Pan	Pan	26.1695	-21.0825	2007	7	2
Makgadikgadi Pan	Pan	26.1759	-21.1421	2008	5	19
Makgadikgadi Pan	Pan	26.1864	-21.1086	2008	7	18
Marcel Pan	Pan	19.4628	-27.1659	2007	11	29
Meob Bay Pan	Pan	14.6217	-24.5596	2006	7	1
Meob Bay Pan	Pan	14.6552	-24.5470	2007	7	3
Meob Bay Pan	Pan	14.6613	-24.5928	2008	8	11
Meob Bay Pan	Pan	14.6680	-24.5528	2006	6	30
Meob Bay Pan	Pan	14.6684	-24.5529	2007	5	11
Meob Bay Pan	Pan	14.7176	-24.6617	2006	7	1
mine tailing	Anthropogenic	16.1486	-28.3398	2007	8	8
mine tailing	Anthropogenic	16.3134	-28.5093	2007	8	8
Morgenzon Pan	Pan	19.3413	-26.1945	2005	6	23
Noenieput	Pan	20.1648	-27.5505	2007	6	25
Omaruru River	River	14.2646	-22.0984	2008	4	21
Omaruru River	River	14.2700	-22.0994	2008	8	11
Omaruru River	River	14.3116	-22.0799	2007	8	8
Omaruru River	River	14.3117	-22.0654	2006	6	30
Omaruru River	River	14.3136	-22.0664	2007	5	12
Omaruru River	River	14.3155	-22.0634	2007	5	6
Omaruru River	River	14.3186	-22.0553	2007	7	2
Omaruru River	River	14.4877	-21.9024	2008	4	22
Omaruru River	River	14.4942	-21.9005	2007	7	15
Omaruru River	River	14.4949	-21.9026	2005	7	9
Omaruru River	River	14.5009	-21.9002	2006	7	1
Omaruru River	River	14.5115	-21.9004	2007	7	31
Ombonde	River	14.1229	-19.3737	2007	7	13

Onanzi Pan	Pan	15.5499	-18.4032	2006	6	20
Orange River	River	16.4924	-28.6412	2007	8	8
Oranjemund	Pan / Mine	16.4411	-28.5936	2006	11	6
Orawab	River	14.4806	-21.3869	2005	9	19
Quoxo River	River	24.3257	-23.1469	2005	10	3
Rock Bay	River	14.4687	-22.4634	2007	5	12
Rock Bay	River	14.4832	-22.4687	2006	5	22
Rocky Point	Pan	12.4776	-18.9554	2005	7	9
Rocky Point	Pan	12.4954	-18.9931	2005	7	9
Salt Pan	Pan	18.9748	-25.9386	2005	6	23
Salztal Pan	Pan	19.4414	-26.5754	2008	2	12
Samahaling Pan	Pan	19.5797	-27.0568	2007	11	29
Samahaling Pan	Pan	19.6098	-27.0602	2005	6	23
Saulstraatpan	Pan	20.0996	-27.0128	2005	6	23
Sechomib	River	12.2770	-18.6931	2008	4	4
Sechomib	River	12.3024	-18.6071	2005	7	9
Skemerhoek Pan	Pan	19.8195	-24.9260	2007	9	11
Swaartput se Pan	Pan	19.2907	-26.5136	2005	6	23
Swaartput se Pan	Pan	19.2952	-26.5165	2005	9	30
Swakop River	River	14.5338	-22.6812	2006	6	30
Swakop River	River	14.5435	-22.6817	2007	7	14
Swakop River	River	14.5663	-22.6864	2007	5	7
Terrace Bay 2	Pan	13.0568	-20.0576	2007	7	14
Terrace Bay 2	Pan	13.0698	-20.0710	2005	7	9
Terrace Bay 2	Pan	13.0791	-20.0782	2008	4	22
Terrace Bay 2	Pan	13.1093	-20.1141	2007	5	12
Torra Bay Pan	Pan	13.2609	-20.4143	2008	4	22
Torra Bay Pan	Pan	13.2672	-20.3816	2005	7	9
Torra Bay Pan	Pan	13.3155	-20.5481	2008	8	10
Toscanini Pan	Pan	13.4025	-20.8185	2005	7	9
Tsauchab River / Sossusvlei	River/Pan	15.3157	-24.7296	2005	11	14

Tsauchab River / Sossusvlei	River/Pan	15.3251	-24.7236	2007	5	22
Tsauchab River / Sossusvlei	River/Pan	15.3360	-24.7265	2008	4	21
Tsauchab River / Sossusvlei	River/Pan	15.3475	-24.7144	2007	7	2
Tsondab River/Pan	River/Pan	15.4383	-24.0005	2007	5	22
Tsondab River/Pan	River/Pan	15.4514	-23.9970	2007	8	7
Tumas River	River	14.6030	-22.8939	2007	7	2
Tumas River	River	14.6878	-22.9076	2008	8	11
Ugab Pan 1	Pan	13.6840	-21.2354	2008	8	10
Ugab Pan 1	Pan	13.6933	-21.2487	2007	5	7
Ugab Pan 1	Pan	13.7037	-21.2570	2007	7	31
Ugab Pan 1	Pan	13.7055	-21.2500	2008	4	22
Ugab Pan 1	Pan	13.7147	-21.2709	2006	6	30
Ugab Pan 3	Pan	13.7935	-21.3828	2007	8	8
Ugab Pan 3	Pan	13.7993	-21.3916	2006	5	22
Ugab Pan 4	Pan	13.8518	-21.4750	2006	5	22
Ugab Pan 5	Pan	13.8706	-21.5239	2005	7	9
Ugab River	River	13.6345	-21.1849	2007	7	31
Ugab River	River	13.6397	-21.1752	2007	7	15
Ugab River	River	13.6481	-21.1820	2006	6	30
Ugab River	River	13.6576	-21.1734	2005	7	9
Ugab River	River	13.6644	-21.1678	2007	5	7
Uniab River	River	13.1906	-20.1865	2007	7	15
Uniab River	River	13.1950	-20.1985	2008	8	10
Uniab River	River	13.1965	-20.1954	2006	5	22
Uniab River	River	13.1999	-20.1856	2006	6	30
Uniab River	River	13.2034	-20.1971	2007	7	31
Uniab River	River	13.2052	-20.1887	2007	7	14
Uniab River	River	13.2192	-20.2547	2007	5	12
Uniab River	River	13.2456	-20.2203	2008	4	22
Uniab River	River	13.2824	-20.1734	2008	4	4

Unknown 1	Unknown	13.0277	-19.8648	2005	7	9
Unknown 10	Unknown (river)	14.5535	-22.8007	2007	5	12
Unknown 11	Unknown river	14.5715	-22.7888	2008	8	10
Unknown 12	River	14.6024	-22.7832	2006	5	22
Unknown 13	River	14.6169	-22.5304	2007	5	6
Unknown 14	River	14.6948	-22.1677	2006	6	20
Unknown 15	River	14.5219	-22.5649	2006	6	30
Unknown 16	Pan	14.9655	-26.1560	2007	5	22
Unknown 17	Pan	14.9972	-26.2928	2006	6	30
Unknown 18	unknown	15.9597	-28.1290	2006	4	26
Unknown 2	River	14.2044	-21.8139	2005	7	9
Unknown 3	River	14.3571	-22.2255	2006	6	30
Unknown 4	Unknown (Poss river)	14.4225	-22.3247	2007	5	12
Unknown 5	River	14.5124	-22.2470	2006	6	30
Unknown 6	Unknown (River)	14.5380	-22.7163	2008	8	11
Unknown 7	Unknown (River)	14.5384	-22.7436	2006	6	20
Unknown 8	Unknown (River)	14.5442	-22.7294	2007	5	6
Unknown 9	Unknown (River)	14.5471	-22.7821	2005	7	9
Unknown River	River	14.0010	-21.6520	2006	6	30
Vrysoutpan	Pan	20.8294	-27.3382	2005	6	23
White Lady Salt Pan	Pan	13.9698	-21.7734	2007	5	12
White Lady Salt Pan	Pan	13.9873	-21.7767	2005	7	7

3.3 RESULTS

In terms of all the dust emissions that were observed between January 2005 to December 2008, 16% where from the Makgadikgadi Pans, 9% from Etosha Pan, 7% from Kuiseb River and 4% from Omaruru River (Figure 3-2). The other 64% is from various other smaller discrete sources which in all cases did not contribute more than 3% each.

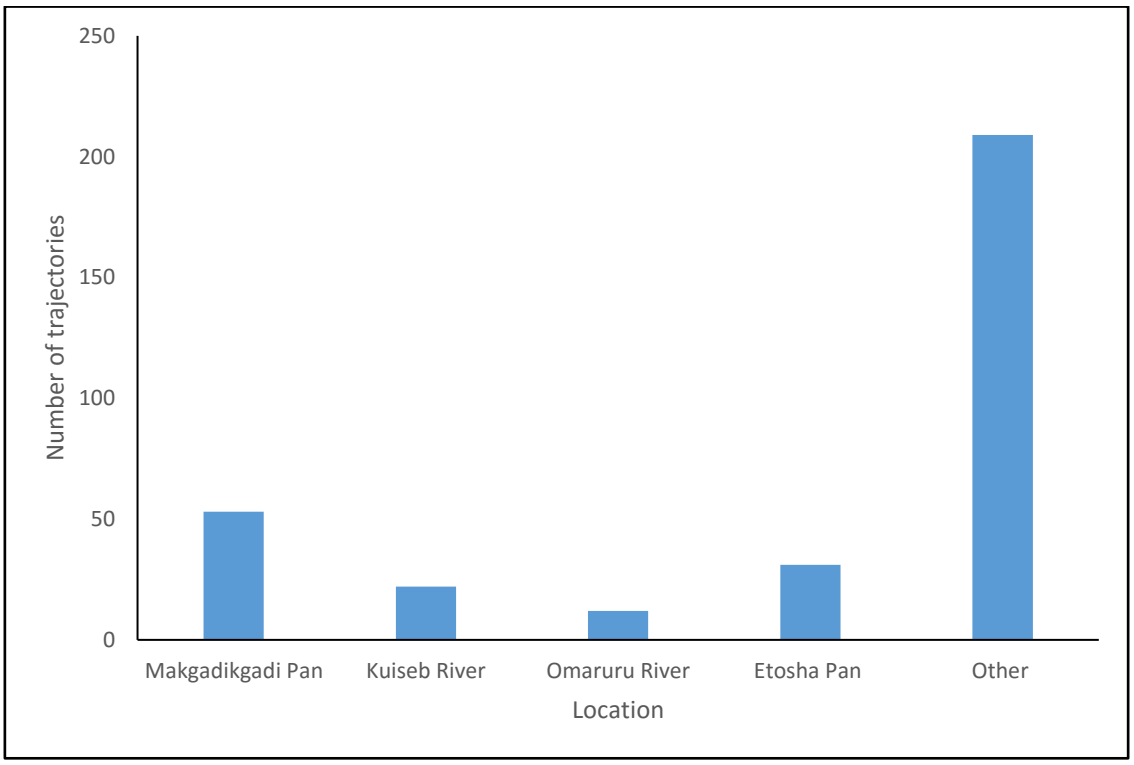

Figure 3-2 Dust emitting contributions from various locations in southern Africa between January 2005 to December 2008.

Trajectory maps presented in this section are from the chosen locations based on the variables used as discussed in the methods section. The maps for all the trajectories are presented in Appendix B, while what is displayed here are the trajectory maps for the chosen dust emitting sources and different seasons.

For the source locations only the chosen dust emitting sources were used in the Hysplit Model namely being Etosha Pan, Kuiseb river, Makgadikgadi Pan and Omaruru River (Figure 3-3), while for different seasons, all emissions from the sources were considered (Figure 3-4).

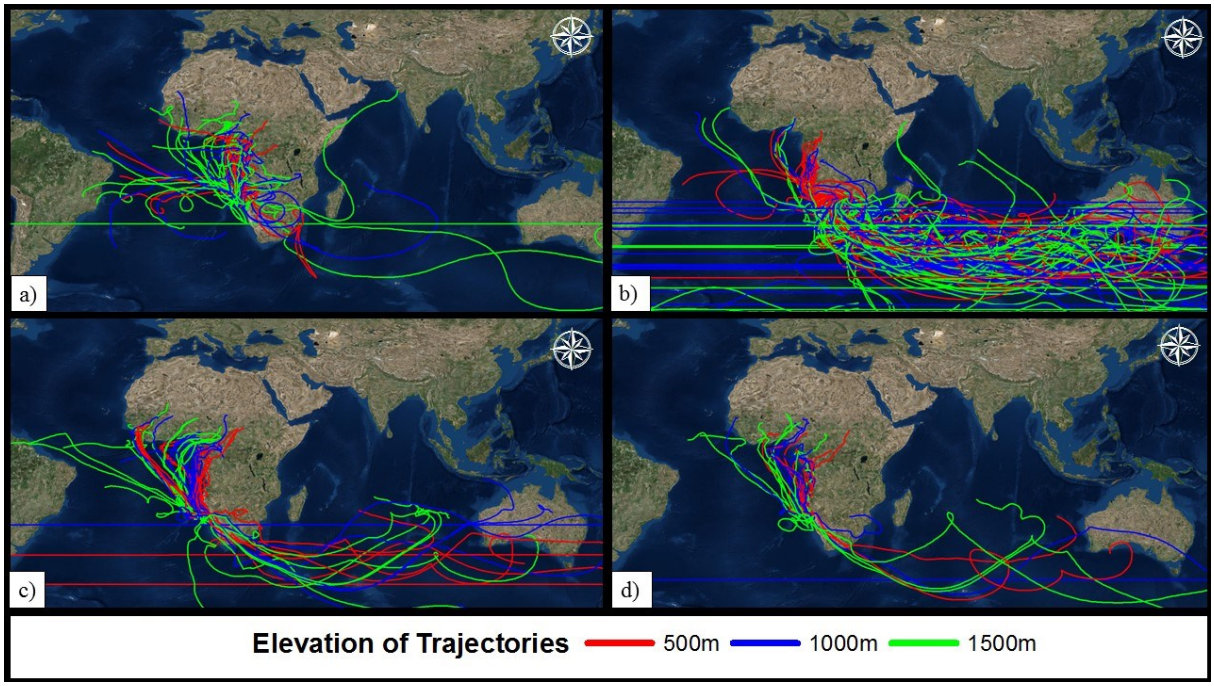

Figure 3-3 Hysplit modelled forward trajectories for the different dust emitting sources, with the different line trajectories representing different heights (a) Etosha Pan, (b) Makgadikgadi Pan (c) Kuiseb River and (d) Omaruru River for all the seasons.

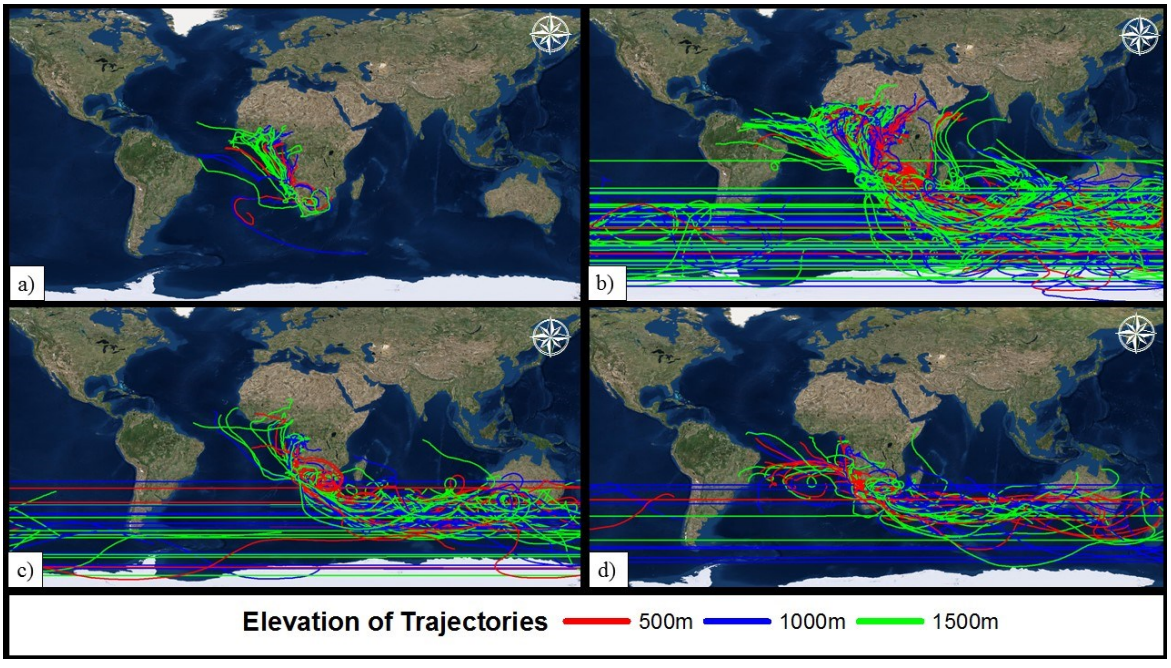

Figure 3-4 Hysplit modelled trajectories for the different seasons for all four selected dust emitting sources. The different line trajectories represent different heights (a) Autumn (1st Feb to 31st Apr), (b) Winter (1st May to 31st Jul) (c) Summer (1st Oct to 30th Jan) and (d) Spring (1st Aug to 30th Sep).

The modelled trajectories at the highest elevation tend to travel the furthest, while the trajectories from 500 m height does not travel as far from the source, although this was not consistent with all the trajectories. Some of the modelled trajectories recirculated and travelled long distances, which showed the high variability in the models (Figure 3-3). Individual trajectories are more challenging to interpret; hence these results were summarised into density maps for better interpretation which will be discussed in the next section. Most of the trajectories, sometimes from the same sources tend to travel in various directions based on the modelled initial height. Most of the dust emissions occurred from Makgadikgadi Pan, while the two ephemeral rivers had lower emissions (Figure 3-4).

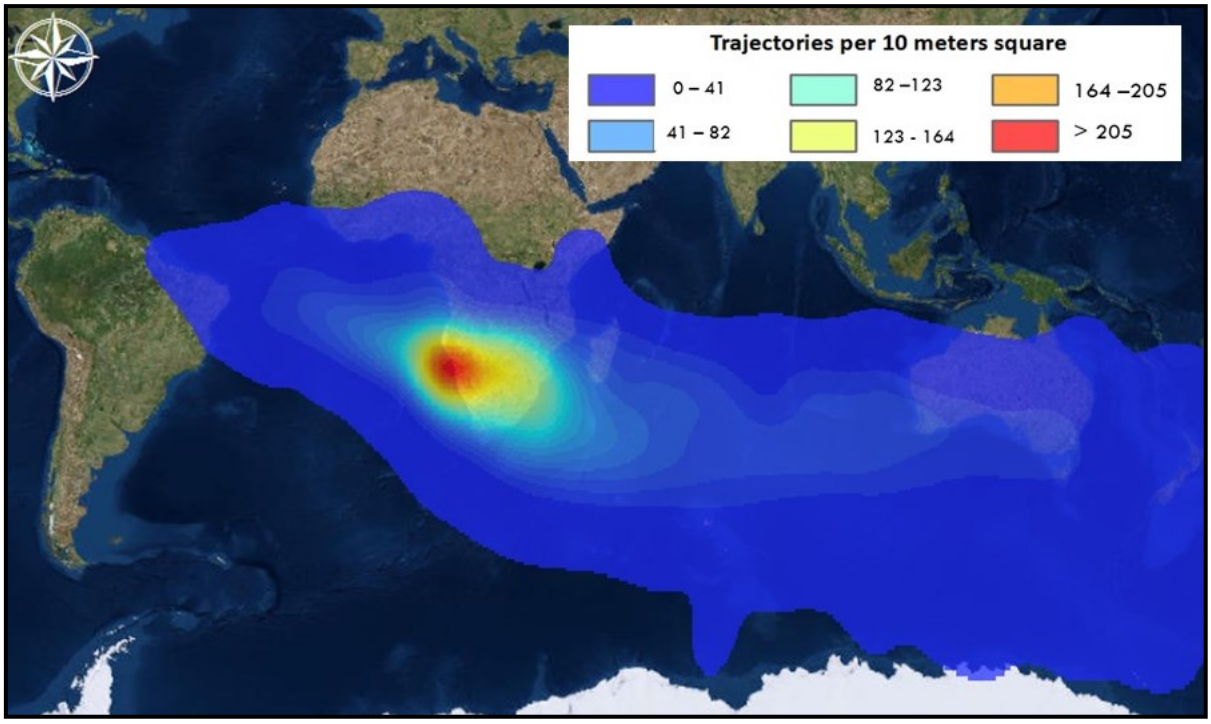

Figure 3-5 Plume frequency contours passing over the surface summarising all the modelled trajectories using the online Hysplit Modelling software between the period of 2005 to 2008 as observed by Vickery et al (2013), from the known dust plume sources in southern African.

Based on these chosen variables (as discussed in Section 3.2), of all the recorded 327 dust plumes modelled at the three different heights, 60% of the dust plumes travelled towards the north-west direction passing over the Benguela Current. Most of the trajectories travelled along the western coast towards the northern direction (Figure 3-5). The rest of the 40% trajectories travelled towards the southern oceans, with a substantial portion travelling towards the Indian Ocean (29%), while a lower portion travelled towards the western Southern Ocean (5%) (Figure 3-6).

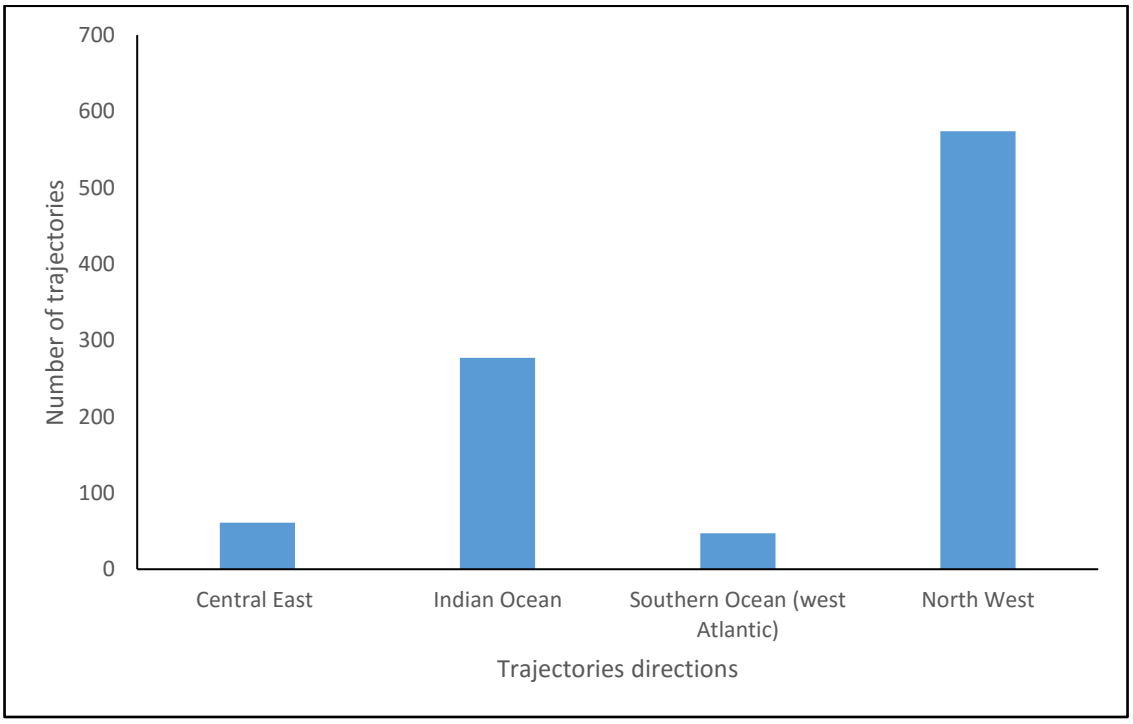

Figure 3-6 Air mass pathways directions from all the dust emissions in southern Africa between 1st January 2005 to 31st December 2008.

When analysing based on the different locations, from the 108 locations, 44 locations dust plumes predominantly travelled towards the north west while from the 57 locations (Table 3-1), even though dust plumes were mainly only individual dust plumes. Only less than 10 locations trajectories the travelled towards the Southern Oceans.

3.3.1 Locations

Density maps were created from the Hysplit models based on the four locations and the three trajectory elevations, where merged into a single shape file. The maps based on the locations will be presented in this section.

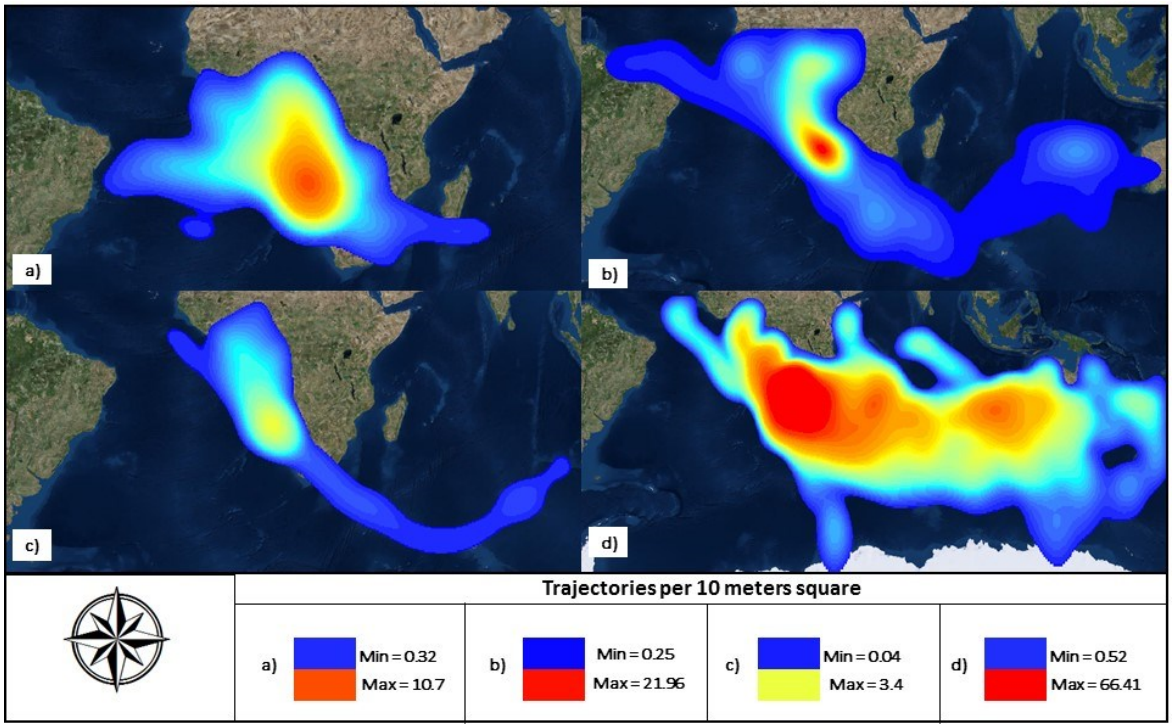

Figure 3-7 Trajectory density contours for all modelled trajectories for the dust emitting sources in the period between 2005-2008 (a) Etosha Pan, (b) Kuiseb River, (c) Omaruru River and (d) Makgadikgadi Pan.

3.3.1.1 Etosha Pan

About seven out of 33 (23%), of all dust emissions detected from Etosha travels towards the south, while 77 % travels towards the north and dominantly towards the north west. The largest number of trajectories are found on the eastern part of Etosha, but does affect the larger part of north western African region extending into the Atlantic Ocean (Figure 3-7). Only trajectories at heights of 500-1000 m (coloured in green and red) are capable of reaching the Indian Ocean and potentially the Southern Ocean (Appendix B). Trajectories in this layer are also capable of penetrating the south eastern part of African to countries such as Zambia, Mozambique and Zimbabwe with not many trajectories travelling beyond 30° S. Our models reveal that dust from

the Etosha Pan are more likely to fertilise the north western Atlantic Ocean than Indian or Southern Ocean.

3.3.1.2 Makgadikgadi Pan

A total of 52 dust emissions were detected from the Makgadikgadi Pans, with a mere 7% travel towards north western African region while the rest tends to migrate more towards the central and south eastern region. For the Makgadikgadi Pan, 44 of the modelled dust plumes travelled towards the southern oceans, predominantly the Indian Ocean. Eight of the projections travelled towards the north west. A significant number of the trajectories can potentially reach the Southern Ocean. Dust emissions from the Makgadikgadi were dispersed as far as Australia and Southern Ocean.

3.3.1.3 Kuiseb River

For the Kuiseb River, most of the projections travel towards the north west or south east with 57 of the dust plumes travelling towards that direction. From all the dust plumes, seven travelled towards the southern regions with 15 of the trajectories modelled at 1000 m heights travelling almost towards the Southern Ocean although most of the projections travelled more towards the south east into the Indian Ocean and potentially all the way to Australia over 10 days. The density plots for Kuiseb River display an undoubtedly distinct north west to south east travelling direction. The highest concentrations are skewed towards the north western part of the African continent, with a few trajectories affecting the South American continent. The higher trajectories dominantly travel towards the south east in comparison to the north west.

3.3.1.4 Omaruru River

The modelled trajectories for the Omaruru River also showed that eight trajectories travelled towards the north west (similar pathway to Kuiseb River). Only two travelled towards the south eastern regions towards the Indian Ocean. None of the projections appeared to move towards the South Atlantic Ocean. The trajectories from the Omaruru River show a similar trend to the Kuiseb River with a clearly defined north west and south east orientation. The trajectories from

these areas clearly regularly affect the West African region, while the higher trajectories tend to move more towards the Indian Ocean (Appendix B).

3.3.2 Different seasons

Models were also run to determine the air mass directions based on the different seasons (Section 3.3.2). The biggest proportion of the dust emissions occur during the winter months (64%), followed by emissions during spring (19%), while the least emissions occur during the summer (9%) and autumn (8%) seasons as shown in Figure 3-8.

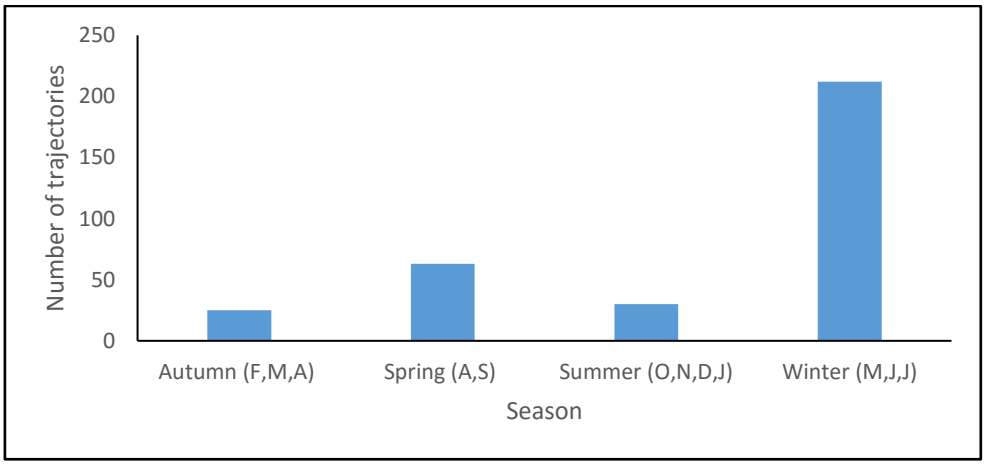

Figure 3-8 The number of dust emissions from southern Africa based on the different seasons

3.3.2.1 Summer (1st October to 31st January)

The summer trajectories appeared to travel very far from the southern African sources, though less far south or north west when compared to the winter. Most of the air masses do not dominantly reach the Southern Ocean or west African regions. However, some of the trajectories can extend as far as Australia and the Indian Ocean (Figure 3-9). The high altitude trajectories travel a longer distance. Air masses during this season are less extensive and fewer in comparison to the winter and spring seasons.

3.3.2.2 Winter (1st May to 31st July)

Dust storm emissions are greatest in southern Africa during the winter when it is dry and little rain occurs, which makes it favourable for dust to be emitted (contributes about 64%). The air

masses show a high concentration of dust transported towards the north west and south eastern region off the southern African continent. The air masses tend to move more towards the south east into the Indian Ocean sector and all the way to the Australian continent. The higher air masses dominantly travel towards the south east and north west (Figure 3-9). Fewer trajectories travel towards east Africa, while trajectories from southern Africa has the potential to travel as far as South America and Antarctica. There appears to be a significant transfer of air mass off southern Africa towards the southern oceans during the winter months.

3.3.2.3 Spring (1st August to 30th September)

There were more dust emissions from southern Africa during the spring months, which tend to travel towards the north west Atlantic Ocean. A significant proportion also travel towards the Indian Ocean. There is also a considerable number of air masses traveling towards the south east Indian Ocean (Figure 3-9).

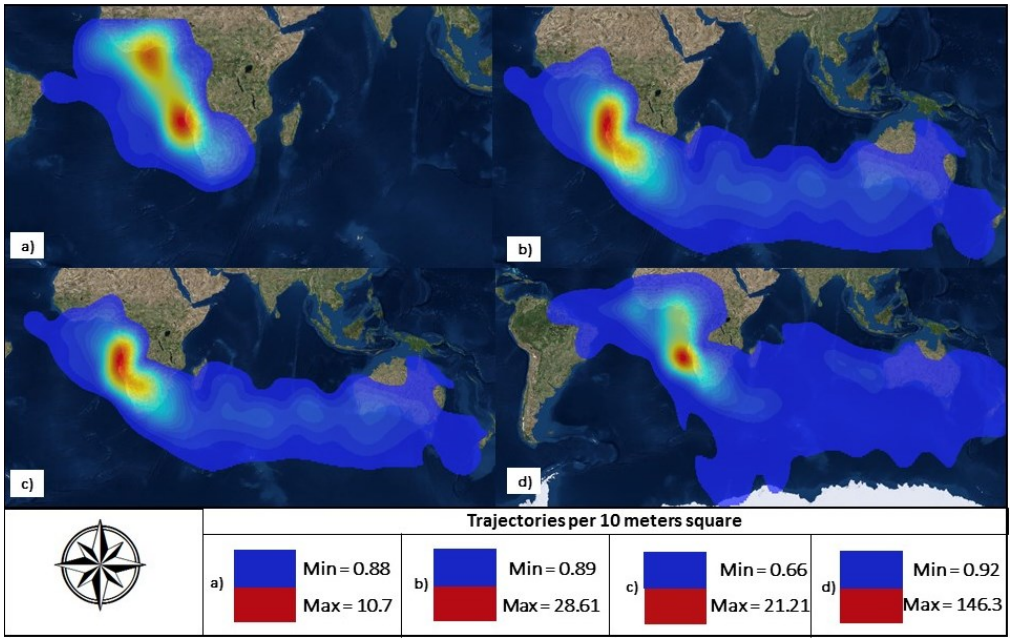

Figure 3-9 All modelled trajectories for the (a) Autumn, (b) Spring (c) Summer and (d) Winter detected dust emissions for the period between January 2005 to December 2008

3.3.2.4 Autumn (1st February to 31st April)

Most of the trajectories from the autumn months tend to travel towards the north west. Only three of the trajectories travelled towards the Southern Ocean. One of the trajectories travelled towards the Indian Ocean. In autumn, few air, masses migrated towards the south.

3.3.3 Traveling directions

The preferred travelling direction of the trajectories appeared to be based on the locations. Most of the northerly based emitting sources tend to travel towards the north west direction, influencing the northern Atlantic Ocean, while southern counter parts tend to travel towards the Indian Ocean. Most of the emissions from the Namibian coastline travelled towards the north west, while the inland emissions appeared to travel more towards the Indian Ocean.

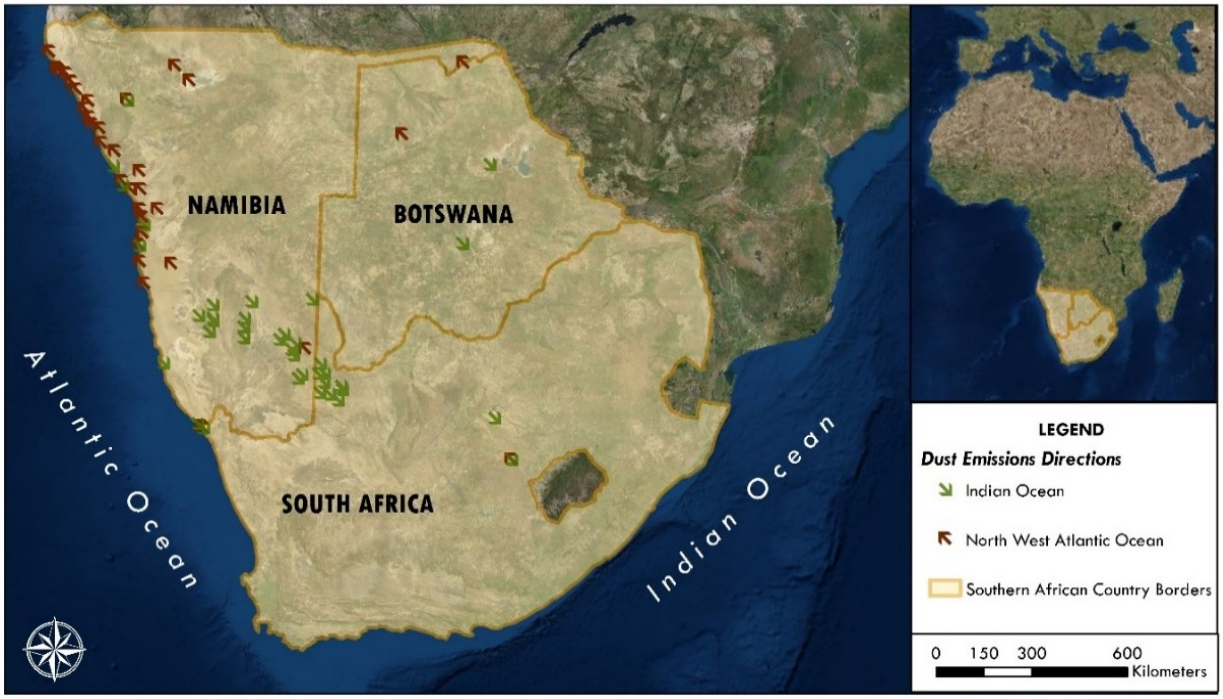

Figure 3-10 Direction of the dust emitting sources classified as travelling either towards the Indian Ocean or the north west Atlantic Ocean sector.

The biggest proportion (60%) of air masses from southern Africa tend to travel towards the north west of the Atlantic Ocean. Dust emissions that travel towards the Indian Ocean

contributes 29% of all the total air mass that leave southern Africa. Much less dust emissions travel towards the central east Indian Ocean (6%) and Southern Ocean (5%) respectively.

Table 3-2 Different dust plume locations and travelling direction which were recorded during the period from 2008 to 2010 by Vickery and Eckardt (2013).

North West	Cape Cross Pan, Cape Fria Pan, Conception Bay Pan, Etosha Pan, Gui uin, Hoanib, Hoarusib, Huan Pan, Hunkab Pan, Ihea Point, Khan River, Kiriis Ost Pan, Khumib, Koigab Pan 1, Kuiseb River, Lake Ngoni, Langer Werner, Torra Bay Pan, Toscanini, Tsauchab River Sossusvlei, Latitude Pan, Linyandi, Marshlands, Makgadikgadi Pans, Meob Bay, Omaruru River, Ombonde, Onanzi Pan, Oranjemund, Orawab, Rock Bay, Sechomib, Swakop River, Terrace Bay, Tsondab River Pan, Uniab River
Indian Ocean	Bloemfontein, Donnovan Se Pan, Duwisib River, Fish River, Gamanas Pan, Gannapan/Bloemhofdam, Gemsbokbrak, Grasheuwel Pan, Grundorner, Groot Witpan, Hakskeenpan, Haseweb River, Helmeering River, Ilhea Point, Isirub River, Kanibes River, Koeipan Koppieskraal Pan, Konkiep, Kuubmanville, Marcel Pan, Morgenzon Pan, Noeniput, Orange River, Quoxo River, Salt Pan, Samahaling Pan, Saulstraat Pan, Skemerhoek Pan, Swaartput Se Pan, Vrysoutpan, White Lady Salt Pan**,** Tumas River, Ugab Pan
Central East Atlantic Ocean	Klein Aarpan, Kongapan, Saltztal Pan

Most of the dust emissions in the inland southern Africa tend to travel towards the Indian Ocean, while most of the emissions in the northern southern African and Namib coastline appeared to travel north west (

Table 3-2). Although there are few emissions in the northern region that travel towards the Indian Ocean (Figure 3-10).

3.4 DISCUSSION

Although, dust emissions in southern Africa might not be as large as the Northern Hemisphere counterparts, these dust sources do contribute to the global emissions and are significant to global models. The dust emissions investigated during this study greatly contribute to the dust emissions that occur in the Southern Hemisphere. Hysplit model trajectories presented during this study show that most of the forward trajectories from these sources travel long distances under favourable conditions and could potentially fertilise phytoplankton communities that are depleted in essential trace elements. With the use of Hysplit, we have managed to map the extent that air parcels can potentially travel to and from the observed sites. However, determining where the dust travels tends to be a complicated aspect when analysing the trajectories based on the Hysplit Modelling software because of the high variability in the different pathways. This is because a single trajectory cannot accurately represent the development of a dust plume because the wind fields vary in space and height. These data can reveal that a significant amount of dust is emitted out of southern Africa and can potentially reach the Indian Ocean and extending all the to Australia in a period of less than two weeks of transport under favourable conditions. These results show that dust from southern Africa may affect a large part of the Indian Ocean, much of the north west Atlantic Ocean.

3.4.1 Dust travelling potential

Dust emissions from the central to northern regions of southern Africa (60%) tend to travel towards the north west regions associated with south easterly trade winds on the lower latitudes of the southern African regions. A significant proportion of air parcels also tend to travel towards the southern regions of the Indian Ocean and to a lesser proportion towards the Southern Ocean caused mainly by the westerlies. These two pathways appeared to be the dominating travel pathways out of Southern Africa. There are smaller variable air mass travelling pathways, which for example is responsible for transporting dust towards the Southern Ocean. Mineral dust from southern regions appear to be travelling in a south easterly path because of the south easterly trade winds (Schultz 1980) and this can be seen with a significant amount of air mass travelling towards the north west Atlantic Ocean. Dust from southern Africa can travel towards the north western part of Africa as far as potentially Ghana, Nigeria, Liberia and Senegal among other western African countries. Most of these dust plumes that travel towards the north west are along the Namibian coastlines where the landscape is

mainly dominated by dry river valleys, ephemeral rivers and the Namib desert. Such locations appear to be far up north and are less influenced by the easterly winds. The variation in the air mass pathways based on models at different heights appeared to be very low, meaning the models generally showed a similar direction irrespective of the height. This is mainly because the southern African continent lies beneath a stable layer around approximately 5500 m above sea level (Cosijn & Tyson 1996). The majority of the aerosols transported towards the west Atlantic Ocean are caused by the south east trade winds off southern Africa (Gingele 1996; Stuut & Jansen 2000; Stuut et al. 2002). In rare occasions, westerlies (usually very weak in the southern African continent) tend to reach high velocities and can transport significant amount of dust towards the south Atlantic Ocean (Tllhalerwa et al. 2005).

Most of the dust emissions along the Namibian coastline which are travelling towards the north west must have been influenced by the south easterly trade winds. Satellite images observations have revealed that dust sources in the northern Namibia (mainly due to strong south east trade winds) can contribute to transport off to proximal oceans (Eckardt et al. 2001). Most of the atmospheric aerosols in southern Africa appear to be highly recirculated in long range transport before deposition (Tyson et al. 2002). The geographic location of the Etosha Pan and the Makgadikgadi Pan, which are the most dynamic dust sources in southern Africa delays the transport of dust to the Southern Ocean as only 15% of the trajectories travel south of 40° S (Bhattachan et al. 2015). This is evident in our study, especially for the Etosha Pan where almost none of the air masses travels towards the south. Dust particles from the Makgadikgadi Pan has been observed to travel as far as Johannesburg, South Africa (e.g. Resane et al. 2004) and this study has shown that it can potentially be a considerable source of trace elements to the Indian Ocean and Southern Ocean. The geographic location of the Makgadikgadi Pan reduces the transport of aeolian aerosols to the Southern Ocean as only less than 10% of the trajectories travel south of 40° S (Bhattachan et al. 2015).

Our models revealed and are in agreement that almost no dust emissions from the Etosha Pan travels towards southern direction, and a contributing factor could be that berg winds which are the only winds that can transport substantial quantities of mineral dust offshore are not strong enough where Etosha Pan is located. Berg winds are much stronger and more favourable in the south but their occurrences are episodic and seem to decrease rapidly offshore which

results in few strong possible dust plumes towards the southern Atlantic Ocean (Tllhalerwa et al. 2005). Berg winds occur principally during the cold and dry periods of the year, when a resilient anticyclone lodges the central part of southern Africa and produces a steady discharge from the central highlands towards the coastal low lying land (Goudie & Middleton 2006). Etosha pan is influenced by weak but more persistent south east trade winds as the main transport proxies according to Chester (1990). Work by Chester (1990) showed that westerlies are responsible for the transport of dust towards the south, but they are not strong enough to make large deposits of aerosols towards the Southern Oceans. Another factor is the fact that most of the dust emissions occur in the upper northern regions which also ultimately weakens the dust loading potential to reach the Southern Ocean.

3.4.2 How seasonality and location influences pathways direction

Dust that travels occasionally off the south western Atlantic and potentially towards the Southern Ocean (a region which is depleted in micronutrients) is mostly influenced by berg winds which tend to be less frequent and very episodic (Tllhalerwa et al. 2005). All trajectories maps revealed that this phenomenon is possible although it is not as dominant as in the other two regions (being the Indian Ocean and north west Atlantic Ocean). The berg winds are the only winds that can transport significant quantities of dust to proximal oceanic regions at a particular time. Berg winds are episodic, appear to favour dry and hot weather conditions, hence they are very scarce (occurring occasionally annually) (Vickery & Eckardt 2013). Such meteorological conditions occur predominantly only during winter, which will make sense as it is the time that most (64%) dust emissions occur from southern Africa from studied archives.

Most of the dust plumes in southern Africa occur in winter which is partially influenced by the position of the subtropical high-pressure belt, with an average yearly circulation at approximately 1200 metres height over southern Africa is anti-cyclonic (Tyson et al. 1996). The semi-permanent south Atlantic anticyclone over southern Africa is responsible for transport of aeolian dust and gases in the lower troposphere (Zunckel et al. 2000). Southern Africa is driest during the winter season with prominent dust emission occurring during this season. Between June and July these pans dry out and dust deflation occurs. An increase in dust activity begins from June-July and reaches a maximum between August and October.

Most dust activities occur predominantly in winter along the Namib desert due to the great extent but low occurrence of north easterly winds (Vickery et al. 2013).

About 29% of the all the dust emissions air mass travels towards the south to south eastern part of the Indian Ocean. Our trajectory models reveal that air parcels can travel through the Indian Ocean to Australia and New Zealand. Garstang et al. (1996) and Tyson et al. (1996), obtained similar results although their estimations where much higher. This implies that both the anticyclone circulations and westerly disturbances will produce conducive conditions for the transport mineral dust from Africa to the east over the Indian Ocean (Tyson et al. 1996). Prevailing winds that blow in winter trigger the dust dispersion and leads to strong dust emissions occurring in winter rather than in other seasons. Another factor could be the fact that it is much drier during the winter to spring seasons which could then result in more emissions travelling (Bryant et al. 2007).

Bryant et al. (2007) has established that during the dust season, most of the emissions off the Makgadikgadi Basin travels in the eastern direction (90° – 100°). These findings are in agreement with our results which show that dust from the Makgadikgadi Pan travels predominantly in the eastern to south-eastern direction. Another factor that could influence dust emissions in southern Africa is precipitation, since there will be little to no dust emissions during the rainy season. Precipitation variation in Botswana and southern Africa has been strongly connected with the El Niño -Southern Oscillation (ENSO) (Bryant et al. 2007).

3.4.3 Impact on phytoplankton

Although light may serve as a limiting factor during the winter months, the bioactive trace elements in dust will possibly be stored as a reserve for the subsequent season when light is available. Another factor, which might influence the effect of mineral dust deposition on open oceans, is the nutrient requirements of the phytoplankton, which might not be limited by the dust. Hence, the effect of dust might not fertilise or inhibit the growth of phytoplankton communities might be low due to requirements other than the dust. Other factors might be the inhibitory or toxic effects of the trace elements on the ecosystems (Paytan et al. 2009), although its highly influence by the concentration, speciation and ecosystem resilience. Our results more importantly show that under favourable conditions, southern African dust can reach regions which are isolated from any nearby continents and can extend well beyond regions than

previously thought. For example, southern African dust can affect a huge portion of the Indian Ocean and extending as far as Australia. Eastward transport over the ten days can also potentially provide nutrients to the Eastern African countries providing nutrients to the terrestrial region. Hence, dust from southern Africa has the potential to affect a major part of the Indian Ocean, influence primary marine productivity in the massive open ocean regions. Southern African dust can also affect a significant portion of the north west Atlantic Ocean. In addition, global models forecast a poleward movement and strengthening of Southern Hemisphere air masses (Yin 2005), which then can potentially increase the transport of the essential bioactive trace metals dust to the open surface oceans in the next decades.

3.4.4 Air mass pathways climatology in southern Africa

Tyson et al. (1996), found that the westerly winds occur more regularly during the spring season which is agreement with our findings showing that most of the emissions during October travelled towards the Indian Ocean. In contrast, westerly distances occur more regularly throughout the year with a peak occurrence of 40% in spring (October). The autumnal peak that would give the semi-annual cycle in many parts of the mid-latitudes of the southern hemisphere is weakened (Tyson, et al. 1996) and this phenomenon explains why almost none of the autumn trajectories travel towards the southern oceans but more predominantly towards the north western coastal regions. Ginoux et al. (2012) using remote sensing showed that dust emissions occur gradually from austral spring to summer months from the western regions into the central regions. These results are consistent with our results because most emissions occur close to the coastline to tend to deplete when moving inland. Dust plumes along the Namibian coastline are active during most seasons (Ginoux et al. 2012; Eckardt & Kuring 2005; Vickery et al. 2013), which leads to them being dispersed a high variety of directions which ultimately leads to difficult to contextualised their preferred pathway. Our models show a high variability in the air mass pathways along the coastline mainly due to this high variety of wind directions but they mostly tend to favour the north west direction rather than Southern Ocean.

3.4.5 Travel distance/long range transport, residence time and re-circulation

Aerosols residence time in the atmosphere is hugely influenced by whether aerosol particles are mostly in the lower or upper troposphere, with the upper troposphere having longer

atmospheric lifetime for aerosols than the lower troposphere were are removed from suspension much faster (Bolin & Rodhe 1973). At times, air masses can be transported directly from southern Africa to Antarctica in four to five days (Tyson, et al. 1996) while others can be transported to lower latitudes and deposited in the India Ocean. While the variability may be so high that on occasion based on the three (lower, middle, higher) troposphere levels may be dissociated to the degree that transport from southern Africa can travel in all directions at different heights. Mean residence times of aerosols of about seven days at higher latitudes appear to be of the same order as the recirculation period of air over southern Africa (Tyson 1996). Aerosol recirculation times are dependent on the size fraction of particles in the aerosol and whether dry deposition occurs by fallout from the atmosphere and direct uptake at the surface, or on whether wet deposition occurs in precipitation. Investigations in the variation of dust pathways based on different heights showed no major significant difference in the models, which is interpreted that the masses pathways do not vary significantly, based on heights. Aerosols from the Etosha pan are most susceptible to recirculation mainly due to their fine grain size and the fact that they will be most suspended for the longest time in the atmosphere.

Li et al. (2008) showed dust plume emissions in the Southern Hemisphere and found that dust from southern Africa is relatively restricted to proximal source areas due to the insignificant strength of emissions. Our observations directly contradict this, showing that emissions from southern Africa are dispersed over thousands of kilometres and may not necessarily be localised. Their study also stated that the fact that most dust sources are located in lower latitudes in southern Africa in comparison to sources from Australia and South America. This contributes to the localization of southern African dust because this region is distant and isolated from the impact of the westerlies. The northern location of the Africa continent serves as a disadvantage in terms of being a potential supplier of micronutrients to the Southern Ocean. Not all the dust sources along the Namibian coastline are evenly distributed, with the prominent and largest collection found in the northern Namib Desert region along the Skeleton Coast. This fact means that weaker westerlies will have an effect such sources travelling towards the southern regions. South of the Kuiseb River, the Namib Sand Sea prevents all of the highland rivers from reaching the coastline and more importantly the production of dust from inland lakes such as the Sossusvlei and the end-point of the Tsauchab River, for example (Eckardt & Kuring 2005).

There are numerous discrete dust sources that are located along the Namibian west coast line which are influenced by northerly orientated winds affected by the high-pressure system which stretches east of the South Atlantic Ocean. This high pressure system stops noticeable and southerly oriented transport of dust from southern Africa (Li et al. 2008). The large scale distribution of Southern Hemisphere dust is primarily attained through transport of westerly directed winds (McGowan & Clark 2008). Westerlies from Southern Africa are weak and do not carry sufficient dust towards the southern oceans. Although, there might be significant dust emissions in southern Africa regions, predominantly cloudy conditions and diffusion of plumes during transport possess a challenge in tracking emissions off the south west Atlantic Ocean. To overcome this problem, remote sensing techniques such as MODIS and OMI satellites should be coupled with simulation calculations to achieve a consistent description of the transport and deposition of dust (Gasso & Stein 2007).

3.4.6 Hysplit modelling method application in South America and Australia

Hysplit modelling is most commonly applied in back-trajectory investigations to locate the source of air mases and asses the relationship between source and deposition sites. Worth noting is the fact that most of the backward modelling using the Hysplit model in southern Oceans tend to circulate around the Antarctic but do not necessarily go to the Patagonia or southern Africa which are projected to be the major sources for Southern Atlantic Oceans. However, majority of the projections from Patagonia are deposited into the Southern Atlantic Oceans especially the HNCL zones. It is only in current years that a more descriptive information and data of the major dust source regions at regional and global scales has materialized with most supporting sources from Australia (e.g., Mackie et al. 2008; McGowan & Clark 2008) and Patagonia (Gasso & Stein 2007; Johnson & Meskhidze 2013), although work in southern Africa is missing. Our findings so far show that the dust concentrations travel off to the Indian Ocean from southern Africa can be comparable to the ones travelling west coast of Africa. Over southern Africa, Tyson and Preston-Whyte (2000) proposed that despite the multiple synoptic circulation fields that occur in the surface boundary layer and the seasonal migration of pressure fields, the transport of air and entrained aerosols is predominantly towards the east coast and the Indian Ocean. There are two major air mass pathways that originate from the southern African landform, one being a predominantly off to the north west Atlantic Ocean direction and the second being towards the south eastern Indian Ocean sector.

The findings of Tyson and Preston-Whyte (2000) are in agreement with the results that we observed in our models which shows that majority of the trajectories were indeed travelling towards the Indian Ocean and east coast.

When the Hysplit is initiated at a very low height, it rapidly hits the ground and stops calculating; this is clearly demonstrated in the 500 m heights. The calculations work well if initiated at a higher elevation. A single trajectory cannot properly represent the development of a dust trail when the wind field varies in space and height. That is why the simulation must be conducted using many points to generate a multiple possible favourable pathway direction. The initial insert data quality hugely influences the output results because the trajectory model has a three-dimensional input dataset. Initial conditions highly influence the average speed of the advected parcel (which displays the air mases pathways). The accuracy and quality of the simulated trajectories is also influenced by the length of calculated time. Reliable models are usually the ones calculated for short time periods in comparison to increased times.

Other studies such as Gasso & Stein (2007) used the Hysplit to simulate a dust event that occurred to study phytoplankton blooms in open oceans, and their Hysplit results agreed with the location observed with remote sensing satellites such as MODIS and OMI respectively. The correlation amongst the calculated simulations and satellite observation strongly recommends the existence of emissions in the band of high Aerosol Optical Depths (AOD) observed by MODIS (Gasso & Stein, 2007). In addition, Ashrafi et al. (2014), used Hysplit modelling to simulate a dust storm over Iran, and to support the model results, they also used a MODIS satellite images which confirmed the results Hysplit dust modelling. In Australia, McGowan & Clark (2008), also used Hysplit modelling to simulate air masses pathways from Lake Eyre; their results were in agreement with dust plumes observed in the surrounding regions. Therefore, Hysplit simulation models tend to show similar trends to actual observations from satellites (Gasso & Stein 2007; Mcgowan & Clark 2008; Stein et al. 2015; Ashrafi et al. 2014). The models from South America and Australia all show a strong westerlies effect which leads to many aerosols travelling towards the Southern Ocean.

From a southern African perspective, Bhattachan et al. (2012) used Hysplit to model dust pathways from the Southern Kalahari and the Makgadikgadi Pan for years 1999-2009. Overall,

their results are in agreement with ours with 28% of their trajectories getting to regions south of 40° S within a week of transport from sources (Bhattachan et al. 2012). They also found that most trajectories travelling towards the Southern Oceans occur during the winter months (33%), when light is most probably low and restricting marine productivity in the Southern Ocean. They also found that there is no major variance in the spatial dispersion of terminal points if the initial height is altered, which is in agreement with our findings. These shows that the Hysplit model is an effective tool and can produce reliable data on the various air masses pathways. Our study also compared the various air masses pathways with chlorophyll a content in global oceans.

Our results show that the region where most of our dust plumes travel to oceanic regions thousands of kilometres from sources hence fertilising large oceanic regions. This further proves that dust from southern Africa does play a significant role in the fertilisation of open oceanic regions, although we do agree that there might be other sources of nutrients that might also supply these regions. It should also be taken into account that there is usually a lag time between dust emissions, travelling directions and eventually to the time it gets deposited in ocean. Another factor is that once the dust is deposited on surface waters, other various conditions such as for example light needs to be available for phytoplankton blooms to occur. Although light may the regulating factor in austral winter, the dust deposited can likely be stored as a reserve for spring when there is light especially in the Southern Ocean.

3.5 CONCLUSION

Our results show that dust from southern Africa can be a potential source of micronutrients if dust is emitted under the right conditions and season. The existence of large-scale plumes migrating to the eastern Indian and north western Atlantic Ocean from this region is now confidently confirmed. The different seasons that these plumes might be occurring are also modelled as well the potential air masses pathway direction from the sources. Current modelling can expose that the aerosols from southern Africa influences the southern Indian Ocean from South Africa, Mozambique and all the way to Australia which can potentially be a region of major carbon sink. Aerosols general pathways are fairly homogenous at different heights which further shows that the atmospheric system in southern Africa is capped by a stable layer which long period climatologies have proven to be around 500 hPa level in the troposphere.

There is enough evidence to support the notion that atmospheric transport of mineral dust from southern Africa can supply limited bioactive trace metals to microorganisms in marine environments eventually increasing primary productivity in the Indian Ocean. Current anthropogenic effects such as overgrazing, tourisms, deforestation, dam constructions and mining activities can result in new dust emitting sources, which can potentially produce new frequent dust emitting sources in southern Africa.

The low frequency of berg winds in southern Africa is one of the main reasons why there is low deposition of dust to the Southern Ocean from southern African continent. However, berg winds are still one of the most vital dust transport and deposition proxies to the proximal regions along the Namibian and South Africa coastlines. However, the location of most of the ephemeral rivers in southern Africa (especially, the proximity) to the coastline can be an indication that dust can be a significant source of micronutrients to surrounding areas. One of the major limitation of trace elements in the Southern Ocean could be attributed to the fact that most of the dust emissions from southern African tend to travel during the winter months, when there is limited light which is a fundamental requirement for photosynthesis.

CHAPTER 4:

TRACE METAL COMPOSITIONS, PARTICLE SIZE ANALYSIS AND BIOAVAILABILITY OF THE DUST

NOTE: A presentation of the prepared research paper:

This research manuscript will be prepared for a journal submission. I am the lead author on the work and Dr Susanne Fietz, Prof. Alakendra Roychoudhury, Prof Frank Eckardt and Mrs Johanna von Holdt are co-authors.

I was responsible for data compilation, written work and the creation of all diagrams. Samples that were used for the analytical experiments were collected by Johanna von Holdt. My co-authors mainly played a supervisory role in developing this chapter.

TRACE METAL COMPOSITIONS, PARTICLE SIZE ANALYSIS AND BIOAVAILABILITY OF THE SEDIMENTS

K. Kangueehi [a], S.Fietz [a], A. N. Roychoudhury[a], F. D. Eckardt [b], J. Von Holdt [b]

[a] *Earth Science Department, University of Stellenbosch, South Africa*

[b] *Environmental and Geographical Science Department, University of Cape Town, South Africa*

ABSTRACT

Sediments were analysed from the four major dust emitting regions in southern Africa, namely the Etosha and Makgadikgadi Pans and the Omaruru and Kuiseb Rivers. Dust emitting from ephemeral rivers can be potential fertilizers to open oceans, but the possibility has largely been overlooked. This study investigates soil/sediments the particle size distribution, trace elemental concentrations, solubility and mineralogical characteristics of four ephemeral pans and rivers in southern Africa. Particle size distribution revealed that Etosha, Kuiseb and Omaruru samples were predominantly fine grained compared to the Makgadikgadi Pan. Makgadikgadi Pans being coarser with parent rock fragments found in samples. Bulk trace metal analysis showed that Kuiseb and Omaruru River dust sources are enriched in Ti, Al, Fe, Cu and Zn which are vital micronutrients to phytoplankton communities. Etosha, in distinction, was enriched in Mg and Ca, most probably controlled by the bedrock geology dominated by dolomites. Continuous flow-through experiment was used to leach bioactive trace metals from aerosol samples from the four dust emitting sources for approximately one day. Trace metal solubility (proxy for bioavailability) was determined from these experiments to characterize and compare which source is most suitable as a fertilizer for open oceans. The Etosha Pan had the highest Fe (%) solubility although Kuiseb and Omaruru River appeared to be enriched in bulk trace metal compositions. The ephemeral rivers and pans trace elements concentrations in southern Africa can potentially play an essential role in fertilizing marine systems where trace elements are limited.

4.1 INTRODUCTION

Trace elements play an essential role in ocean biogeochemistry as micronutrients for marine life. Dust deposited into the oceans provide essential trace elements that fertilise phytoplankton communities (Mahowald et al. 2006). Trace metals bioavailability to phytoplankton communities stimulates primary productivity which then removes carbon dioxide from the atmosphere via photosynthesis (Johnson et al. 1997). This sequestration of carbon dioxide from the atmosphere by phytoplankton has attracted a worldwide interest among researchers and stakeholders due to the consequences of global warming (Martin et al. 1990; Merkel et al. 2014). The CO_2 in the atmosphere is usually taken up by the ocean through gas exchange processes and then gets transformed into inorganic carbon (DIC) such as carbonic acid, bicarbonate and carbonate ions in seawater (Raven & Falkowski 1999; Sarmiento et al. 1992), therefore leading to a decrease in pH of ocean waters. This process is known as the "solubility pump". Based on current trends in the CO_2 emissions, a doubling of present atmospheric CO_2 concentrations paralleled by a concomitant threefold increase in H^+ ions are expected to occur before the end of this century (Caldeira & Wickett 2000; Passow et al. 2014)). Then the DIC can be converted into organic materials (Chrisholm & Morel 1991; IPCC 2013). This process is known as the "biological pump". The carbon that sinks to the bottom of the ocean can be stored in the sediments for thousands to millions of years, therefore reducing CO_2 from the atmosphere. Recent models have shown that the Southern Ocean is very subtle to changing climatic conditions and its study is crucial to reliably forecast the dynamics of the global carbon cycle in the future (Breviere et al. 2006).

Dust represents an important land-ocean-climate feedback mechanism, with the overall nutrient loading of dust widely recognised as essential to marine primary productivity (Mahowald et al. 2009). Mineral aerosols deposition on surface oceans contain notable concentrations of essential trace elements, hence it can be considered to have fertilisation potential. Largest deposits of sediments to oceans are fluvial deposits (Poulton & Canfield 2005), while glacial sediments tend to supply over a longer timescale, the next largest contributor of sediment and nutrients to the oceans is aeolian transport and deposition (Mahowald et al. 2008). Aeolian aerosol transport has the potential to disperse and be transported by wind for long distances to isolated open ocean regions. Largest sources of mineral aerosols are ephemeral lakes in arid and semi-arid regions, for example the Bodélé Depression in Lake Chad which is largest in the world (Prospero et al. 2002; Mahowald et al. 2014), the Makgadikgadi Pan system and Etosha

Pan (Prospero et al. 2002; Bryant et al. 2007). In southern Africa, ephemeral rivers have also been regarded is significant dust emitters with regional dust emissions observed in remote sensing studies (Eckardt & Kuring 2005; Vickery et al. 2013; Vickery & Eckardt 2013).

Most of the dust research in southern Africa has focussed on dust emissions and sources characteristics (Vickery 2014; Eckardt & Kuring 2005; Bryant 2003), long distance transport and ephemeral lakes as a potential sources of minerals for ocean fertilisation (Bhattachan et al. 2015; Bhattachan et al. 2012; Piketh et al. 2000), rather than the potential role of ephemeral rivers as sources of micronutrients through airborne transport to proximal oceans. The trace elemental concentrations and mineralogical compositions of ephemeral rivers as potential sources nutrients to open oceans has not been investigated to date. The potential role that trace elements can play to fertilise the oceans is mainly influenced by the bioavailability of the dust. Solubility of sediments is usually used as a proxy for bioavailability (Paris et al. 2011; Raiswell et al. 2008a; Shi et al. 2015).

The high variety in geological origin of underlying rocks, usually highly influences the desert soils chemical and physical compositions while major components such as iron can contribute up to 3.5% (on a weight basis) (Jickells & Moore 2015). The mineralogical characteristics of the dust are vital factors in determining the dissolution rates, solubility and therefore the bioavailability of the trace metals (Wang et al. 2015). The variation in the mineralogy can provide an indication of the grain size distribution and the physical characteristics that affected the grains during transport. Most of the fine grained particles (clay-sized minerals such as kaolinite, montmorillonite, illite) are typically produced through chemical weathering of country bedrocks (Pedro 1984). More weathering resistant minerals such as phyllosilicates are frequently silt-sized or occasionally coarse grained (Mitchell & Soga 2005). More weathering resistant minerals such as quartz, calcite and feldspars appear to be found in all soil size fractions from fine to coarse, but predominantly in the silt-sized portion (Chatenet et al. 1996). Most arid regions soils are frequently rich in calcite, especially in the large soil fractions such as silt-size to coarse, and much less in the clay fraction (Abtahi 1980). Primary minerals such as quartz, mica, feldspars are commonly abundant in the silt-sized class, while the weathered clay minerals are associated with clay sized fraction (Journet et al. 2014).

The mineralogical composition of the dust ultimately influences the chemistry. This highlights the importance of studying the mineralogical characteristics of dust as associated to that of the soil. The choice of reagents (leach solutions) used also plays a huge role in the determination of bioavailability of Fe. Experimental artefacts, the dissimilar nature of surface sea water and deposited mineral dust are likely to add to the large reported variation in the calculations and measurements of bioavailability (Morton et al. 2013). For aeolian aerosols, chemical concentrations and particle size distribution are crucial in determining the dust impacts when deposited in surface oceans (e.g. Mahowald et al. 2011)). For mineral aerosols, both composition and size vary greatly over space and time (Mahowald et al. 2014). Higher solubilities are also observed at lower total iron concentrations (Sholkovitz et al. 2012). Some metals, like Zn, Fe and Co, are essential for phytoplankton growth (Sunda 2012) while others, like Cu, may be toxic (Brand et al. 1986) such that an acidification-induced change in bioavailability could affect the productivity of marine ecosystems.

The overall aim of this chapter is to determine the trace elemental composition of the known dust emitting ephemeral lakes and rivers from southern Africa. In addition, the project aims at determining how mineralogy might influence trace elemental chemistry. Secondly, the project aims to determine the dissolution of the soil samples when using deionized water as a reagent and how it is influenced by the particle size distribution.

4.2 METHODOLOGY

Soil/sediment samples from the top 50 mm of the ephemeral rivers and pan were collected at the four different sites, namely the Omaruru and Kuiseb Rivers and Etosha and Makgadikgadi Pans (figure 4-2). At least replicates or triplicates from each site was used for the different analysis depending on the availability of the material. These grabbed samples are not necessarily a representative of the overall grain size or mineralogical composition of the studied areas but we believe they give a good representation of the probable variables in the studied areas.

4.2.1 XRD analysis

The XRD was used to identify and semi-quantitatively assess the mineralogical composition of the sediment/soil particles. A brief description of this method can be found in Appendix C. XRD results are merely a complimentary component because critics believe that XRD is not sensitive enough to detect and a fortiori identify or differentiate between the different Fe oxides. This is often due to the less crystalline structure (very broad peaks), overlap of the main diagnostic peaks of Fe-oxides and the low amounts of such oxides in the samples (usually a few % in mass) (Shi et al. 2012). Variation in mineral dust composition leads to changes in the refractive indices, which may lead to positive or negative radiative forcing by dust aerosols

The XRD analysis were conducted with the BRUKER AXS Advance diffractometer at the iThemba Labs in Cape Town, South Africa, with measurements conducted continuously as the scan in locked coupled mode. A Cu-Kα radiation X-ray beam of wavelength 1.5406Å was used. Samples were detected by the LynxEye (Position sensitive detector). All data were collected with the standard X-ray generator settings of 40 kV and 40 mA. All samples were analysed for a duration of 20 minutes.

4.2.2 Particle size analysis

The laser diffractrometry via the Malvern Laser sizer was used to characterize the particle size distribution for the sediments. Approximately 10 g of the sample was first mixed and then split to create a representative composite sample. Thereafter, approximately 1 g of the split sample

was continuously added to the Malvern instrument. To minimize errors, the samples were analysed as triplicates. A brief description of the particle size analysis method can be found in appendix H.

4.2.3 Complete digestion method

0.1g of each of the four sieved sediment dust sample was weighed in the microwave vessels and then 6.5 ml HNO_3 and 0.5ml HCl was added to it. The samples were then allowed to stand for 20 min to predigest before sealing the vessels and proceeding to the heating program. The MARS microwave instrument was used with settings at a power level of 1600 W with a ramp time of 25 minutes at which the sample is heated from 20°C to 185°C at a pressure of 800 psi and temperature of 235°C. Holding time was 15 minutes that the sample spends in the microwave under the above mentioned conditions. The cool down time is 25 minutes (default setting of the microwave). After microwaving, 43 g of deionized water was weight out in a sample bottle that was cleaned in 5% HNO_3 and then added it to the digested sample in the microwave vessel to make up 50 ml. The sample was then stirred in the microwave vessel and then transferred into the sample bottle.

4.2.4 Cation analysis- ICP-MS

Trace elemental concentrations in the soil samples were measured using the trace cation analysis, an Agilent 7700 ICP-MS (Inductively Coupled Plasma - Mass Spectrometer) at the University of Stellenbosch. 0.2 g of each of the four sieved sediment dust sample was weighed in the microwave vessels and then 6.5 ml HNO_3 and 0.5 ml HCl was added to it. The samples were then allowed to stand for 20 min to predigest before sealing the vessels and proceeding to the heating program. The MARS microwave instrument was used with microwave set at a power level of 1600 W with a ramp time of 25 minute where sample is heat from 20 degrees to 185 degrees at a pressure of 800 psi and temperature of 235 ^{0}C. Holding time was 15 minutes that the sample spends in the microwave under the above mentioned conditions. Cool down time is 25 minutes (default setting of the microwave). After microwaving, 43 g of deionized water was weight out in a sample bottle that was cleaned in 5% HNO_3 and then added it to the digested sample in the microwave vessel to make up 50 ml. The sample was then stirred in the microwave vessel and then transferred into the sample bottle for complete digestion analysis.

4.2.5 Bioavailable leaching experiment

All chemicals were analytical grade and de-ionized water (Milli-Q, 18 mΩ com-1) was used. All glassware, falcon tubes and containers were washed and soaked overnight with HCL (6 M) and then rinsed several times with ultrapure water. The samples were pre-sieved at different mesh sizes. For the sieving process, the samples were left in an electric shaker for more than 48 hours. After the sieving process, samples processed in the laminar flow hoot to preserve the samples in a clean room environment with minimum handling. All the analyzed samples were weight to a mass of approximately 0.5 g. The weighted sample were then placed and spread out evenly on a filter (extraction system). Filter was then covered with another cleaned filter on top to prevent the sample from spilling.

In order to study the rate of dissolution, it is important to establish the time of the leaching experiments. Time of dissolutions can be either instant solubility or slow solubility which ranges from several minutes to a couple of hours have been recorded in various studies. Aguilar-Islas et al. (2010) measured iron dissolution rates over short period intervals ranging from 1 minute, 3 minutes and 90 minutes, while Baker et al. (2006) measured the iron solubility after a dissolution lasting 1 to 2 hours. This study measured the dissolution of trace elements from a period of one day, with samples collected every 30 minutes for the first 2 hours and then every 3 hours for the duration of the day. Determining the bioavailability of trace elements in mineral dust is based on laboratory leaching experiments. This involves the leaching of sediments to generate operationally defined solubility patterns sensitive to extraction volume, different solvent pH and mechanical agitation.

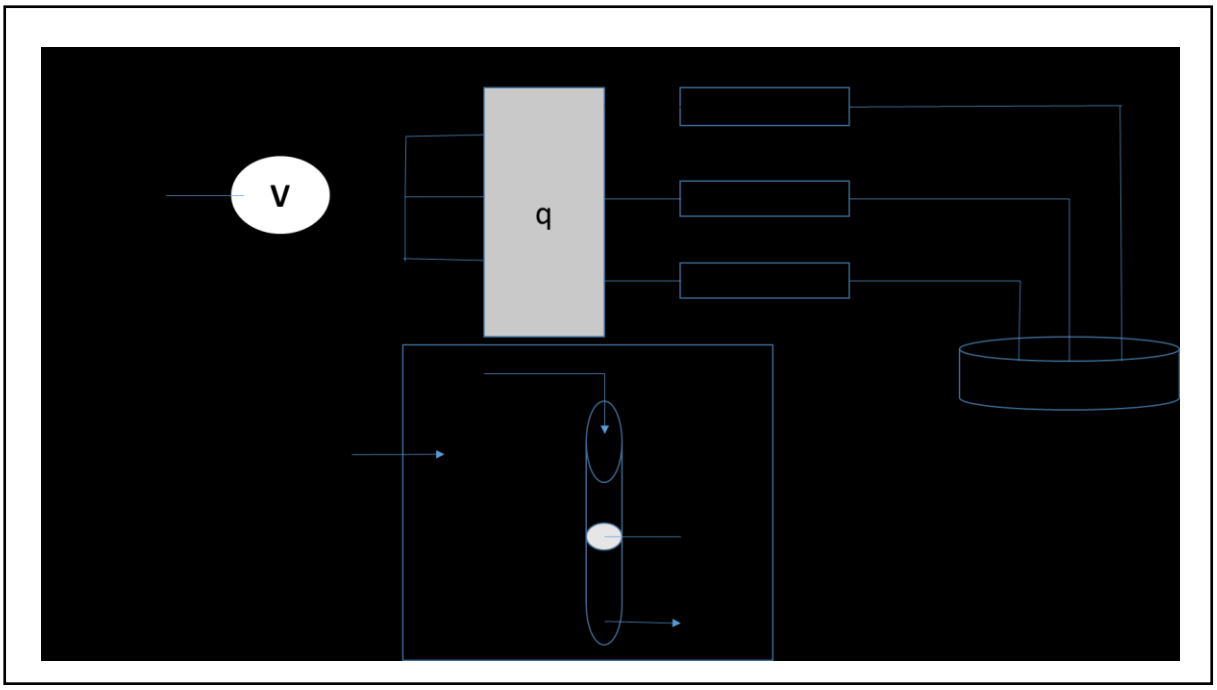

Figure 4-1 (a) “Schematic outline of the continuous flow system for soil/sediments trace elemental dissolution rates measurements. P.P. Peristaltic pump; q: flow rate ;V: Volume for reagents (Milli Q water) ; ES: leaching system (ES_1: duplicates of the sediments ; b) Extraction system ;S: sample ; f1: filter of cellulose acetate tow; f2: filter membrane (0.45 mm) (adapted from a schematic diagram of a continuous flow method from Simonella et al., (2014))”.

Samples were inserted in a two-filter system and then the flow system was connected to a peristaltic pump. The flow system was designed in such a way that there was constant flow of Milli-Q (deionized) water when the leaching of the sediments was initiated (Figure 4-1). A peristatic pump was connected to the flow system to allow constant flow of Milli-Q water into the filters. The continuous flow through system is connected to a peristaltic pump as a propulsion system that allows for multiple analyzes to be conducted at once. After multiple testing sessions, a flow rate of 0.2 mL min-1 was used. All experiments were conducted for approximately 24 hours. The samples were then buffered to a pH 1.7-1.8 using concentrated hydrochloric acid to prevent Fe from precipitation. The acid used was Geo-traces grade acid, with the acidification blanks also collected and analyzed to determine external addition of trace elements. Analysis were carried out in the shortest possible time after sampling, because of Fe high reactivity.

4.3 RESULTS

4.3.1 General Sedimentological Characteristics of the Samples

Etosha Pan samples appeared to be very fine grained, with well-rounded grains, powdery, porous and fine fluff texture. Sample was collected from a crust and was very light in weight. Sample had a white to creamy colour with almost no grains visible with the naked eye (figure 4-2 (a)). Sample from Makgadikgadi Pan appeared to be medium to coarse grained, with numerous angular grains, poorly sorted and predominantly light grey to creamish white colour. Minerals could be seen with the naked eye and were predominantly calcite and carbonate rock fragments showing a wide range grain size variation. Kuiseb river samples was fine grained, most probably mud to silt-sized with well-rounded and sorted grains. Organic matter fragments such as roots and leaves were find to be aggregated to the mud to silt-sized grains. Sample had a medium to dark brown colour. Omaruru river sample appeared to be fine grained with also well rounded and sorted grains. None of the grains could be identified with the naked eye and the sample had a muddy cracked texture. Sample could be classified as a clay-sized due to the very fine grain texture. Sample had a light brown colour.

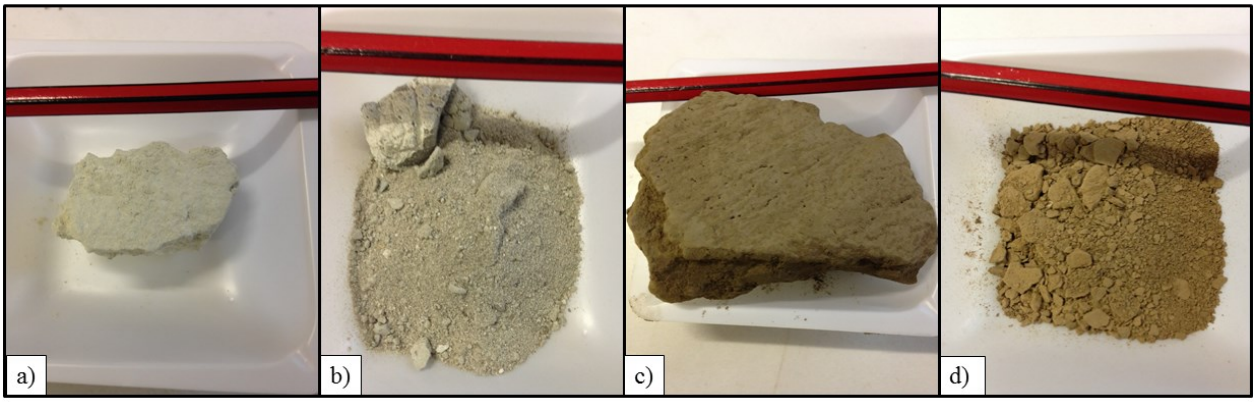

Figure 4-2 Grab samples of the analysed sediments from (a) Etosha Pan, (b) Makgadikgadi Pan, (c) Kuiseb River and (d) Omaruru river with the pencil used as a scale.

4.3.2 XRD Results

The sediment samples are predominantly made up of quartz and calcite (Appendix C-F), while the silt-sized fraction is dominated mostly by kaolinite with much lesser amounts of smectite and illite. Not surprisingly, there is high presence of micas, especially muscovite mainly due to the geology of the area which is abundant with Kuiseb schists, Swakop and Karibib marbles. Etosha samples had Na-rich clay minerals namely analcime and montmorillonite.

The Etosha Pan sample was mostly abundant with calcite, quartz, analcime and montmorillonite, although calcite appeared to be the dominant mineral (Figure 4-3). More of the XRD results for Etosha are in appendix D.

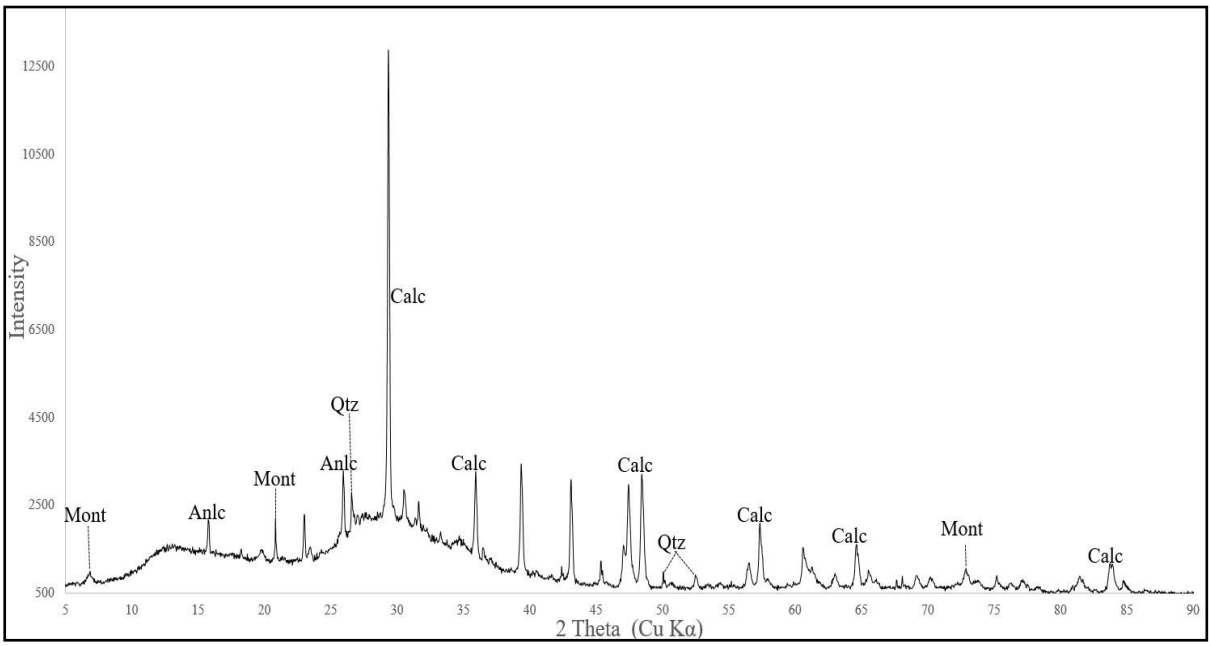

Figure 4-3 XRD mineralogical analytical results for Etosha Pan

Makgadikgadi Pan was also abundant with quartz, calcite and silica oxide, but quartz appeared to be the dominant mineral from this area (Figure 4-4). More of the XRD results for the Makgadikgadi Pan are displayed in the Appendix D.

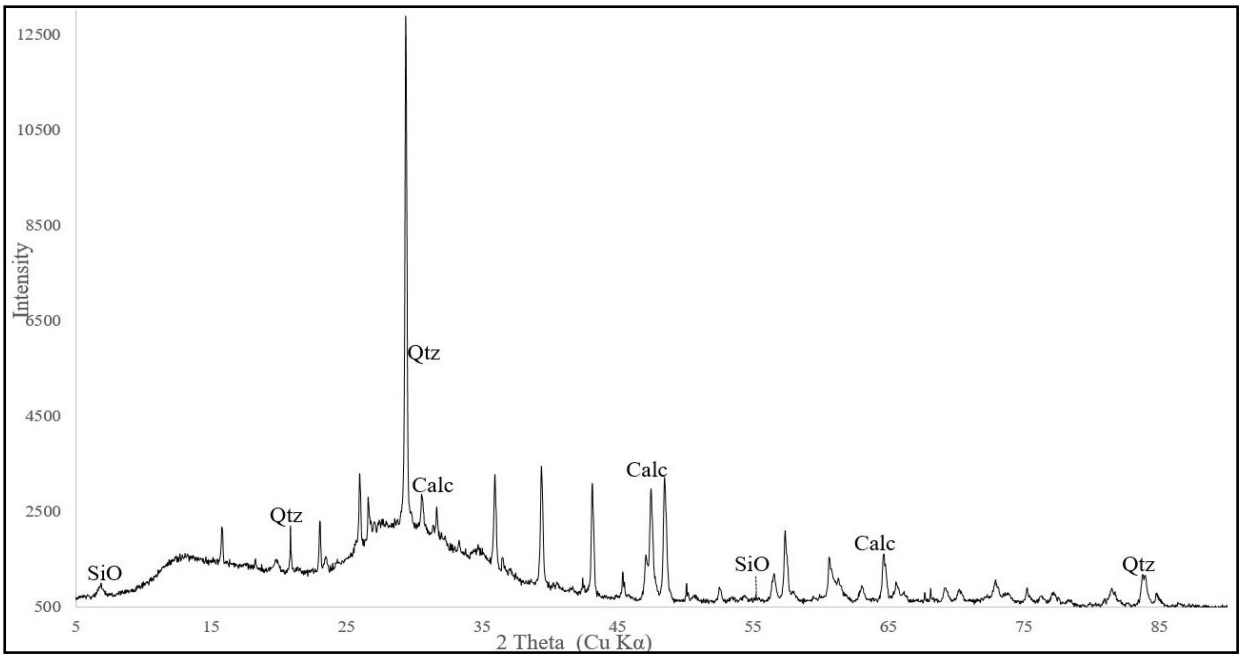

Figure 4-4 XRD mineralogical analytical results for Makgadikgadi Pan

Kuiseb River was abundant with quartz, illite, muscovite and kaolinite. Quartz appeared to be the dominant mineral but with a relatively high abundance of kaolinite and muscovite as well (Figure 4-5). More XRD results from the Kuiseb River can be found in Appendix D.

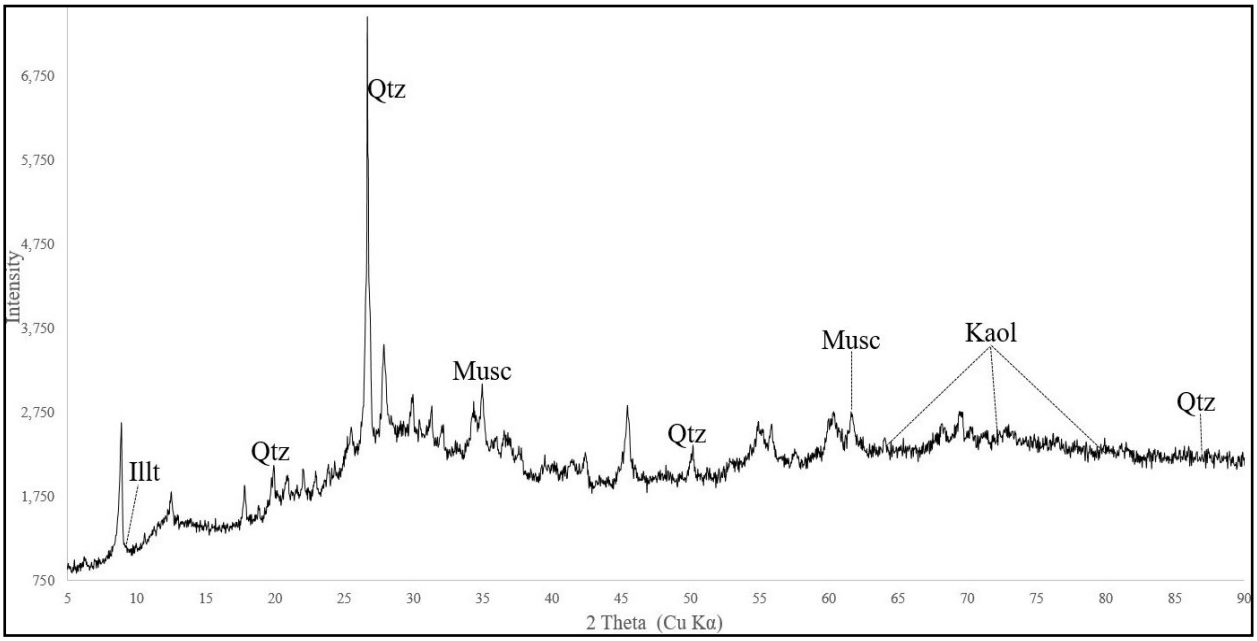

Figure 4-5 XRD mineralogical analytical results for Kuiseb River

Samples from Omaruru River was mainly abundant with quartz, illite, anorthite, muscovite and kaolinite. The dominant mineral is also quartz with also a relatively high abundance of muscovite. More of the XRD results from the Omaruru River are displayed in Appendix E.

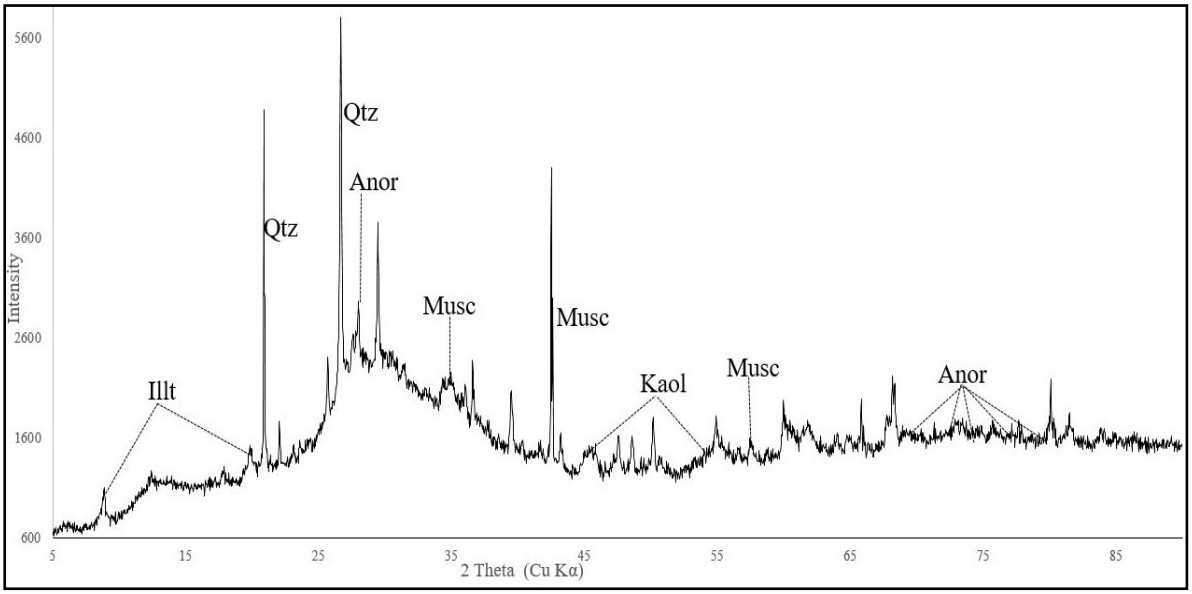

Figure 4-6 XRD mineralogical analytical results for Omaruru River

Comparison of the mineralogy between the two rivers and the pans show that the pan is more enriched in calcite bearing minerals while the rivers are enriched alumino-silicate bearing minerals. River sediments appeared to be abundant with illite which was absent in the pan sediments (Table 4-1). The pans appeared to be enriched in calcite and quartz, with quartz being more abundant in Makgadikgadi pan in comparison to Etosha Pan. In addition, Etosha Pan has clay minerals such as montmorillonite and analcime.

Table 4-1 XRD results from the different dust emitting sources.

Sample Source	Minerals
Etosha Pan	Quartz (SiO_2), Calcite ($CaCO_3$), Iron Silicon (Fe_3Si), Analcime ($Na(Si_2Al)O_6.H_2O$, Montmorillonite ($Na_x(Al,Mg)_2SiO_4$
Makgadikgadi Pan	Quartz (SiO_2), Calcite ($CaCO_3$), Silicon Oxide (SiO_2)
Kuiseb River	Quartz (SiO_2), Muscovite ($H_2KAl_3(SiO_4)_3$, Illite ($K_{0.5}(Al, Fe, Mg)_3(Si, Al)_4O_{10}(OH)_2$ Kaolinite ($Al_2(Si_2O_5)(OH)_4$
Omaruru River	Quartz (SiO_2), Calcite ($CaCO_3$), Anorthite ($CaAl_2Si_2O_8$), Muscovite ($H_2KAl_3(SiO_4)_3$, Illite ($K_{0.5}(Al, Fe, Mg)_3(Si, Al)_4O_{10}(OH)_2$

4.3.3 Particle size analysis

The particle size analysis for the four dust emitting sources were analyzed, with four samples from Kuiseb River, six samples from Omaruru river, seven samples from Etosha Pan and five samples from the Makgadikgadi Pan (All results are in Appendix H). Figure 4-7 presents mean particle size data in the study. These data demonstrate the general characteristics of the units. The particle sizes from each of the individual sources looked very similar; hence, the average particle size of the analyzed samples was used to produce a distribution curve that represent that particular source.

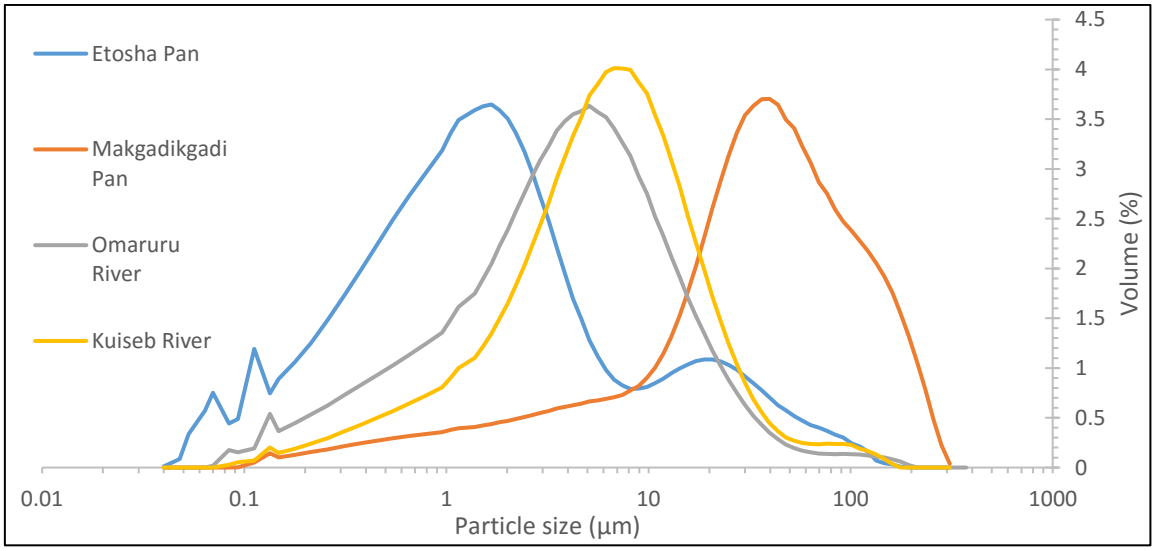

Figure 4-7 Grain size histograms of four samples from the known dust emitters in southern Africa, Etosha Basin, Makgadikgadi Basin, Omaruru River and Kuiseb River.

The grain size distribution for Kuiseb and Omaruru River shows that the sediments have a similar particle size distribution. Majority of the grains ranges from 1 to <100 µm. Grain size distribution for the Etosha Pan area shows a range from approximately 3 µm to 16 µm which is the finest grained in comparison to all the other dust emitters. Etosha sediments grain size contains approximately 75% clay to medium silt sediments which proofed to be the finest of the four sources (Figure 4-8). Only less than 25% is coarse silt to medium sand with negligible coarse sand. This distribution can be classified as clay based on the upper limit Wentworth (1922) classification scheme. The Omaruru and Kuiseb River are having a similar overall grain size distribution ranges from approximately 0.45 µm as the lowest grain size to 787 µm as the highest grain size.

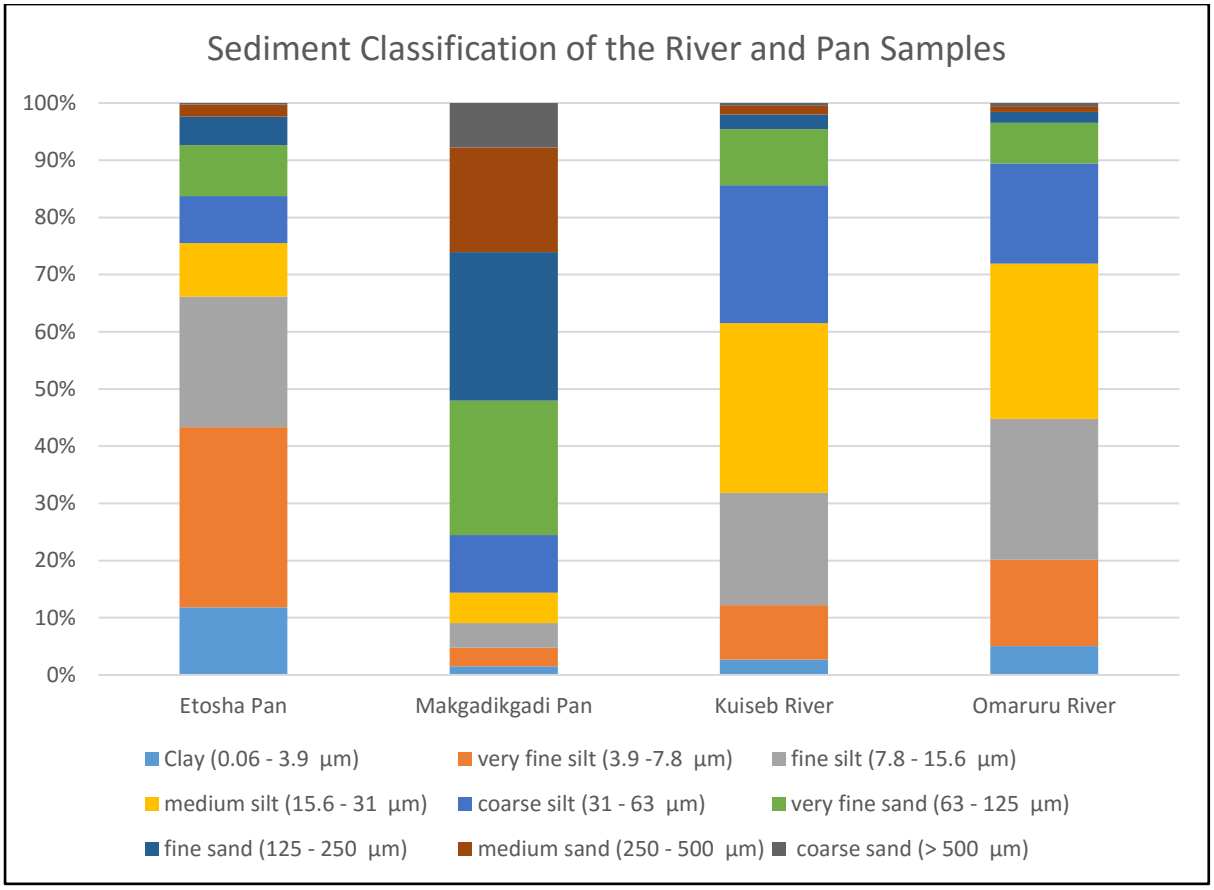

Figure 4-8 Average particle size fractions for the four different locations based on the Wentworth (1922) classification scheme (Table 2).

The Kuiseb River appeared to have a slightly coarser grain size distribution than the Omaruru River although they roughly contain more than 60% clay to medium silt sediment content with a less than 15% sand content (Figure 4-8). The grain size distribution for the Makgadikgadi Pan reveals that the grain size distribution dominantly ranging from approximately 48 µm to 787 µm. Makgadikgadi Pan has the coarsest grain size distribution in comparison to all the dust emitting sources with more than 75% sediments being sand, while less than 25% being silt with little to almost no clay content. In summary, the grain size distribution shows that Etosha Pan is the finest grained followed by the Omaruru and Kuiseb River which both have a very similar grain size distribution, while the Makgadikgadi Pan is the coarsest grain in comparison to all the dust emitting sources. The soil texture of the samples from all four sites vary from coarse silt to very fine sand.

4.3.4 Analytical results and findings

In this section, we present the trace metal concentration of soils in southern Africa from the four dust emitting sources, namely the Omaruru and Kuiseb River, the Etosha (all in Namibia) and Makgadikgadi Pan in Botswana. The focus will mainly be Mg, because it is a major component of crustal materials and Fe, Cu, Zn and Cd for their biogeochemical properties.

Trace elements in the soil samples (in descending order in mg/kg concentration) included Ca, Al, Fe, Na, Ti, Co, Zn (Figure 4-9). The Kuiseb River area is enriched in Cu, Fe, Mn, V, Ti, Zn and K in comparison to all the other sources while the Omaruru River has the highest second concentration with 23.9 mg/kg. The Makgadikgadi and the Etosha both have fairly lower concentrations for the presented trace elements. For the trace element Zn, Omaruru River area is more enriched in comparison to all the other sources with a concentration of 94.6 mg/kg while the Kuiseb River has the highest second concentration with 91.1 mg/kg. The Makgadikgadi and the Etosha both have low Zn concentrations with values of 10.6 and 11.8 mg/kg respectively.

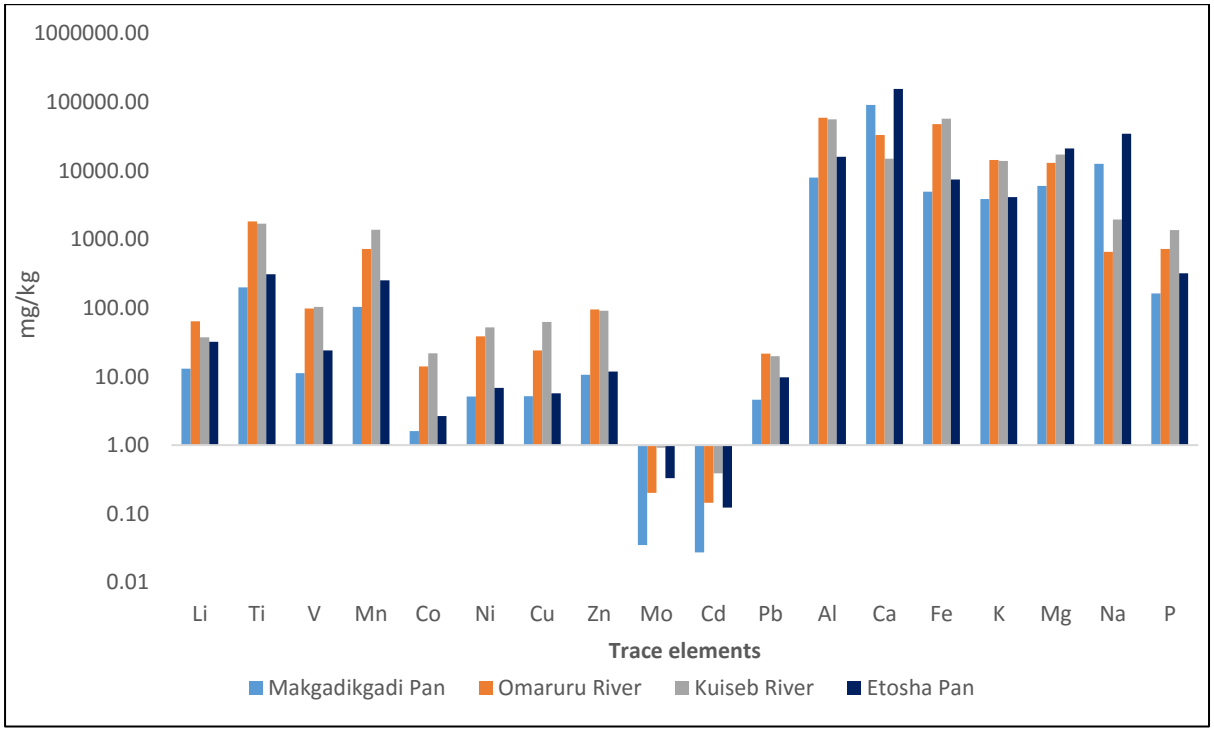

Figure 4-9 Distribution of trace elemental compositions (mg/kg) of the soil samples collected from the four dust emitting sources in southern Africa.

In terms of Fe, the Kuiseb River area is enriched in comparison to all the other dust sources with a concentration of 57.2 g/kg while the Omaruru River has the highest second concentration with 47.7 g/kg. The Makgadikgadi and the Etosha Pans both have fairly lower iron concentrations with values of 49.3 and 74.6 g/kg respectively. For Cd, the Kuiseb River area is enriched in comparison to all the other dust sources area with a concentration of 0.39 mg/kg while the Omaruru River has the highest second concentration with 0.14 mg/kg. The Makgadikgadi and the Etosha Pans both have low cadmium concentrations with values of 0.03 and 0.12 mg/kg respectively. For all the other trace elements, there appears to be a similar pattern in terms of variation, with the Kuiseb River dust being the most enriched, followed very closely by the Omaruru River, which also has high concentrations. The two ephemeral pans, namely the Etosha and Makgadikgadi Pans have low bulk trace elemental compositions but the Etosha Pan is enriched when comparing to only the two ephemeral pans.

4.3.5 Solubility of dust emissions

There is a steep increase in concentration for all the trace elements for the first 3 hours for all the various dust-emitting sources (Figure 4-10). Al and Fe are the enriched in terms of concentrations. Ni and Cd concentrations appear to be showing a much less increase over duration of the experiment. Trace elements such as Cu, Co, V, Mn and to less extent Zn seem to be to not enriched but show a similar trend to Fe and Al but much more gradually in terms of increasing concentrations. There appears to be little to no change in terms of concentrations for all trace elements after approximately seven hours. Cd is below detection limit after one hour. Al is the most enriched of all the trace elements in all the various dust emitters.

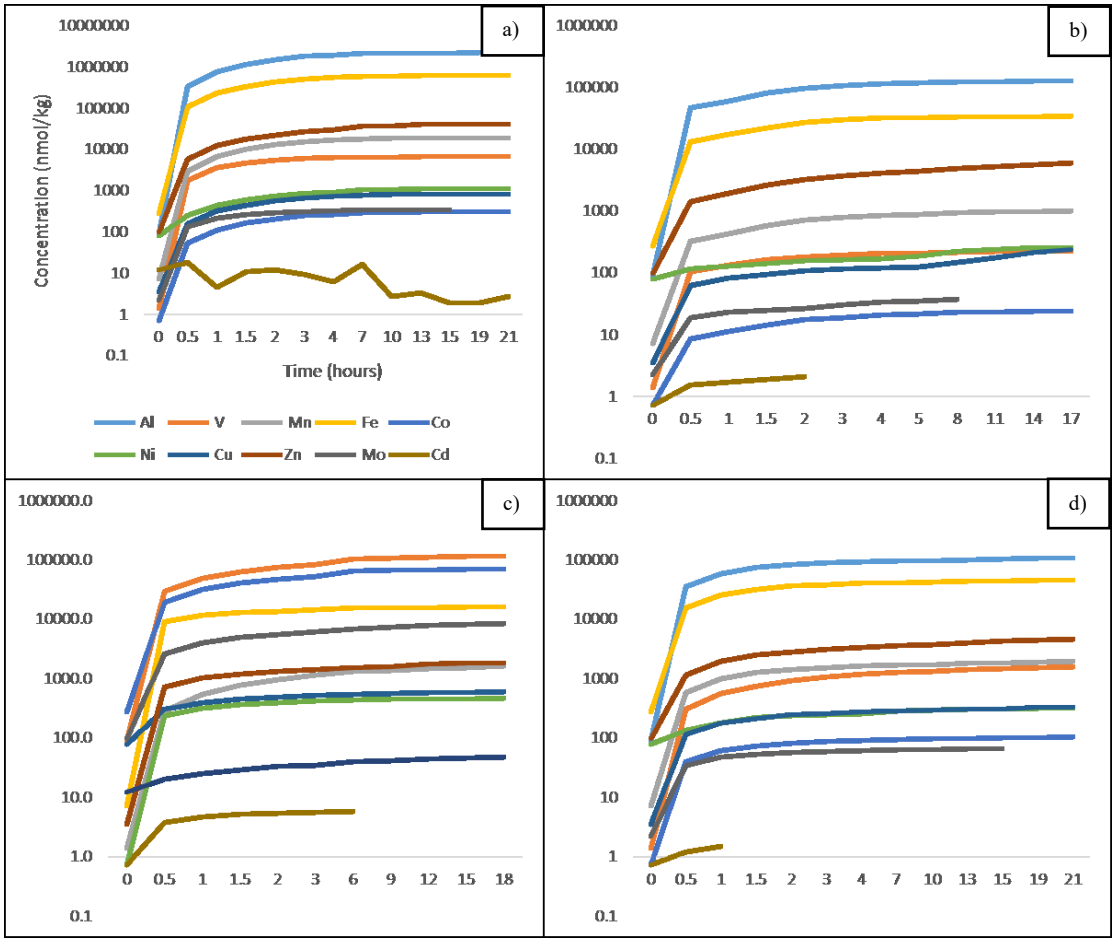

Figure 4-10 Solubility of sediments from the various dust emitters over different time (hours) (a) Etosha Pan, (b) Makgadikgadi Pan, (c) Kuiseb River and (d) Omaruru River.

Al and Fe have the highest trace elemental solute for the sediments samples from the Etosha Basin. Trace elements such as Zn, Mn, V, Co, Mo and Zn show a similar trend as Fe and Al but their concentrations are much lower in comparison to Fe and Al. Cd is below detection limits and shows a more irregular behavior. There appears to be little to no change in concentration after 4 hours.

There is a steep increase in concentration for all the trace elements in the first two hours for Makgadikgadi Basin. Al and Fe are the most enriched in terms of concentrations. Trace elements such as Cu, Mo, Co, V, Mn and to less extent Zn seem to be to not enriched but show a similar trend to Fe and Al but much more gradually in terms of increasing concentrations over time. There appears to be little to no change in concentrations after three hours. Cd is below detection limits after 2 hours.

Al and Fe have the highest trace elemental composition for the sediments samples from the Kuiseb River, with Mn having a relatively high concentration in comparison to other trace elements. Trace elements such as Zn, Mn, V, Co, and Mo show a similar trend as Fe and Al but their concentrations are much lower in comparison to the two. Ni and Pb show a much gradual increase in terms concentrations. Cd is below detection limits and shows a more irregular behavior. There appears to be little to no change in concentration after 6 hours, which seem to be the longest compared to all the other dust emitters.

4.3.6 Omaruru and Kuiseb River (30 micrometers sieved)

In terms of analyzing the fine-grained fraction, only samples from the Omaruru and Kuiseb River could not have sieved to the 30 µm mesh size. Samples from Etosha and Makgadikgadi Pan appeared to be coarser and not enough sample could be retrieved for analytical procedures. The sieving of soil samples to separate the fine fractions from the coarse is exceptionally difficult with the use of dry sieving even with an electric shaker. Wet sieving could not be used because it can potentially alter the soluble fraction of Fe present.

Al and Fe have the highest trace elemental composition for the sediments samples from the Omaruru River, but all trace elements tend to show a similar trend (Figure 4-11). Trace elements such as Mn, V, Co, Mo and Zn show a similar trend as Fe and Al but their concentrations are much lower in comparison to the two. All trace elements show a much faster extraction rate, with no increase in concentration after 30 minutes. There appears to be an increase in Zn over the 14 hour duration.

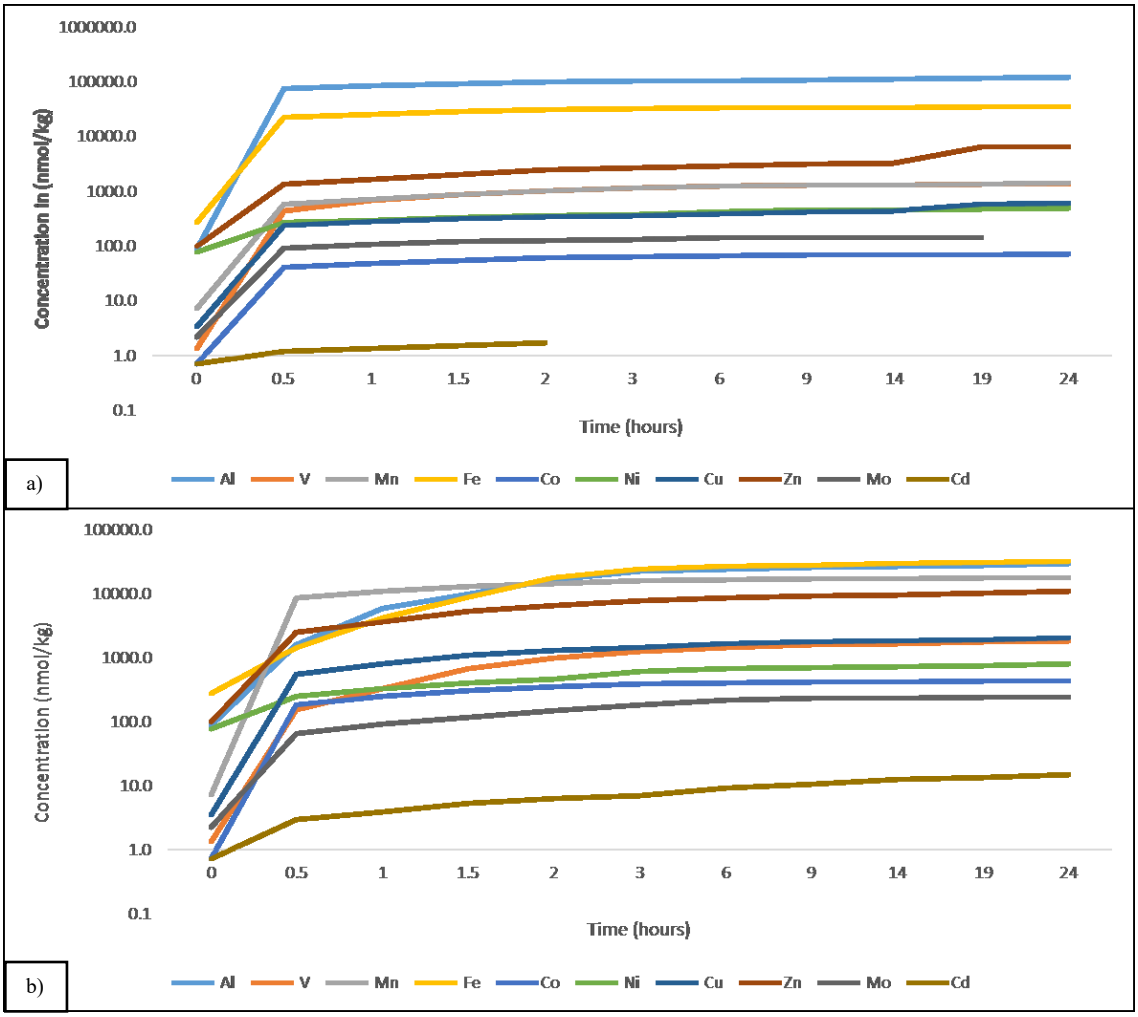

Figure 4-11 Solubility of sediments from the (a) Kuiseb River (30 microns) over 21 hours duration and for (b) Omaruru River (30 microns).

4.3.7 Kuiseb River (30 µm)

There appeared to be a much gradual increase in terms of Al and Fe have the highest trace elemental composition for the sediments samples from the Kuiseb River, with Mn having a relatively high concentration in comparison to other trace elements (Figure 4-11). However, the behavior of Fe and Al for fine fraction of the Kuiseb sample is very different compared to all the other samples from the various sources. Trace elements such as Zn, Mn, V, Co, Mo and Zn show a similar trend as Fe and Al but their concentrations are much lower in comparison to the two. Ni and Pb show a much gradual increase in terms concentrations. Cd is below detection limits and shows a more irregular behavior. There appears to be little to no change in concentration after 6 hours which seem to be the longest compared to all the other dust emitters.

4.4 DISCUSSION

4.4.1 Particle size characteristics

The mean particle size distribution of the sediments showed a general relative abundance of fine sediments (<100 µm) with the exception of Makgadikgadi Pan. Sample from Makgadikgadi appeared to be coarser and angular grained which is an indication that it must have been collected close to the source rocks. The presence of fragments of calcite, dolomite and halite is also an indication that the samples must be close to the bedrock. Occasional flooding and extreme drying events of the ephemeral pan surfaces results in salts on or near the surface and over geological timescales, such minerals accumulated in the pan (Eckardt et al. 2008). In comparison to the other samples, the Makgadikgadi sample is the most poorly sorted, collected as soil sample, while the Etosha, Kuiseb and Omaruru appeared to be crust samples. Hence, naturally the crust samples are more sorted, finer grained and more exposed to longer fluvial transport mechanisms which will influence particle size distribution results. Studies by Dansie et al (2017) found that Etosha and Makgadikgadi Pan had very similar particle size distribution with some instances, Etosha Pan being coarser grained such as in the valleys. The coarse grained texture of the Makgadikgadi sample is merely a representative of the collected sample, while other studies such having recorded finer grain size distributions for the area (Dansie et al. 2017; Vickery 2014; Bhattachan et al. 2015). Particle size distribution of the samples from Kuiseb and Omaruru river is in similar ranges to other ephemeral rivers along the Namibian coastline which predominantly had over 80% of <1000 µm grains (Dansie et al. 2017; Von Holdt 2013).

4.4.2 Mineralogy of known dust emitting sources

Ultimately, the mineralogical composition hugely influences the trace geochemistry of the sediments. Heine & Völkel (2010) mapped and described clay minerals across Namibia and Botswana with their results being comparable to our study because of various reasons, among them being that they sampled in similar localities and used a similar analytical technique, which is the XRD in this case. Overall, their findings showed that most of the samples mineral compositions ranged from quartz, feldspars, Fe-oxides (goethite), calcite, dolomite and traces of other non-clay species (Heine & Völkel 2010). Their findings showed that the Kuiseb and Ugab valleys are dominated by illite, with smectite, kaolinite from weathered feldspars and a

mixed layer clay minerals and chlorite being important components as well. They found no palygorskite which was interpreted to be a sign that there is minimal dispersion of dust by wind dispersion transported from the central mountainous regions to the Namib Desert flat plains (Heine & Völkel 2010). Although our results are generally in agreement with the findings by Heine & Völkel (2010), we found muscovite as one of the minerals, which their previous work did not observe. The absence of palygorskite should not be interpreted as a lack of mineral dust dispersed from the Kuiseb River to the Namib Desert because recent work Vickery et al. (2013) and Eckardt & Kuring (2005) have shown in remote sensing studies that the Kuiseb River is the most active dust emitting river in southern Africa. This is an indication that there is constant, active aeolian transport and emissions from the river contrary to the findings by Heine & Völkel (2010).

However, Omaruru sediments contained up to 10% palygorskite with dominantly illite (50-90%), smectite contributing (15-25%) which means that there is an impact from the central mountainous regions, kaolinite is present with 10-20% (Heine & Heine 2002). These findings are in agreement with what we found in the samples from Omaruru although in addition we found muscovite and anorthite. The local geology around between Swakopmund and Henties Bay is dominated by arkosic, micaceous gneisses and feldspathic quartzites of the Etusis Formation outcrop in narrow zones around the granitic or gneissic cores of domes and anticlines (Lehtonen et al. 1996). The rocks from these formations can be eroded and weathered into the Omaruru River and can therefore be found in the sediment samples. The muscovite and anorthite might most probably be from the surrounding geology with most of the rocks in the area from the Damara Sequence have abundant micaeous minerals such as muscovite and biotite (Lehtonen et al. 1996).

The Etosha Pan is characterised by fairly high amounts of sepiolite (80-100% in some samples) and palygorskite according to Heine & Völkel (2010). The weathered minerals in the Etosha Pan are also enrich in sepiolite and palygorskite, which are the main clay minerals in the underlying geological rocks (carbonaceous rocks such as dolomites and limestones). Sediments found in the bed surface of the Etosha Pan are part of the Kalahari Group (Thomas & Shaw 1991) which are usually covered of bedrock composed of Etosha calcrete and Etosha Pan Clay (Bush and Rose 1996). The occasional flooding and drying of the pan results in surface

evaporites rich in halite, carbonate, and dolomite (Buch and Rose, 1996). Our study in addition found considerable amount of montmorillonite, iron silicon and analcime during the XRD analysis (Appendix D-F). The fine portion of the Etosha pan sediments is due to constant inflows of complex ephemeral networks which are the major contributor of fine-grained sediments from the northern regions (Bryant 2003). The geochemical and physical characteristics of sediments in the Etosha and Makgadikgadi Pans are mainly due to the occasional flooding and drying processes coupled with weathering and dispersion of the suspended finer sediments (Bhattachan et al. 2015). Analcime appeared to be very pronounced in the samples and was observed in previous work conducted by Buch & Rose (1996). In most paleo lake environments, the K-feldspar usually replaces the salt rich centres of the lakes. Presence of analcime can be interpreted as the underlying pan was salty and the available solutions were rich in potassium and dissolved silica (SiO_2) according to Buch & Rose (1996). Work by Buch & Rose (1996) also found higher calcite content in the Etosha Pan in comparison to the Makgadikgadi Pan, which was interpreted as an indication of wetter meteorological conditions in the Makgadikgadi system.

In the Makgadikgadi Pans, the clay content of the soils is characterised by high fractions of smectite (80%) and low fractions of palygorskite (10%), as well as illite and mixed-layer clay minerals (5%). Eitel (2000) indicated that high content of palygorskite in the clay fractions show that clay has been recycled (and that means aeolian long distance transport). Work by Eckardt et al (2008) has shown that the sources of ions in the Makgadikgadi Pan are related to the network of streams flowing (or that used to flow) into the basin and the underlying geology and atmospheric inputs. A significant portion of the dust production is due to inundation events, which leaves the pan surface dry with precipitated calcite, dolomite and halite (Eckardt et al. 2008), occurring over long periods and accumulation of salt deposits in the pan floors. The occurrence of calcite, quartz and silicon oxide is in agreement with the mineralogy observed by work of Eckardt et al., (2008) and Heine & Völkel (2010). Calcite has been associated with fluffy sediments and suggested to be able to rise the onset of wind speed necessary for deflation (Goudie & Middleton 2006). The particle size distribution of the sediments from both pans and rivers have grain sizes dominantly ranging at < 100 µm which shows that these sediments can potentially be airborne dust. Mahowald et al. (2009) revealed that the size range most commonly found in airborne dust is usually under 100 µm. surface samples collected from these river and sources are also known to emit dust (Vickery et al. 2013).

4.4.3 Trace elemental chemistry

Evaluating the dust elemental composition is significant to predict the potential micro and macronutrients provided to oceans from sources, hence affecting the biological productivity (Zhang et al. 2015). Eltayeb et al. (1992) analysed different soil fraction from the Namib dessert and found that for dust concentrations of elements such as Al, Si, K, Rb and Sr where not varying based on the particle size, while concentration of elements such as Ca, Ti, Mn, Fe, Y and Zr tend to rise with a decrease in the particle size distribution. This showed that both major and trace elements display specific partitioning patterns based on size fractions. Similar studies analysed over 200 soil samples from the Namib and found that the average calcium content in the region is double as high as the global measured concentrations (Evens. 1978). The main minerals in the Namib desert are feldspar and quartz near the coast, and feldspar, garnet, monazite, opaque and ore minerals towards the central regions (Eltayeb et al. 1993). Our assumption is that most of the above mentioned minerals must predominantly be coarse grained fraction and will not necessarily be found in the river valleys. Some studies have indicated that based on particle size distributions, major and trace elements can vary (Eltayeb et al. 1992).

Studies by Qu (2016) compared elemental compositions from Patagonia and Namibia soils and found the mean Fe_2O_3 concentration was 6.3 ± 1.8% for dust from Patagonia and 8.2 ± 2.1% for dust in Namibia. That study also found that there is no significant difference in iron concentration between dust and parent sediments in Patagonia, while a difference was observed in the Namibian soils. That study concluded that the Namibian samples were more enriched in most of the trace elements in comparison to dust from Patagonia. The high calcium content of southern African dust than the global average content could increase solubility which will ultimately lead to high bioavailability. Work by Baker et al. (2013) identified that Fe and Al solubilities from Sahara sources lie in the lower ranges in comparison to Southern Hemisphere sources.

This study focused on the trace metal composition of the sediments in the dust emitting rivers and pans in Namibia and Botswana, with an emphasis on the bioactive trace elements such as Cu, Zn, Fe, Cd, and Si and Mg as crustal materials. Majority of the other trace metals displayed a complex degree of variation in Omaruru and Kuiseb River soils concentration in comparison

to the Etosha and Makgadikgadi Pan. There is a correlation between Li, Ti, V, Mn, Co, Ni, Cu, Zn, Mo, Cd, Al, K, Fe and P which can be due to the alumino-silicates such as (kaolinite, illite and montmorillonite), especially for Si, Al, K and Fe in the dust fraction (Qu 2016). Aluminium showed a similar variation and behaviour pattern to Fe. Areas such as Omaruru and Kuiseb River show high Cu concentrations which might be toxic to the phytoplankton communities, work by Paytan (2009), revealed that the brink toxicity in laboratory experiments was between 0.2 and 2 µg of Cu per microgram of Chlorophyll A in some organisms. The Cu concentrations for both these sources are already over this threshold, and dust solubility tend to increase as it travels in the atmosphere, meaning such dust could potentially be toxic to the phytoplankton communities.

4.4.4 Bioavailability of dust emitters

Dust iron bioavailability is usually altered during airborne transport by factors such as photochemical reduction, aqueous complexation and chelating effect of organic ligands (Sholkovitz et al. 2012). This means that low iron solubility values from sources should be taken with the consideration that during atmospheric transport, the aerosols can potentially become more soluble and hence bioavailable. Iron solubility is also influenced by numerous factors such as mineral dust particle sizes, microbial organisms activities, and the occurrence of seawater iron-complexing organic ligands (Baker & Croot 2010). The estimations being described in this study will be used to relate the iron content among the diverse dust emitting regions. The bioavailability content of Fe and other trace elements from the Etosha pan is the highest which could most probably be explained by the aerosol size fractions. Samples from the Etosha pan appears to be having the highest solubility, which makes sense because Ca-enriched minerals are easily soluble than Fe-enriched minerals. The area off the Namibian coastline have been found to contain permanent low lying clouds which are usually polluted with smoke from inland biomass burning (black carbon) (Venter et al. 2015). These could possibly reduce the pH of the clouds in the area, which could potentially increase the solubility of the trace elements as they travel from inland sources to the various different directions.

Samples from Etosha pan appeared to be the most soluble compared to all the different dust emitters. Higher solubility and dissolution behaviour for Ca-rich minerals is in agreement with similar studies conducted by Aghanatios et al. (2014), who supposed that a high proportion of calcite and dolomite (Aghanatios et al., 2014). The dissolution (bioavailability) of the

Makgadikgadi pan is higher than for the two ephemeral rivers (Omaruru and Kuiseb River). In terms of Fe chemistry from the different locations revealed that the Etosha, has the lowest overall trace elemental composition but has the highest solubility, which appears to be a trend between mineral dust and iron solubility. When sediments contain low iron concentration, the comparative solubility of iron is high, while the reverse occurs when the sediments contain high iron concentration, solubility tends to be low (Sholkovitz et al. 2012). These results showed that bioavailability is rather influenced by the mineralogy rather than the particle sizes.

The results from our leaching/filtering experiments indicated that the dissolution of the soils from southern Africa is very low, with values ranging from 0.01 to 25%. However, what was surprising is the fact that the samples from the fine grained fraction of the Kuiseb River has the lowest solubility. The overall expectation is that the finer grained fraction should be more soluble because of greater surface areas and more adsorption sites for dissolution to take place. Fine mode aerosols seem to produce larger iron solubility than coarse grained mineral dust sediments (Baker & Jickells 2006). The higher solubility associated with the Etosha pan is in agreement with our general expectations because the Etosha samples has the finest grain size distribution and has high calcite abundance which is more easily soluble in comparison to the other minerals associated with the other dust emitting sources. Fung et al. (2010) showed that soluble iron in sediments contributes only roughly 0.5% of complete iron. Work by Hand et al. (2004) also found similar values which showed very low for soluble iron in soils although measurements of soluble iron of aerosols in the atmosphere. Fe solubility is much higher in the atmosphere which can be interpreted as that there is processing of soluble iron during transport from sources to oceans where the Fe eventually gets deposited (Zhuang et al. 1992). Studies on bioavailability of sediments/soils from Namibia and Patagonia by Qu et al. (2016) has shown that the solubility of Fe in pure water fluctuated from 0.4% to 8.6%, with geometric average solubility of 2.6 ±1.0% (geomean ± SD) (Qu 2016). These values are in correlation with our values although the solubility for the Etosha sample was 26%. Aghnatios et al. (2014), found dissolved Fe solubility for alluvial soil in Tunisia to be 0.04% with ultrapure water as a reagent (Table 4-2). Work by Baker et al. (2006) and Jickells et al. (1995) demonstrated that elements such as Al and Mn show a slightly higher solubility than Fe is in agreement with our results. Ca-rich minerals tend to dissociate much faster in comparison to Al-rich minerals, which have stronger chemical bonding between the particles to dissociate iron-bearing minerals.

Table 4-2 Estimation of soluble iron for soil in this study.

Sample Type	Leaching Solution	Leaching time	DFe %
Etosha Pan	Ultrapure water	21 hours	25.8
Makgadikgadi Pan	Ultrapure water	17 hours	0.58
Kuiseb River	Ultrapure water	18 hours	0.002
Omaruru River	Ultrapure water	21 hours	0.1
Kuiseb River (30 µm sieved)	Ultrapure water	24 hours	0.07
Omaruru River (30 µm sieved)	Ultrapure water	24 hours	0.07

When comparing the percentage of dissolved iron (DFe%) in this study with other similar studies which looked at the dissolution of Fe, some of our values are similar to some of the studies besides the huge range (Table 4-3). This further shows the need for a more standard method to determine the solubility of Fe and standard reagents and set leaching time to have a more universal comparison of the results.

Table 4-3 Some preceding approximations of iron solubility conducted at a variety of leaching experimental methods

Reference	Sample Type	Leaching Solution	Leaching time	DFe%
Spokes and Jickells (1995)	Saharan aerosol collected by North African coast	pH2	24 hours	4.7 ± 0.2
		pH 5.5		0.3
		pH8		0.1
Aghnatois et al (2014)	Alluvial soil from Tunisia, <20 µm	Ultrapure water	4 min	0.04
		pH5 HNO_3		0.07
		pH3 HNO_3		0.26
		pH1 HNO_3		0.93
Aguilar-Islas et al. (2010)	Alaska Coastal urban aerosol	Ultrapure	1, 30, 90 min	1.8, 2.1, 2.3
		UV oxidized seawater		1.5, 1.7, 1.8
		UVSW + deferrals		2.6, 2.8, 3.2

Reference	Sample Type	Leaching Solution	Leaching time	DFe%
Buck et al (2010)	Aerosol collected over North Atlantic	Ultrapure water	Instantaneous	3 - 47
	Saharan aerosol collected over North Atlantic	seawater		1 – 26
Heimburger et al. (2013)	Rainwater collected over Kerguelen		Instantaneous	51 - 91
Edwards and Sedwick (2001)	Surface snow in East Antarctica		After melting	9 - 89

This solubility is increased during transport by chemical and photochemical mechanisms through the atmosphere which would be achievable during laboratory results (Spokes et al. 2001). Solubility variety is from as low as 0.01% to as high as 80% and are vastly unrelated in space and time (Mahowald et al. 2005). Although, the solubility of the bioactive trace elements is low and show low enrichment, the atmospheric transport processing that will lead to increase bioavailability of trace metals in aerosols from southern Africa can play a key role on ocean primary productivity. Although, under oxic condition and active photochemistry, iron is known to have low fractional solubility in comparison to the trace metals. (Jickells et al. 2005). The large variation in iron solubility results is mainly due the heterogeneous nature of the ocean and atmospheric systems, but also due the high variation of methods by researchers on how to determine the solubility of Fe. Work by Witt et al (2010) showed that with atmospheric transport, iron fractional solubility can increase by approximately 5% in samples collected in the south east Indian Ocean along the coast of Madagascar. This demonstrates the fact that aerosol processing during transport make Fe more soluble. Mineral dust originating from southern Africa appear to have high iron concentrations in comparison to the mean concentration of the global mainland crust (Witt et al. 2006; Witt et al. 2010).

Other studies which investigated the bioavailability of Fe in southern African sources is the work by Bhattachan et al (2015) and Dansie et al (2017), has shown that ferrous iron (Fe^{2+}) was higher in the parent material (< 63 µm – 2000 µm) than the fine faction (<63 µm). Dansie et al (2017) found that there was much higher bioavailable Fe in the ephemeral rivers in comparison to the ephemeral pans. However, more importantly these results cannot be directly related to our study because of the different methods used to determine the bioavailable iron. Those two studies analysed their samples bioavailable iron through the DTPA extraction with

flame Atomic Absorption OR ICP spectrometry method (Bhattachan et al. 2015; Dansie et al. 2017), which is completely different from a continuous flow through method.

4.4.5 Continuous flow method

One of the major advantages of using the flow through continuous method in comparison to the traditionally widely used batch leaching is because it is less expensive. Majority of the solubility all the trace elements occur during the first 3 hours, which means that the continuous flow method can save time and the use of less reagents for solubility experiments. The time span of roughly one day, which was implemented in this study, shows that there is insignificant extraction of trace elements after 3 hours and extraction experiments could be stopped by then already. Majority of the samples, we observed a fast extraction of trace elements for the first 30 – 60 minutes of sediment contact with the reagent (Milli-Q water). Aerosols become more soluble with a decrease in pH, with work by Longo (2016), showing that aerosols become more acidic with increased transport time (>15 days), meaning the aerosols deposited are expected to have higher solubility due to the transport from sources. This suggests that the proton reactions are solubilizing the trace elements (including Fe) during transport.

There is still no agreement on the most suitable method that can yield the accurate value of iron solubility. However, what is commonly agreed upon is that a standard aerosol filtering procedure would be an essential stride to an enhanced understanding of mineral dust trace elemental solubility rates. This can be achieved by focusing on the mineralogical characteristics of aerosols at fine grained scale. The utilization of deionized water as one of the reagents in continuous flow through experiments is one way of making results comparable. Some researchers argue that deionized water has high pureness which offers a reliable and repeatable filtering solution, allowing assessment among various field studies and investigations (Buck et al. 2006; Sedwick et al. 2007). Several studies have used deionized water, which has a comparable pH to that of non-acidified cloud. Leaching aerosols and sediments with deionized water at pH of approximately 5.5 simulates the dissolution of mineral iron-enriched dust in wet deposition (Buck et al. 2010). However, this extraction solution has weak to no buffer capacity and essential pH fluctuations are anticipated when batch experiments using sediment samples with different mineralogical characteristics are studied (Simonella et al. 2014). The continuous

flow methodology uses much less water as the solutions are continuously reintroduced during the method (Simonella et al. 2014).

Most studies tend to utilise soil/sediment as a substitute for mineral dust although preferably research investigating dust, will ideally use airborne dust but airborne dust is difficult to get and not always readily obtainable in large amounts (grams), which is a necessity for most of the metal leaching and extracting experiments. Samples collected as airborne are usually limited in mass, usually obtainable in very small quantities (Simonella et al. 2014), forcing researchers to place dust with sediment/soil as a substitute (Desboefs et al. 1999; Mackie et al. 2006). However, when using soil/sediment samples important factors such the sand abrasion, chemical processing during transport and disaggregation of grains during transport are neglected. Another factor is that to obtain a representative sample of the dust, it is essential to find sieving techniques to separate different size fractions time efficiently without compromising on the quality of the samples (Simonella et al. 2014).

4.5 CONCLUSION

The results of the laboratory analyses showed the potential dissolution rate of sediments southern African and how it potentially can be the source of limited bioactive trace elements to phytoplankton communities. The dissolution of trace metals (and Fe in particular) in the continental crust is a crucial part for developing a greater understanding of the role of bioactive trace elements in the biological pump and the carbon cycle which can ultimately remove carbon dioxide from the atmosphere. Our results show the important role that sources from southern Africa can play in terms of fertilising oceans, especially the ephemeral rivers which are regions that have never been investigated for bioavailability to proximal oceanic regions. As the refractive index of mineral dust is contingent on the mineralogical characteristics and geochemical composition of dust over any area, additional research is essential to identify the predominant mineralogical composition of dust over different source areas (Choobari & Sturman 2014).

The proximity of the ephemeral rivers to the ocean in comparison to Etosha (approximately 400 km away from Atlantic Ocean) and Makgadikgadi Pans (1200 km from open oceans) means that rivers will have increased incidence of deposition over the ocean and can prove to be important sources of trace elements to marine productivity. We hypothesise that the mineralogy coupled with the fine grained particles of Etosha pan most probably controls the high solubility as compared to the two ephemeral rivers. Our results support the findings of Journet et al. (2008), who report that the mineralogical composition of mineral aerosols, independent of particle surface area, was the primary determinant for Fe bioavailability. In addition, the results show that the ephemeral rivers and pans in southern Africa are a source of bioavailable trace elements, which are of a particle size suitable for long range transport, and are therefore probable to play a part in the fertilisation of the South Atlantic.

The continuous flow method aims to mimic the mechanism of bioactive trace metals dissolution during atmospheric transport while interacting with clouds prior to the exchange sediments with surface oceanic deposition (Simonella et al. 2014). Work by Simonella et al. (2014) has highlighted the advantages of the continuous flow method, which include: the fact that most of the common used reagents are readily available in many laboratories, permits dissolution rates studies with insignificant sum of samples and with great repetition. The

dissolution process can track in near real time conditions, which cannot be conducted through bunch techniques.

CHAPTER 5: OVERALL DISCUSSION AND CONCLUSIONS

Our study shows that dust emissions from southern Africa can be a significant source of trace elements to the surrounding oceans which are in proximity and capable of fertilising regions which are thousands of kilometres away. The location of the dominant sources which is in the northern parts of southern Africa weakens the ability of dust to travel substantial distances especially to the Southern Ocean region, which is a region limited in this bio-active trace elements. A significant proportion of the dust tend to travel towards the north-west Atlantic Ocean and the south-east. Indian Ocean region which are areas which not necessarily depleted in micronutrients. Only a small proportion of dust from southern Africa travels towards the Southern Ocean. The proximity of the rivers to the ocean is expected to cause in a higher deposition of trace elements into the ocean, even in periods when the emissions are not strong. Our findings clearly show that the ephemeral rivers must have a significant contribution of aerosols to the open oceans and can influence the biogeochemical and marine productivity should be highly considered in further studies. Our models also show that the region where dust emissions preferentially travel to from southern Africa are not bio-limited, which could mean that these regions might be supplied with dusts from the southern African region.

The dissolution rates experiments have revealed that the highest trace element composition does not necessarily mean that it will higher bioavailability. Two ephemeral rivers, namely the Omaruru and Kuiseb are more enriched overall in terms of the trace elements. This did not show the highest solubility (bioavailability) which indicates that the high trace elemental composition is not available to the phytoplankton communities. Highest solubility was observed in the Etosha pan samples, which could have been attributed to the fine grain texture and the fact that the dominant minerals are Ca-rich which are highly soluble. However, the low solubility of the two ephemeral rivers should be taken into account that during transport, most probably the coarse fractions minerals such as quartz and feldspar will settle out leaving the clay minerals, which will ultimately increase the solubility. Our findings showed that mineralogical composition appeared to affect the solubility more in comparison to particle size in contrast to previous studies.

Although the solubility of the trace elements appeared to be influenced by the grain size to a certain extent between the different dust emitting sources, the same cannot be said when it comes to sieved fraction of the two ephemeral rivers. There appeared to be a higher solubility in the coarser fraction in comparison to the finer fraction, which could mean that soluble phase is associated with the coarser fraction rather than the fine fraction. Hence, the relationship between the particle size and solubility is not linear (Baker & Jickells 2006), there might be instances where the coarser fraction will have higher solubility.

5.1 OVERALL RECOMMENDATIONS

More field sampling measurements are needed to better quantify the amount of dust emitted from the various sources and collect more long term records which can be used to compare the evolution of aerosols over a long term period. Actual dust concentration data from the field dust traps will be valuable to minimise possible sources and calculate the modelling results (Li et al. 2008). Especially in the Southern Ocean were the remote sensing observations are hindered by the predominantly cloudy atmospheres (Gasso & Stein. 2007). More shipboard measurements of atmospheric aerosol composition are also recommended. Measurements of more vertical distributions of atmospheric dust, such as the use of CALIPSO is needed to better estimate the dust migration from these source regions (Figure 5-1). Scanning Electron Microscope (SEM) examination analyses are also recommended to better understanding the individual grain sizes and chemistry of the grains.

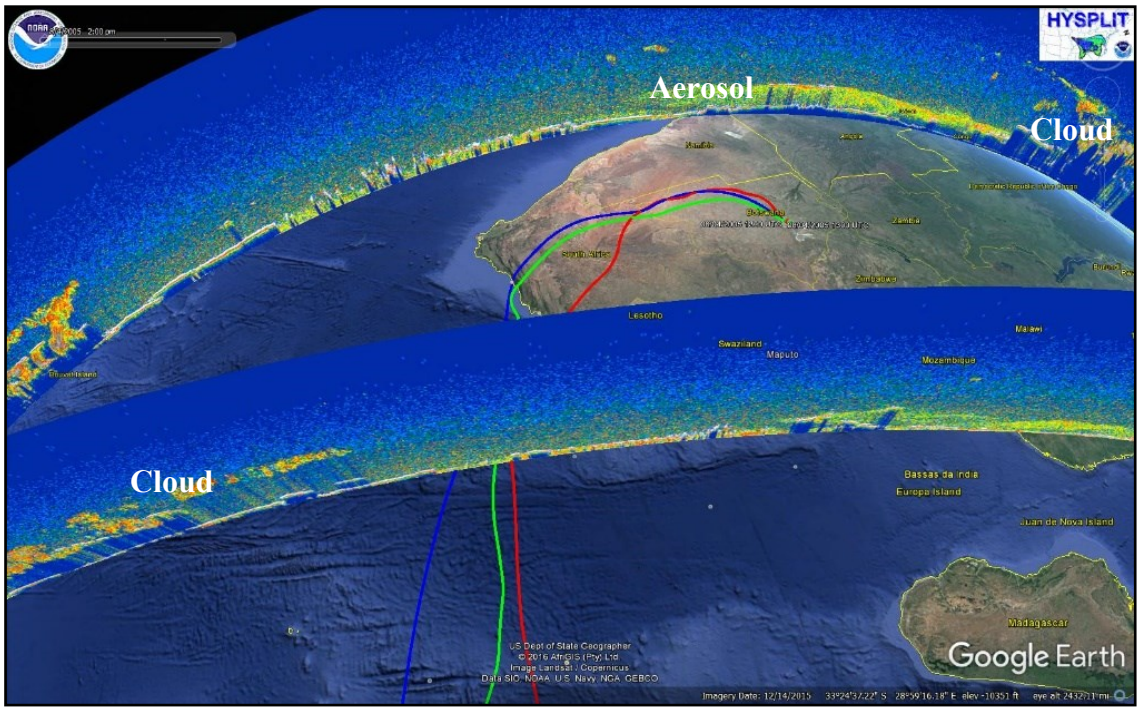

Figure 5-1 CALIPSO Screenshot showing the presence of dust (aerosols) around the height of 5000 m above sea level from southern Africa off to the Atlantic Ocean.

Space-borne LiDAR interpretations of aerosols research (ranging from clouds, smoke and mineral dust) over southern Africa display that on incidents a permanent aerosol layer is covered at the roughly 500 hPa level for areas surpassing 500 square kilometres (Winker et al., 1996). CALIPSO is effective at providing dimensions of aerosol vertical outlines and it can roughly separate among numerous aerosol types such as dust, smoke and pollution. We have used CALIPSO night time observations for dust mass flux, for the high superiority of night time records. An understood hypothesis is that a CALIPSO detected aerosol shape at night is a good illustration of the daily mean (Yu et al. 2016).

More monitoring stations are needed to specifically sample for actually airborne dust to better quantify the amount of dust that gets transported from the sources, as well as what is potentially caused by the anthropogenic effects. Specifically, the bioavailable phase. A major concern when monitoring and running dust collecting exhibitions is the lack of getting sufficient material to conduct experiments, and this is the contributing factor why so many studies use soil as a surrogate for dust. There is a necessity for thorough data on global mineralogy to advance predictions of the environmental and climatic influences of dust. There is a lack of data on the parent soils mineralogical compositions and physical characteristics globally (Journet et al. 2014). In order to truly understand the Fe that becomes bioavailable to the phytoplankton communities, studies should also focus on measuring the portion in the atmosphere to enhanced comprehend the sources and the processes of the bioavailable trace metals deposits to the open oceans. There is a necessity for a global standard technique/measuring method for the bioavailable portion in measurements. There needs to be a better agreement in terms of the leaching experiment that can be used measure the solubility of the aerosols.

Although this study focussed on whether southern African dust can fertilise the open oceans thousands of kilometres away, regions such as the Benguela upwelling system may also be limited in trace elements such as Fe. Therefore, this study can assist the fishing industry companies along the Namibian and South Africa coastlines as to the effects of dust on the surrounding open oceans. Dust emissions from sources such as the Kuiseb and Omaruru river could potentially be toxic to the phytoplankton along the entire Namibia, South Africa and Angolan coastlines if it becomes bioavailable. The existence of the black-carbon rich low-level

clouds off the Namibian and Angolan coastlines could potentially increase the solubility of the dust that is being transported from inland to oceans, this in turn can increase the bioavailability of the southern African dust. In contrast, current climatic models predict that dust and aerosols in the atmosphere will decrease by up to 60% which will result in a double increase of atmospheric carbon dioxide (Mahowald et al. 2009). Our data aims to contribute to the global climatic models, in terms of fillings gaps on the dust pathways from southern Africa.

REFERENCES

Aguilar-Islas, Ana M, Jingfeng Wu, Robert Rember, Anne M Johansen, and Lindsey M Shank. 2010. "Dissolution of Aerosol-Derived Iron in Seawater: Leach Solution Chemistry, Aerosol Type, and Colloidal Iron Fraction." *Marine Chemistry* 120 (1–4). Elsevier B.V.: 25–33. doi:10.1016/j.marchem.2009.01.011.

Ashrafi, Khosro, Majid Shafiepour-Motlagh, Alireza Aslemand, and Sarmad Ghader. 2014. "Dust storm simulation over Iran using HYSPLIT." *Journal of Environmental Health Science & Engineering* 12 (1): 9. doi:10.1186/2052-336X-12-9.

Baker, A R, and T D Jickells. 2006. "Mineral particle size as a control on aerosol Iron solubility." *Geophysical Research Letters* 33 (17): 1–4. doi:10.1029/2006GL026557.

Baker, Alexander R, and Peter L Croot. 2010. "Atmospheric and marine controls on aerosol Iron solubility in seawater." *Marine Chemistry* 120 (1–4). Elsevier B.V.: 4–13. doi:10.1016/j.marchem.2008.09.003.

Baker, Alex R., M. French, and K. L. Linge. 2006. "Trends in aerosol nutrient solubility along a West-East transect of the Saharan dust plume." *Geophysical Research Letters* 33 (7): 10–13. doi:10.1029/2005GL024764.

Barbeau, K, E L Rue, Kenneth W Bruland, and A Butler. 2001. "Photochemical cycling of Iron in the surface ocean mediated by microbial iron (III) -binding ligands." *Letters of Nature* 413 (1): 410–12. doi:10.1038/35096545.

Bhattachan, A, P D'Odorico, and G S Okin. 2015. "Biogeochemistry of dust sources in southern Africa." *Journal of Arid Environments* 117. Elsevier Ltd: 18–27. doi:10.1016/j.jaridenv.2015.02.013.

Bhattachan, Abinash, Paolo D'Odorico, Matthew C Baddock, Ted M Zobeck, Gregory S Okin, and Nicolas Cassar. 2012. "The Southern Kalahari: A potential new dust source in the Southern Hemisphere?" *Environmental Research Letters* 7 (2): 24001. doi:10.1088/1748-9326/7/2/024001.

Bhattachan, Abinash, Lixin Wang, Molly F Miller, Kathy J Licht, and Paolo D'Odorico. 2015. "Antarctica's Dry Valleys: A potential source of soluble iron to the Southern Ocean?" *Geophysical Research Letters* 42 (6): 1912–18. doi:10.1002/2015GL063419.

Bolin, Bert, and Henning Rodhe. 1973. "A note on the concepts of age distribution and transit time in natural reservoirs." *Tellus* 25 (1): 58–62. doi:10.1111/j.2153-3490.1973.tb01594.x.

Botes, A, J Henderson, T Nakale, K Nantanga, K Schachtschneider, and M Seely. 2003. "Ephemeral rivers and their development: testing an approach to basin management committees on the Kuiseb River, Namibia." *Physics and Chemistry of the Earth* 28 (20–27): 853–58. doi:10.1016/j.pce.2003.08.028.

Boyd, P W, T Jickells, C S Law, S Blain, E A Boyle, K O Buesseler, K H Coale, et al. 2007. "Mesoscale iron enrichment experiments 1993–2005: synthesis and future directions." *Science* 315: 612–17.

Boyd, P W, D S Mackie, and K A Hunter. 2010. "Aerosol iron deposition to the surface ocean - modes of iron supply and biological responses." *Marine Chemistry* 120 (1–4). Elsevier B.V.: 128–43. doi:10.1016/j.marchem.2009.01.008.

Boye, M, A Aldrich, C M G van den Berg, J T M de Jong, H Nirmaier, M Veldhuis, K R Timmermans, and H J W de Baar. 2006. "The chemical speciation of iron in the north-east Atlantic Ocean." *Deep-Sea Research Part I: Oceanographic Research Papers* 53 (4): 667–83.

Bozlaker, Ayse, Joseph M Prospero, Matthew P Fraser, and Shankararaman Chellam. 2013. "Quantifying the contribution of long-range Saharan dust transport on particulate matter concentrations in Houston, Texas, using detailed elemental analysis." *Environmental Science and Technology* 47 (18): 10179–87. doi:10.1021/es4015663.

Brand, Larry E, William G Sunda, and Robert R L Gulillard. 1983. "Limitation of marine phytoplankton reproductive rates by zinc, manganese, and iron." *Limnology and Oceanography* 28 (6): 1182–98.

Breviere, Emily, Nicolas Metlz, Alain Poisson, and Tilbrook Bronte. 2006. “Changes of the oceanic CO_2 sink in the eastern Indian sector of the Southern Ocean.” *Tellus* 58B (February 1997): 438–46. doi:10.1111/j.1600-0889.2006.00220.x.

Bryant, Robert G. 2003. “Monitoring hydrological controls on dust emissions: Preliminary observations from Etosha Pan, Namibia.” *The Geographical Journal* 169 (2): 131–41. doi:10.1111/1475-4959.04977.

Bryant, Robert G. 2013. “Recent advances in our understanding of dust source emission processes.” *Progress in Physical Geography* 37 (3): 397–421. doi:10.1177/0309133313479391.

Bryant, Robert G, Grant R Bigg, Natalie M Mahowald, Frank D Eckardt, and Simon G Ross. 2007. “Dust emission response to climate in southern Africa.” *Journal of Geophysical Research Atmospheres* 112 (9): 1–17. doi:10.1029/2005JD007025.

Buck, Clifton S., William M. Landing, Joseph A. Resing, and Christopher I. Measures. 2010. “The solubility and deposition of aerosol fe and other trace elements in the North Atlantic Ocean: Observations from the A16N CLIVAR/CO2 Repeat Hydrography Section.” *Marine Chemistry* 120 (1–4). Elsevier B.V.: 57–70. doi:10.1016/j.marchem.2008.08.003.

Buck, Clifton S., William M. Resing, Joseph A Resing, and Geoffrey T Lebon. 2006. “Aerosol Iron and aluminum solubility in the northwest Pacific Ocean: Results from the 2002 IOC Cruise.” *Journal of the Earth Sciences* 7 (4): 1–21. doi:10.1029/2005GC000977.

Bullard, Joanna E, Sandy P Harrison, Matthew C Baddock, Nick Drake, Thomas E Gill, Grant McTainsh, and Youbin Sun. 2011. “Preferential Dust Sources: A geomorphological classification designed for use in global dust-cycle models.” *Journal of Geophysical Research: Earth Surface* 116 (4). doi:10.1029/2011JF002061.

Chan, Y C, R W Simpson, G H Mctainsh, P D Vowles, D D Cohen, and G M Bailey. 1999. “Source apportionment of visibility degradation problems in Brisbane (Australia) Using the Multiple Linear Regression Techniques.” *Chemical Analysis* 33: 3237–50.

Chan, Yc, and Rw Simpson. 1997. “Characterisation of chemical species in pm 2.5 and pm 10 aerosols in Brisbane, Australia.” *Atmospheric …* 31 (22): 3773–85.

Chance, Rosie, Timothy D Jickells, and Alex R Baker. 2015. "Atmospheric trace metal concentrations, solubility and deposition fluxes in remote marine air over the South-East Atlantic." *Marine Chemistry* 177. The Authors: 1–12. doi:10.1016/j.marchem.2015.06.028.

Chever, F, E Bucciarelli, G Sarthou, S Speich, M Arhan, P Penven, and A Tagliabue. 2010. "Physical speciation of iron in the Atlantic Sector of the Southern Ocean along a transect from the subtropical domain to the weddell sea gyre." *Journal of Geophysical Research: Oceans* 115 (10): 1–15. doi:10.1029/2009JC005880.

Choobari, O Alizadeh, and A Sturman. 2014. "The global distribution of mineral dust and its impacts on the climate system : A review." *Atmospheric Research* 138. Elsevier B.V.: 152–65. doi:10.1016/j.atmosres.2013.11.007.

Compton, John, Caren Herbert, and Ralph Schneider. 2009. "Organic-rich mud on the western margin of southern Africa: nutrient source to the Southern Ocean?" *Global Biogeochemical Cycles* 23 (4): 1–12. doi:10.1029/2008GB003427.

Cooke, H J. 1979. "The origin of the Makgadikgadi Pans." *Botswana Notes and Records* 11 (1979): 37–42.

Cosijn, C, and P D Tyson. 1996. "Stable discontinuities in the atmosphere over South Africa." *South African Journal of Science* 92 (August).

D'Almeida, Guillaum A. 1986. "A model for Saharan dust transport." *Journal of Climate and Applied Meteorology*. doi:10.1175/1520-0450(1986)025<0903:AMFSDT>2.0.CO;2.

Dansie, A P, G F S Wiggs, and D S G Thomas. 2017. "Iron and nutrient content of wind-erodible sediment in the ephemeral river valleys of Namibia." *Geomorphology*. Elsevier B.V, 1–42. doi:10.1016/j.geomorph.2017.03.016.

Does, Michelle Van Der, Laura F. Korte, Chris I. Munday, Geert Jan A Brummer, and Jan Berend W Stuut. 2016. "Particle size traces modern saharan dust transport and deposition across the Equatorial North Atlantic." *Atmospheric Chemistry and Physics* 16 (21): 13697–710. doi:10.5194/acp-16-13697-2016.

Duce, Robert A, and Neil W Tindale. 1991. “Atmospheric transport of iron and its deposition in the ocean.” *Limnology and Oceanography* 36 (8): 1715–26. doi:10.4319/lo.1991.36.8.1715.

Eckardt, F D, and N Kuring. 2005. “SeaWiFS identifies dust sources in the Namib Desert.” *International Journal of Remote Sensing* 26 (19): 4159–67. doi:10.1080/01431160500113112.

Eckardt, Frank D, Robert G Bryant, Graham McCulloch, Baruch Spiro, and Warren W Wood. 2008. “The hydrochemistry of a semi-arid pan basin case study: Sua Pan, Makgadikgadi, Botswana.” *Applied Geochemistry* 23 (6): 1563–80. doi:10.1016/j.apgeochem.2007.12.033.

Elrod, Virginia A, William M Berelson, Kenneth H Coale, and Kenneth S Johnson. 2004. “The flux of iron from continental shelf sediments: a missing source for global budgets.” *Geophysical Research Letters* 31 (12): 2–5. doi:10.1029/2004GL020216.

Eltayeb, M A H, R E Van Grieken, W Maenhaut, and H A J Annegarn. 1993. “Aerosol-soil fractionation for Namib desert samples.” *Atmospheric Environment* 27 (5): 669–78.

Gabric, A J, R Cropp, G P Ayers, G McTainsh, and R Braddock. 2002. “Coupling between cycles of phytoplankton biomass and aerosol optical depth as derived from SeaWifs time series in the Subantarctic Southern Ocean - Art. No. 1112.” *Geophysical Research Letters* 29 (7): 433-436. doi:10.1029/2001GL013545.

Gaiero, D M, J L Probst, P J Depetris, S M Bidart, and L Leleyter. 2003. “Iron and other transition metals in Patagonian riverborne and windborne materials: geochemical control and transport to the Southern South Atlantic Ocean.” *Geochimica et Cosmochimica Acta* 67 (19): 3603–23. doi:10.1016/S0016-7037(03)00211-4.

Gasso, Santiago, and Ariel F Stein. 2007. "Does Dust from Patagonia Reach the Sub-Antarctic Atlantic Ocean ?" *Geophysical Research Letters* 34 (October 2006): 3–7. doi:10.1029/2006GL027693.

Geyh, M A, and D Ploethner. 1995. "Groundwater isotope study in the Omaruru river delta aquifer, Central Namib Desert, Namibia." In *IAHS-AISH Publication*, 163–70. IAHS.

Ginoux, P, J M Prospero, O Torres, and M Chin. 2004. "Long-term simulation of global dust distribution with the GOCART Model : Correlation with North Atlantic Oscillation." *Environmental Modelling & Software* 19: 113–28. doi:10.1016/S1364-8152(03)00114-2.

Ginoux, Paul, Joseph M. Prospero, Thomas E. Gill, N. Christina Hsu, and Ming Zhao. 2012. "Global-scale attribution of anthropogenic and natural dust sources and their emission rates based on MODIS deep blue aerosol products." *Reviews of Geophysics* 50 (3): 1–36. doi:10.1029/2012RG000388.

Goudie, A S, and N J Middleton. 2001. "Saharan dust storms: nature and consequences." *Earth-Science Reviews* 56 (1–4): 179–204. doi:10.1016/S0012-8252(01)00067-8.

Goudie, Andrew, and Nicholas J Middleton. 2006. *Dust in the Global System*. 1st ed. Berlin Heldenberg: Springer-Verlag Berlin Heidelberg.

Goudie, Andrew S, and Nicholas J. Middleton. 2006. *Desert Dust in the Global System*. Edited by Dieter Czeschlik and Andrea Schlitzberger. First. New York: SPI Publisher Services.

Heimburger, A, R Losno, and S Triquet. 2013. "Solubility of iron and other trace elements in rainwater collected on the Kerguelen Islands (South Indian Ocean)." *Biogeosciences* 10: 6617–28. doi:10.5194/bg-10-6617-2013.

Heine, Klaus, and Jan T Heine. 2002. "A paleohydrologic reinterpretation of the Homeb Silts, Kuiseb River, Central Namib Desert (Namibia) and paleoclimatic implications." *Catena* 48 (1–2): 107–30. doi:10.1016/S0341-8162(02)00012-7.

Heine, Klaus, and Jörg Völkel. 2010. "Soil clay minerals in Namibia and their significance for the terrestrial and marine past global change research." *African Study Monographs. Supplementary Issue* 40 (March): 31–50.

Huneeus, N, M Schulz, Y Balkanski, J Griesfeller, J Prospero, Kinne, S Bauer, et al. 1993. "Global dust model intercomparison in aerocom phase I." *Atmospheric Chemistry and Physics* 11: 7781–7816. doi:10.1029/2007JG000640/abstract.

Huntley, BJ. 1985. "The Kuiseb environment: the development of a monitoring baseline." *Foundation for Research Development, CSIR, Pretoria*. doi:ISBN 0798833971.

Jacobson, P J, K M Jacobson, and M K Seely. 1995. *Ephemeral rivers and their catchments: sustaining people and development in western Namibia.* Ed. Windhoek: Desert Research Foundation of Namibia.

Jickells, T. 1995. "Atmospheric inputs of metals and nutrients to the oceans: their magnitude and effects." *Marine Chemistry* 48 (3–4): 199–214. doi:10.1016/0304-4203(95)92784-P.

Jickells, T D. 2005. "Global iron connections between desert dust, ocean biogeochemistry, and climate." *Science* 308 (5718): 67–71. doi:10.1126/science.1105959.

Jickells, Tim, and C Mark Moore. 2015. "The importance of atmospheric deposition for ocean productivity." *Annual Review of Ecology, Evolution, and Systematics* 46 (1): 481–501. doi:10.1146/annurev-ecolsys-112414-054118.

Johnson, Kenneth S, R Michael Gordon, and Kenneth H Coale. 1997. "What controls dissolved iron concentrations in the world ocean ?" *Marine Chemistry* 57: 137–61.

Johnson, M S, and N Meskhidze. 2013. "Atmospheric dissolved iron deposition to the global oceans: effects of oxalate-promoted fe dissolution, photochemical redox cycling, and dust mineralogy." *Geoscientific Model Development* 6 (4): 1137–55. doi:10.5194/gmd-6-1137-2013.

Johnson, MS, N Meskhidze, VP Kiliyanpilakkil, and S Gasso. 2011. "Understanding the transport of patagonian dust and its influence on marine biological activity in the South Atlantic Ocean." *Atmospheric Chemistry and Physics* 11 (6): 2487–2502. doi:10.5194/acp-11-2487-2011.

Journet, E, Y Balkanski, and S P Harrison. 2014. "A new data set of soil mineralogy for dust-cycle modeling." *Atmospheric Chemistry and Physics* 14 (8): 3801–16. doi:10.5194/acp-14-3801-2014.

Knippertz, Peter, and Jan Berend W Stuut. 2014. *Mineral dust a key player in the earth system*. Edited by Peter Knippertz and Jan Berend W Stuut. First ed. New York: Springer.

Krueger, B J, V H Grassian, J P Cowin, and A Laskin. 2004. "Heterogeneous chemistry of individual mineral dust particles from different dust source regions: the importance of particle mineralogy." *Atmospheric Environment* 38 (36): 6253–61. doi:10.1016/j.atmosenv.2004.07.010.

Lam, Phoebe J, J K B Bishop, Cara C Henning, Matthew A Marcus, Glenn A Waychunas, and Inez Y Fung. 2006. "Wintertime phytoplankton bloom in the subarctic pacific supported by continental margin iron." *Global Biogeochemical Cycles* 20 (1): 1–12. doi:10.1029/2005GB002557.

Lehtonen, M I, T E T Manninen, and U M Schreiber. 1996. "Report : Lithostratigraphy of the area between the Swakop , Khan and Lower Omaruru Rivers , Namib Desert." *Commun. Geological. Survey of Namibia* 11: 71–82.

Li, Fuyu, Paul Ginoux, and V Ramaswamy. 2008. "Distribution , transport , and deposition of mineral dust in the Southern Ocean and Antarctica : Contribution of major sources." *Journal Of Geophysical Research* 113 (December 2007): 1–15. doi:10.1029/2007JD009190.

Mackie, Doug S., Philip W. Boyd, Grant H. McTainsh, Neil W. Tindale, Toby K. Westberry, and Keith A. Hunter. 2008. "Biogeochemistry of iron in Australian dust: from eolian uplift to marine uptake." *Geochemistry, Geophysics, Geosystems* 9 (3). doi:10.1029/2007GC001813.

Mahowald, Natalie, Samuel Albani, Jasper F Kok, Sebastian Engelstaeder, Rachel Scanza, Daniel S Ward, and Mark G Flanner. 2014. "The size distribution of desert dust aerosols and its impact on the earth system." *Aeolian Research* 15. Elsevier B.V.: 53–71. doi:10.1016/j.aeolia.2013.09.002.

Mahowald, Natalie, Timothy D. Jickells, Alex R. Baker, Paulo Artaxo, Claudia R. Benitez-Nelson, Gilles Bergametti, Tami C. Bond, et al. 2008. "Global distribution of atmospheric phosphorus sources, concentrations and deposition rates, and anthropogenic impacts." *Global Biogeochemical Cycles* 22 (4): 1–19. doi:10.1029/2008GB003240.

Mahowald, Natalie M. 2003. “Mineral aerosol and cloud interactions.” *Geophysical Research Letters* 30 (9): 1475. doi:10.1029/2002GL016762.

Mahowald, Natalie M., Alex R. Baker, Gilles Bergametti, Nick Brooks, Robert A. Duce, Timothy D. Jickells, Nilgün Kubilay, Joseph M. Prospero, and Ina Tegen. 2005. “Atmospheric global dust cycle and iron inputs to the ocean.” *Global Biogeochemical Cycles* 19 (4). doi:10.1029/2004GB002402.

Mahowald, Natalie M., Sebastian Engelstaeder, Chao Luo, Andrea Sealy, Paulo Artaxo, Claudia R. Benitez-Nelson, Sophie Bonnet, et al. 2009. “Atmospheric iron deposition : global distribution , variability , and human perturbations.” *Annual Review of Marine Science*, no. 1: 245–78. doi:10.1146/annurev.marine.010908.163727.

Mahowald, Natalie M., Karen Kohfeld, Margaret Hansson, Yves Balkanski, P Harrison, Sandy, I Prentice, Colin, Michael Schulz, and Henning Rodhe. 1999. “Dust sources and deposition during the last glacial maximum and current climate : a comparison of model results with paleodata from ice cores and marine sediments.” *Journal Of Geophysical Research* 104 (July 20): 895–916.

Mahowald, Natalie M., Daniel R. Muhs, Samuel Levis, Philip J. Rasch, Masaru Yoshioka, Charles S. Zender, and Chao Luo. 2006. “Change in atmospheric mineral aerosols in response to climate: last glacial period, preindustrial, modern, and doubled carbon dioxide climates.” *Journal of Geophysical Research Atmospheres* 111 (10). doi:10.1029/2005JD006653.

Mahowald, Natalie M, Alex R Baker, Gilles Bergametti, Nick Brooks, Robert A Duce, Timothy D Jickells, Joseph M Prospero, and Ina Tegen. 2005. “Atmospheric global dust cycle and iron inputs to the ocean.” *Global Biogeochemical Cycles* 19: 1–15. doi:10.1029/2004GB002402.

Mahowald, Natalie M, Robert G Bryant, John del Corral, and Linda Steinberger.(a) 2003. (a) “Ephemeral lakes and desert dust sources.” *Geophysical Research Letters* 30 (2): 30–33. doi:10.1029/2002GL016041.

Mahowald, Natalie M, and Chao Luo. 2003. “A less dusty future?” *Geophys. Res. Lett.* 30 (17): 1903. doi:10.1029/2003gl017880.

Mahowald, Natalie, Daniel S. Ward, Silvia Kloster, Mark G. Flanner, Colette L. Heald, Nicholas G. Heavens, Peter G. Hess, Jean-Francois Lamarque, and Patrick Y. Chuang. 2011.(b) “Aerosol impacts on climate and biogeochemistry.” *Annual Review of Environment and Resources* 36 (1): 45–74. doi:10.1146/annurev-environ-042009-094507.

Marker, M E. 1977. “Aspects of the geomorphology of the Kuiseb River, South West Africa.” *Madoqua*.

Martin, John H., and Steve E. Fitzwater. 1988. “Iron deficiency limits phytoplankton growth in the north-east pacific subarctic.” *Nature*. doi:10.1038/331341a0.

Martin, John H, Steve E Fitzwater, and Michael R Gordon. 1990. “Iron deficiency limits phytoplankton growth in Antartic waters.” *Global Biogeochemical Cycles*, 5–12.

McGowan, Hamish, and Andrew Clark. 2008. “Identification of dust transport pathways from Lake Eyre , Australia using Hysplit.” *Atmospheric Environment* 42: 6915–25. doi:10.1016/j.atmosenv.2008.05.053.

Morton, P.L., W. Landing, S. Hsu, A. Milne, A. Aguilar-Islas, A. Baker, A. Bowie, C. Buck, Y. Gao, and S. Gichuki. 2013. “Methods for the sampling and analysis of marine aerosols: results from the 2008 GEOTRACES aerosol intercalibration experiment.” *Limnology and Oceanography* 11: 62–78. doi:10.4319/lom.2013.11.62.

Muhs, Daniel R. 2013. “The geologic records of dust in the quaternary.” *Aeolian Research* 9. Elsevier B.V.: 3–48. doi:10.1016/j.aeolia.2012.08.001.

Muhs, Daniel R, Joseph M Prospero, Matthew C Baddock, and Thomas E Gill. 2014. “Mineral dust: a key player in earth systems.” In *Identifying Sources of Aeolian Mineral Dust: Present and Past*, 51–74.

Paris, R., K. V. Desboeufs, and E. Journet. 2011. "Variability of dust iron solubility in atmospheric waters: investigation of the role of oxalate organic complexation." *Atmospheric Environment* 45 (36). Elsevier Ltd: 6510–17. doi:10.1016/j.atmosenv.2011.08.068.

Passow, Uta, Christina L De La Rocha, Caitlin Fairfield, and Katrin Schmidt. 2014. "Aggregation as a function of p CO_2 and mineral particles." *Association for the Science of Limnology and Oceanography* 59 (2): 532–47. doi:10.4319/lo.2014.59.2.0532.

Paytan, Adina, Katherine R M Mackey, Ying Chen, Ivan D Lima, Scott C Doney, Natalie Mahowald, Rochelle Labiosa, and Anton F Post. 2009. "Toxicity of Atmospheric Aerosols on Marine Phytoplankton." *PNAS* 106 (12): 4601–5.

Petit, J, R, J Jouzel, D Raynaud, I Barkov, N, M Barnola, J, I Basile, M Bender, et al. 1999. "Climate and atmospheric history of the past 420, 000 years from the Vostok Ice Core, Antartica." *Nature* 399: 429–36.

Piketh, S. J., P. D. Tyson, and W. Steffen. 2000. "Aeolian transport from southern Africa and iron fertilization of marine biota in the South Indian Ocean." *South African Journal of Science*.

Poulton, Simon W, and Donald E Canfield. 2005. "Development of a sequential extraction procedure for iron : implications for iron partitioning in continentally derived particulates." *Chemical Geology* 214: 209–21. doi:10.1016/j.chemgeo.2004.09.003.

Prospero, Joseph M. 1996. "The atmospheric transport of particles to the ocean." In *particle flux in the ocean*, edited by V Ittekkot, P Schafer, S Honjo, and P J Depetris, 19–52. John Wiley & Sons Ltd.

Prospero, Joseph M., Paul Ginoux, Omar Torres, Sharon E. Nicholson, and Thomas E. Gill. 2002. "Environmental characterization of global sources of atmospheric soil dust identified with the NIMBUS 7 Total Ozone Mapping Spectrometer (TOMS) absorbing aerosol product." *Reviews of Geophysics* 40 (1): 1–31. doi:10.1029/2000RG000095.

Prospero, Joseph M., and Olga L Mayol-Bracero. 2011. "Understanding the transport and impact of african dust on the Caribean Basin." *Amer Ican Meteorological Society*, no. September 2013: 1329–37. doi:10.1175/BAMS-D-12-00142.1.

Pye, K. 1987. *Aeolian Dust and Dust Deposits*. 1sted. Orlando: Academic Press, INC.

Qu, Zihan. 2016. "Chemical properties of continental aerosol transported over the Southern Ocean : Patagonian and Namibian Sources." Universit_e Pierre et Marie Curie.PhD Thesis

Raiswell, Rob, Liane G Benning, Martyn Tranter, and Slawek Tulaczyk. 2008a. "Bioavailable iron in the Southern Ocean : The significance of the Iceberg Conveyor Belt." *Geochemical Transactions* 9 (1): 1–9. doi:10.1186/1467-4866-9-7.

Ravi, Sujith, Paolo D Odorico, David D Breshears, Jason P Field, Andrew S Goudie, Travis E Huxman, Junran Li, et al. 2011. "Aeolian processes and the biosphere." *American Geophyical Union*, no. 49: 1–45. doi:10.1029/2010RG000328.1..

Remenyi, Tomas Andrew. 2013. "Investigating the impact of aeolian deposition to the Southern Ocean using dissolved aluminium concentrations." University of Tasmania. PhD Thesis.

Remer, Lorraine A. 2006. "Dust, Fertilization and Sources." *Environmental Research Letters* 1 (1): 11001. doi:10.1088/1748-9326/1/1/011001.

Ridgwell, Andy J. 2002. "Dust in the earth system: the biogeochemical linking of land, air and sea." *Philosophical Transactions. Series A, Mathematical, Physical, and Engineering Sciences* 360 (1801): 2905–24. doi:10.1098/rsta.2002.1096.

Romm, Joseph. 2009. "The next Dust Bowl." *Nature* 478: 450–51.

Sarthou, Géraldine, Alex R. Baker, Stéphane Blain, Eric P. Achterberg, Marie Boye, Andrew R. Bowie, Peter Croot, et al. 2003. "Atmospheric Iron deposition and sea-surface dissolved iron concentrations in the eastern atlantic ocean." *Deep-Sea Research Part I: Oceanographic Research Papers* 50 (10–11): 1339–52. doi:10.1016/S0967-0637(03)00126-2.

Schultz, Lothar. 1980. "Long range transport of desert dust with special emphasis on the Sahara." *Academy of Science* 338: 515–32.

Sedwick, Peter N, Edward R Sholkovitz, and Thomas M Church. 2007. "Impact of anthropogenic combustion emissions on the fractional solubility of aerosol iron: evidence

from the Sargasso Sea." *Journal of Earth Sciences* 8 (10): 1–21. doi:10.1029/2007GC001586.

Shackleton, Nicholas, J. 2000. "The 100,000-year ice-age cycle identified and found to lag temperature, carbon dioxide, and orbital eccentricity." *Science* 289 (5486): 1897–1902.

Shi, Zongbo, Michael D. Krom, Steeve Bonneville, and Liane G. Benning. 2015. "Atmospheric processing outside clouds increases soluble iron in mineral dust." *Environmental Science and Technology* 49 (3): 1472–77. doi:10.1021/es504623x.

Shi, Zongbo, Michael D. Krom, Timothy D. Jickells, Steeve Bonneville, Kenneth S. Carslaw, Nikos Mihalopoulos, Alex R. Baker, and Liane G. Benning. 2012. "Impacts on iron solubility in the mineral dust by processes in the source region and the atmosphere: a review." *Aeolian Research* 5. Elsevier B.V.: 21–42. doi:10.1016/j.aeolia.2012.03.001.

Sholkovitz, Edward R., Peter N. Sedwick, Thomas M. Church, Alexander R. Baker, and Claire F. Powell. 2012. "Fractional solubility of aerosol iron: synthesis of a global-scale data set." *Geochimica et Cosmochimica Acta* 89. Elsevier Ltd: 173–89. doi:10.1016/j.gca.2012.04.022.

Simonella, Lucio E., Diego M. Gaiero, and Miriam E. Palomeque. 2014. "Validation of a continuous flow method for the determination of soluble iron in atmospheric dust and volcanic ash." *Talanta* 128. Elsevier: 248–53. doi:10.1016/j.talanta.2014.04.076.

Soderberg, Keir, and John S. Compton. 2007. "Dust as a nutrient source for fynbos ecosystems, South Africa." *Ecosystems* 10 (4): 550–61. doi:10.1007/s10021-007-9032-0.

Spokes, Lucinda, Tim Jickells, and Kym Jarvis. 2001. "Atmospheric inputs of trace metals to the northeast Atlantic Ocean : the importance of southeasterly flow." *Marine Chemistry* 76: 319–330.

Srivastava, Pradeep, George A. Brook, Eugene Marais, P. Morthekai, and Ashok K. Singhvi. 2006. "Depositional environment and osl chronology of the Homeb Silt Deposits, Kuiseb River, Namibia." *Quaternary Research* 65 (3): 478–91. doi:10.1016/j.yqres.2006.01.010.

Stein, A. F., R. R. Draxler, G. D. Rolph, B. J B Stunder, M. D. Cohen, and F. Ngan. 2015. "Noaa's Hysplit atmospheric transport and dispersion modeling system." *Bulletin of the American Meteorological Society* 96 (12): 2059–77. doi:10.1175/BAMS-D-14-00110.1.

Sunda, William G. 2012. "Feedback interactions between trace metal nutrients and phytoplankton in the ocean." *Frontiers in Microbiology* 3 (JUN): 1–22. doi:10.3389/fmicb.2012.00204.

Swap, R, M Garstang, A Macko, S, D Tyson, P, W Maenhaut, P Artaxo, P Kalberg, and R Talbot. 1996. "The long-range transport of southern African aerosols to the tropical South Atlantic." *Journal of Geophysical Research* 101: 777–91.

Thomas, D S G, and P Shaw. 1991. *The Kalahari Environment*. 1sted. Cambridge: Cambridge University Press.

Tllhalerwa, K., M. T. Freiman, and S. J. Piketh. 2005. "aerosol deposition off the southern African west coast by Berg Winds." *South African Geographical Journal* 87 (2): 152–61. doi:10.1080/03736245.2005.9713838.

Tyson, P D, and P C D'Abreton. 1998. "Transport and recirculation of aerosols off southern Africa - macroscale plume structure." *Atmospheric Environment* 32 (9): 1511–24. doi:10.1016/S1352-2310(97)00392-0.

Tyson, P D, M Garstang, and R Swap. 1996. "Large scale air circulation in southern Africa.pdf." *Journal of Applied Meteorology* 35: 2218–36.

Tyson, P D, M Garstang, R Swap, P Kallberg, and M Edwards. 1996. "an air transport climatology for subtropical southern Africa." *International Journal of Climatology* 16: 265–91.

Tyson, P D, and C K Gatebe. 2001a. “The atmosphere, aerosols, trace gases and biogeochemical change in southern Africa: A Regional Integration.” *South African Journal Of Science*.

Venter, A.D., K. Jaars, W. Booyens, J.P. Beukes, P.G. Van Zyl, M. Josipovic, J. Hendriks, et al. 2015. “plume characterization of a typical South African braai.” *South African Journal of Chemistry* 68: 181–94. doi:10.17159/0379-4350/2015/v68a25.

Vickery, Kathryn J. 2010. “Southern African dust sources as identified by multiple space borne sensors.” University of Cape Town.

Vickery, Kathryn J. 2014. “The nature of pan sediments: A case study on dust supply from the Makgadikgadi Pans, Botswana.” University of Cape Town. PhD Thesis.

Vickery, Kathryn J., and Frank D. Eckardt. 2013. “Dust emission controls on the lower Kuiseb River Valley, Central Namib.” *Aeolian Research* 10. Elsevier B.V.: 125–33. doi:10.1016/j.aeolia.2013.02.006.

Vickery, Kathryn J., Frank D. Eckardt, and Robert G. Bryant. 2013. “A sub-basin scale dust plume source frequency inventory for southern Africa, 2005-2008.” *Geophysical Research Letters* 40 (19): 5274–79. doi:10.1002/grl.50968.

Visser, F, L J A Gerringa, S J Van Der Gaast, H J W De Baar, and K R Timmermans. 2003. “The role of the reactivity and content of iron of aerosol dust on growth rates of two Antarctic diatom species 1.” *Journal of Physiology* 1094: 1085–94.

Von Holdt, Johanna R C. 2013. “Lower Kuiseb River sediments and their control on dust emission.” University of Cape Town. Masters Thesis.

Wang, R., Y. Balkanski, O. Boucher, L. Bopp, A. Chappell, P. Ciais, D. Hauglustaine, J. Peuelas, and S. Tao. 2015. “Sources, transport and deposition of iron in the global atmosphere.” *Atmospheric Chemistry and Physics* 15 (11): 6247–70. doi:10.5194/acp-15-6247-2015.

Washington, Richard, Martin Todd, Nicholas J. Middleton, and Andrew S. Goudie. 2003. "Dust-storm source areas determined by the Total Ozone Monitoring Spectrometer and Surface Observations." *Annals of the Association of American Geographers* 93 (2): 297–313. doi:10.1111/1467-8306.9302003.

Witt, Melanie, Alex R. Baker, and Tim D. Jickells. 2006. "Atmospheric trace metals over the Atlantic and South Indian Oceans: Investigation of metal concentrations and lead isotope ratios in coastal and remote marine aerosols." *Atmospheric Environment* 40 (28): 5435–51. doi:10.1016/j.atmosenv.2006.04.041.

Witt, Melanie L I, Tamsin A. Mather, Alex R. Baker, Jan C M De Hoog, and David M. Pyle. 2010. "Atmospheric trace metals over the South-West Indian Ocean: Total gaseous mercury, aerosol trace metal concentrations and lead isotope ratios." *Marine Chemistry* 121 (1–4). Elsevier B.V.: 2–16. doi:10.1016/j.marchem.2010.02.005.

Zhang, Y., N. Mahowald, R. A. Scanza, E. Journet, K. Desboeufs, S. Albani, J. F. Kok, et al. 2015. "Modeling the global emission, transport and deposition of trace elements associated with mineral dust." *Biogeosciences* 12 (19): 5771–92. doi:10.5194/bg-12-5771-2015.

Zhu, X R, Joseph M. Prospero, and Frank J. Millero. 1997. "Diel variability of soluble fe (ii) and soluble total fe in North African dust in the trade winds at Barbados." *Journal of Geophysical Research* 102 (2): 21297–305.

Zunckel, M, L Robertson, P D Tyson, and H Rodhe. 2000. "Modelled transport and deposition of sulphur over southern Africa." *Atmospheric Environment* 34: 2797–2808.

APPENDICES

APPENDIX A: Hysplit Modeling Software Method

Step 1 is to go on the website http://ready.arl.noaa.gov/HYSPLIT.php. The following window will open:

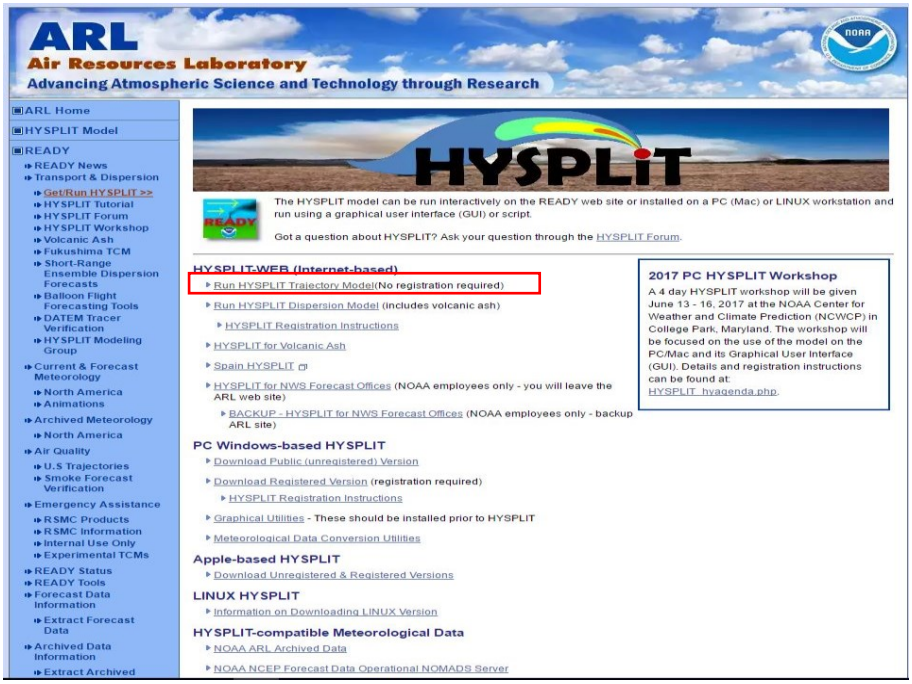

Then choose the 'Run HYSPLIT Trajectory Model'

The following window will open

Then the ‘Compute archive trajectories’ option was chosen because the study aims at modelling air masses pathways that have already occurred.

The following window will open which gives the ‘Type of Trajectories’

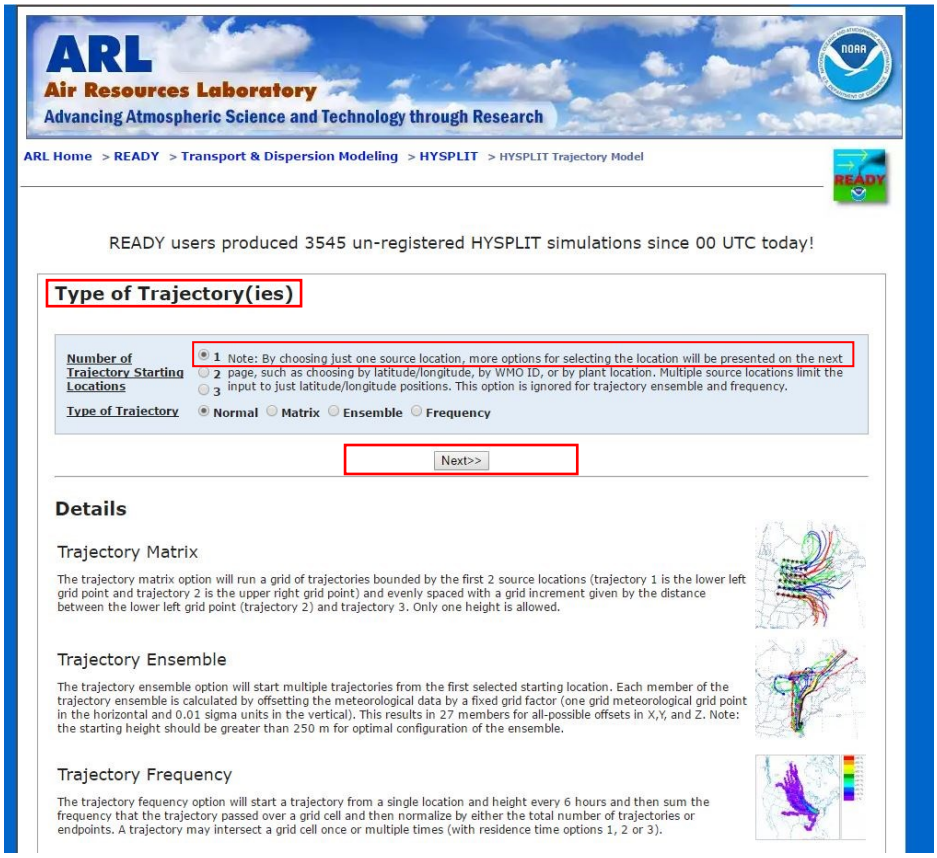

The ‘number of trajectory starting locations selected is 1’, while the type of trajectory chosen is ‘normal’.

Next step is to insert the ‘Meteorology and Starting Location’

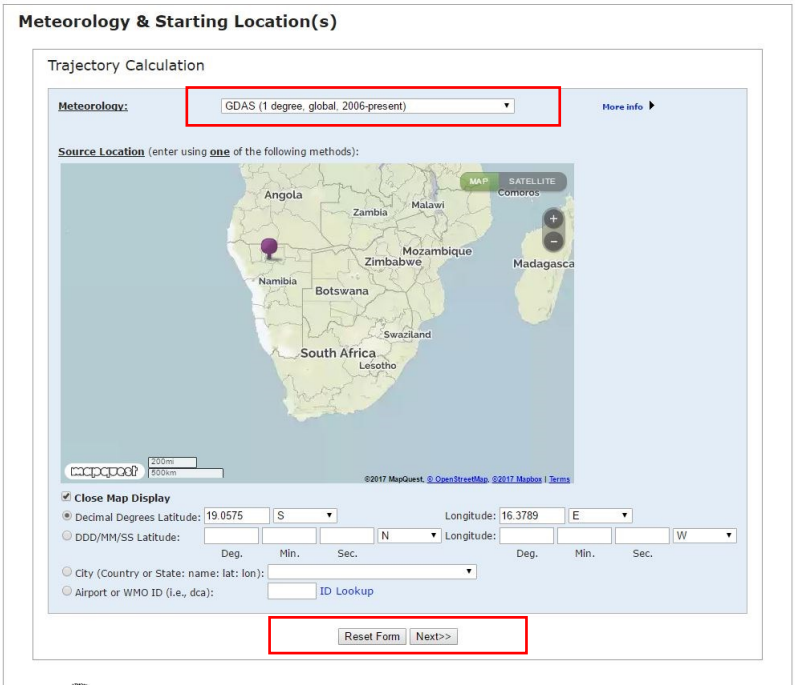

Starting location was selected based on the data described in table 3-1. GDAS (1 degree, global, 2006-present was used

The next window to open will be the ‘Meteorology file”

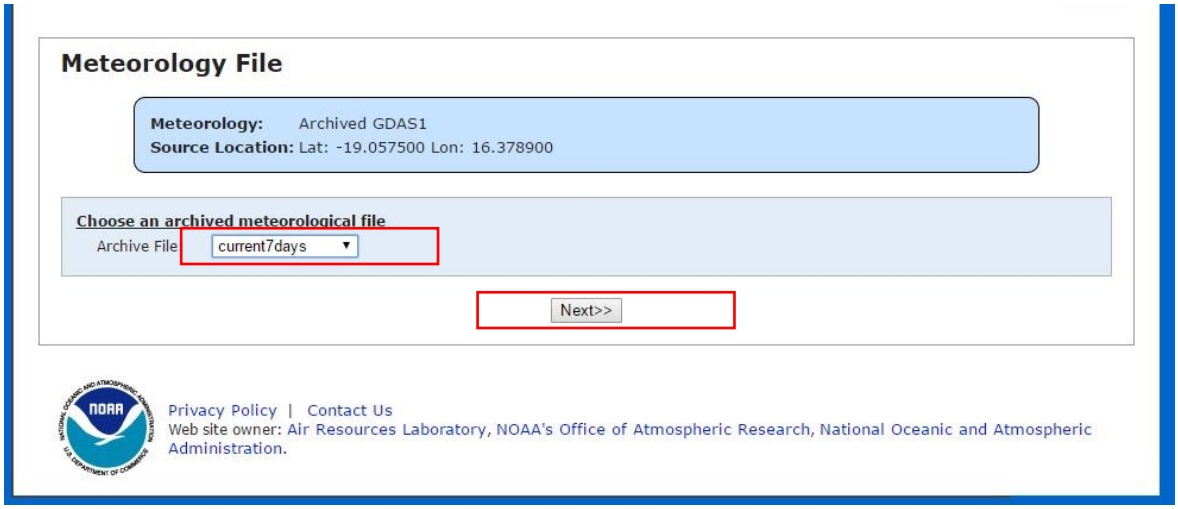

Here, the archive file of when the dust emission occurred based on table 3-1 was inserted. Then next was clicked to open the next window.

The next window was the ‘model run details’

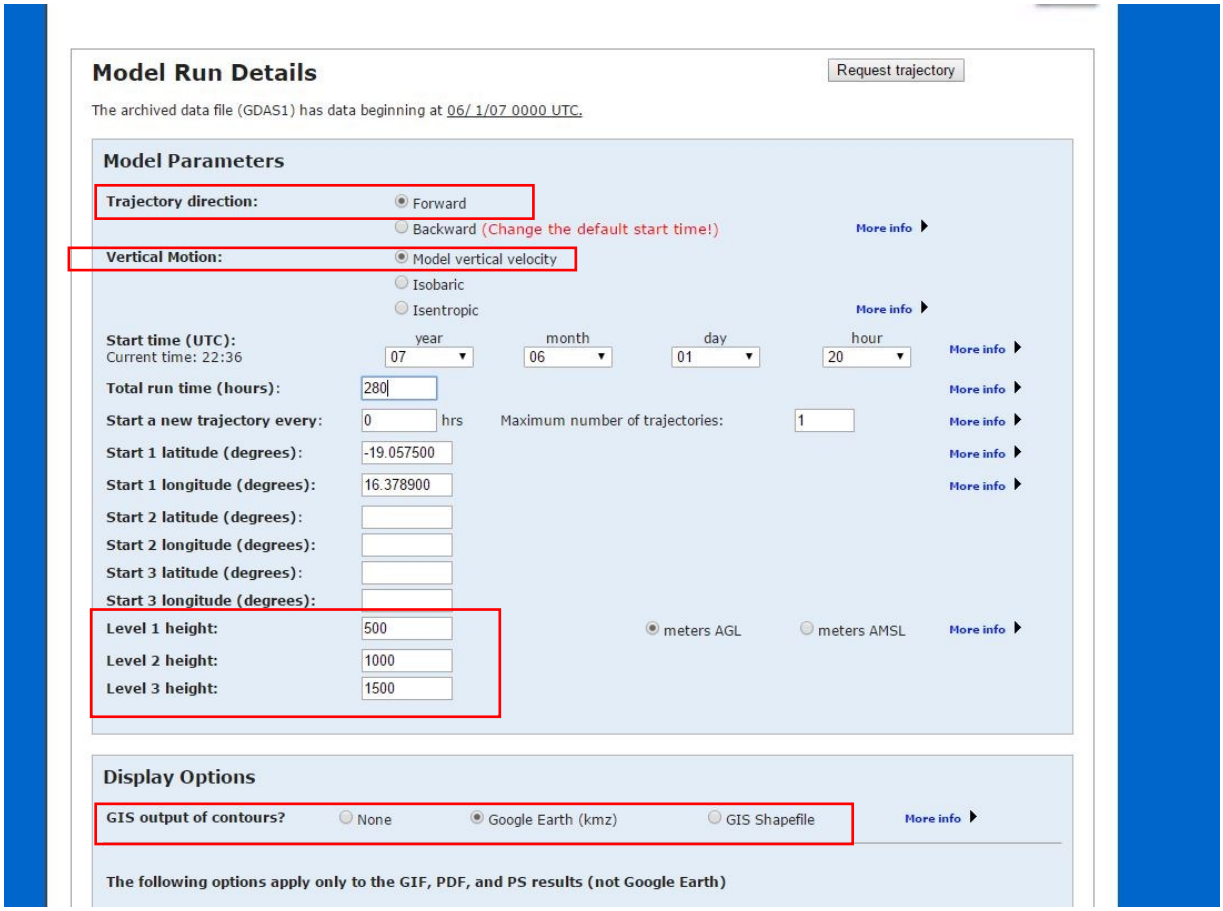

Trajectory direction was forward, vertical motion option chosen was the default “Model vertical velocity” that uses the vertical velocity field from the meteorological data. The starting time was selected as 12:00 for all the emissions. Total run time selected was 240 hours (10 days), with a maximum number of trajectories selected to be one.

The different level heights chosen where 500 m for level 1, 1000 m for level 2 height and 1500 m for level 3 height.

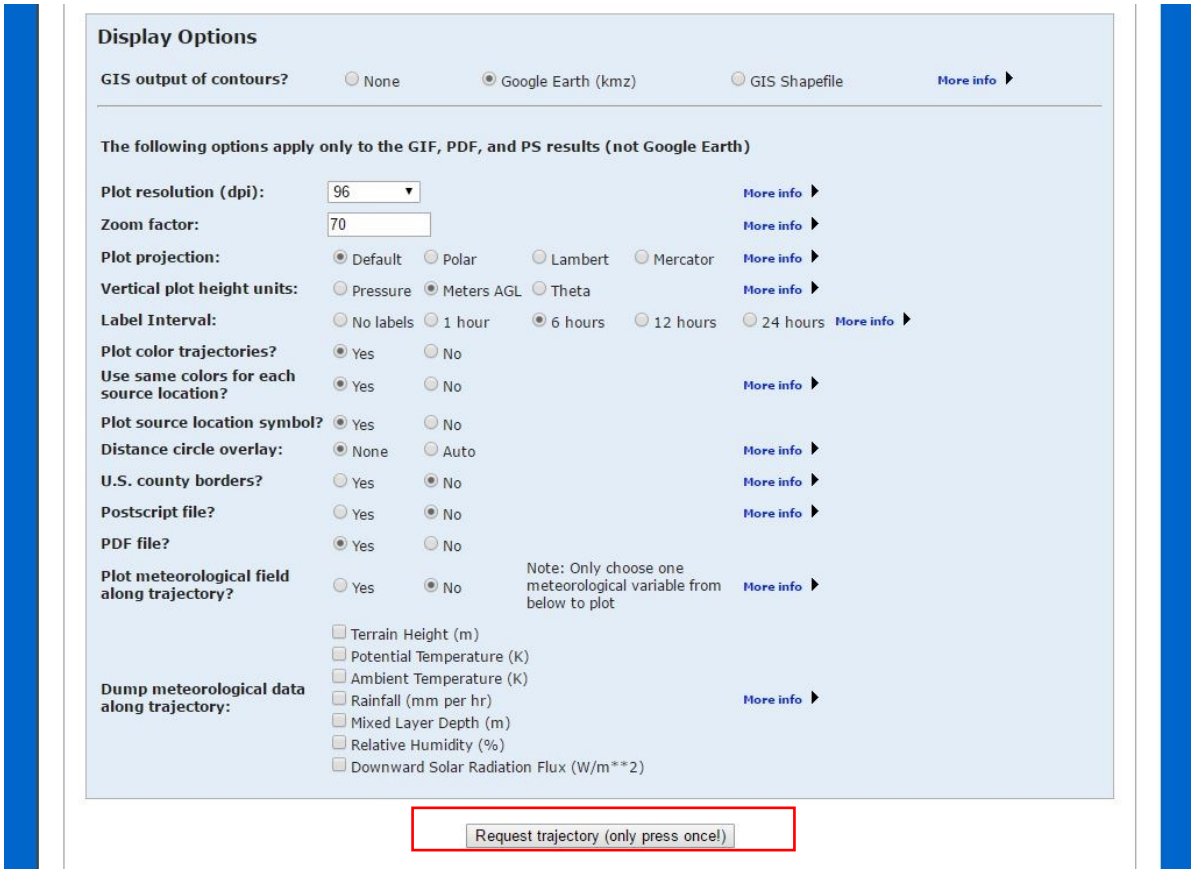

In terms of the display options, GIS output of contours was selected as Google Earth (kmz) and GIS Shape files. The rest of the options where left as default settings, although no labels option was selected. Then the trajectory request option was selected in order for the trajectory to be calculated.

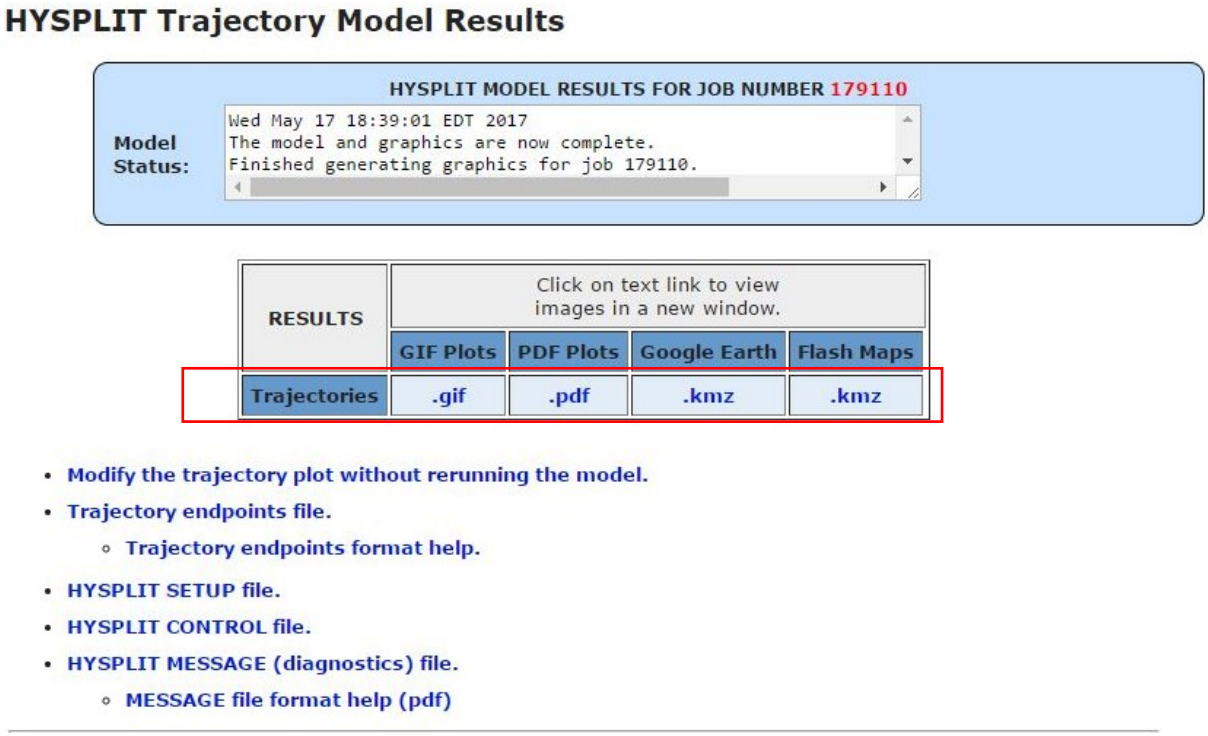

HYSPLIT Trajectory Model Results

HYSPLIT MODEL RESULTS FOR JOB NUMBER 179110

Model Status:

```
Wed May 17 18:39:01 EDT 2017
The model and graphics are now complete.
Finished generating graphics for job 179110.
```

RESULTS	Click on text link to view images in a new window.			
	GIF Plots	PDF Plots	Google Earth	Flash Maps
Trajectories	.gif	.pdf	.kmz	.kmz

- Modify the trajectory plot without rerunning the model.
- Trajectory endpoints file.
  - Trajectory endpoints format help.
- HYSPLIT SETUP file.
- HYSPLIT CONTROL file.
- HYSPLIT MESSAGE (diagnostics) file.
  - MESSAGE file format help (pdf)

Under the Hysplit trajectory model results section, the results can be saved in several options such as either Graphics Interchange Format (GIF), Portable Document Format (PDF) and Keyhole Mark-up Language Zipped (KMZ) files. For this study, the files were saved as pdf and kmz files.

APPENDIX B: Trajectories displayed on the globe using Google earth

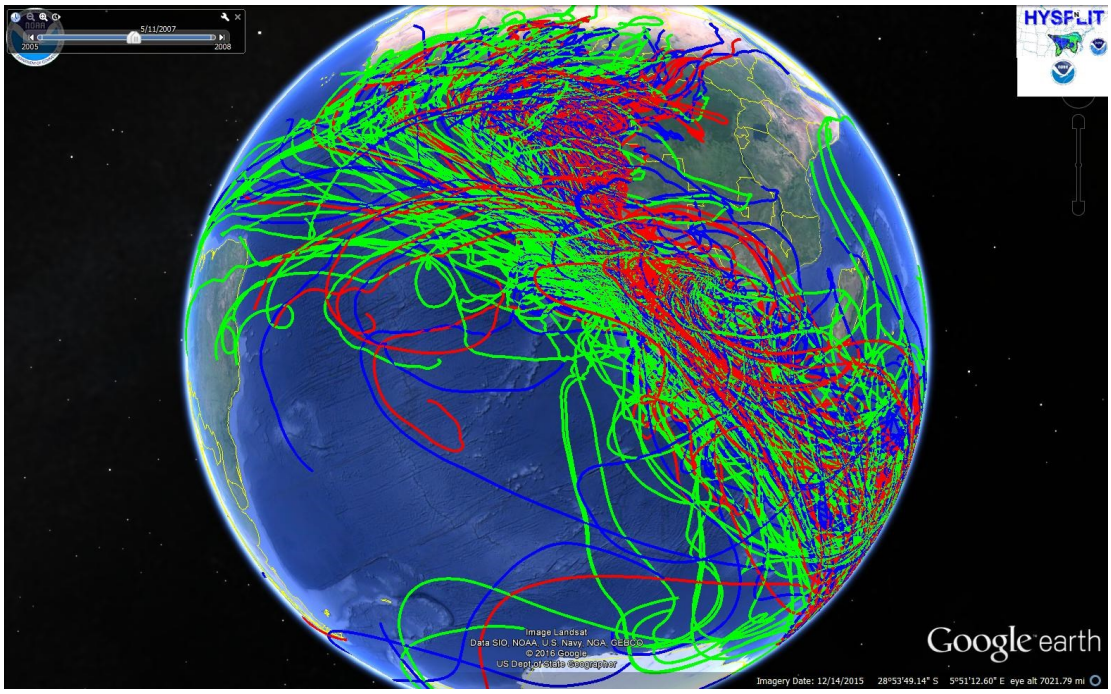

All trajectories displayed above

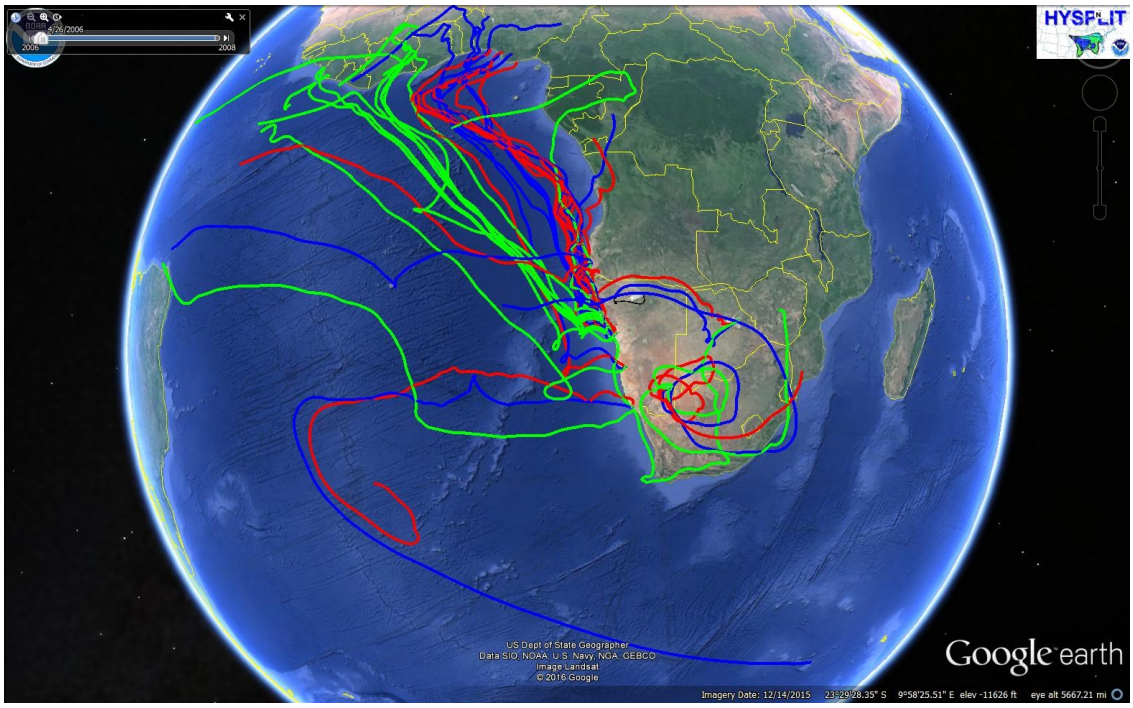

Autumn trajectories map showing the different heights.

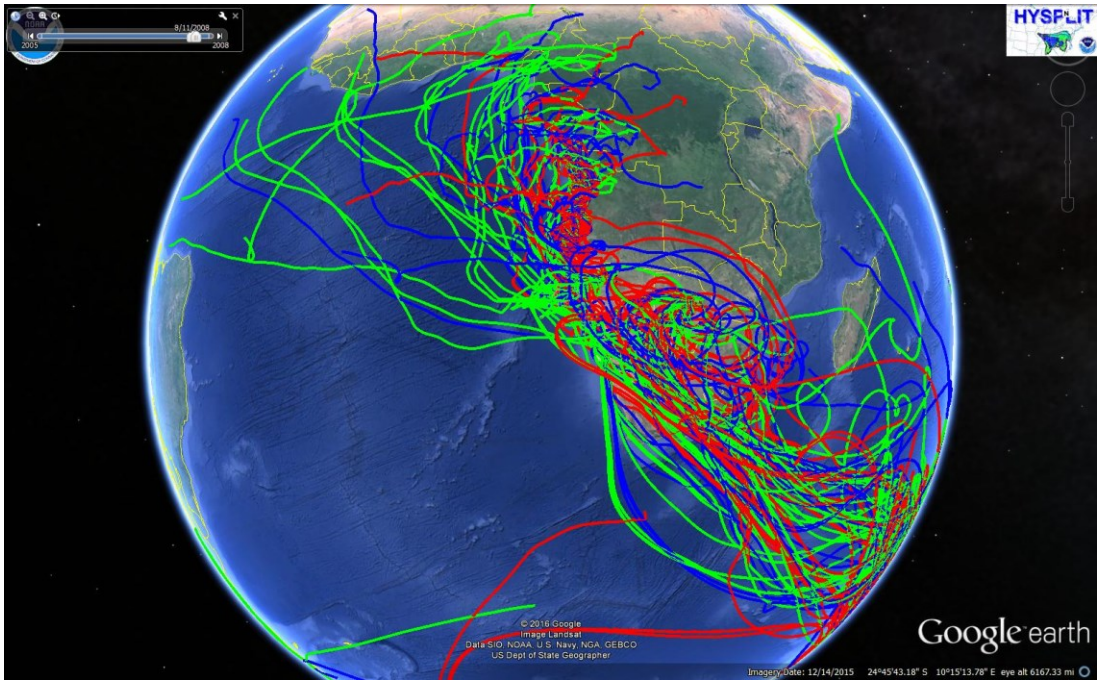

Spring Map trajectories map showing the different heights.

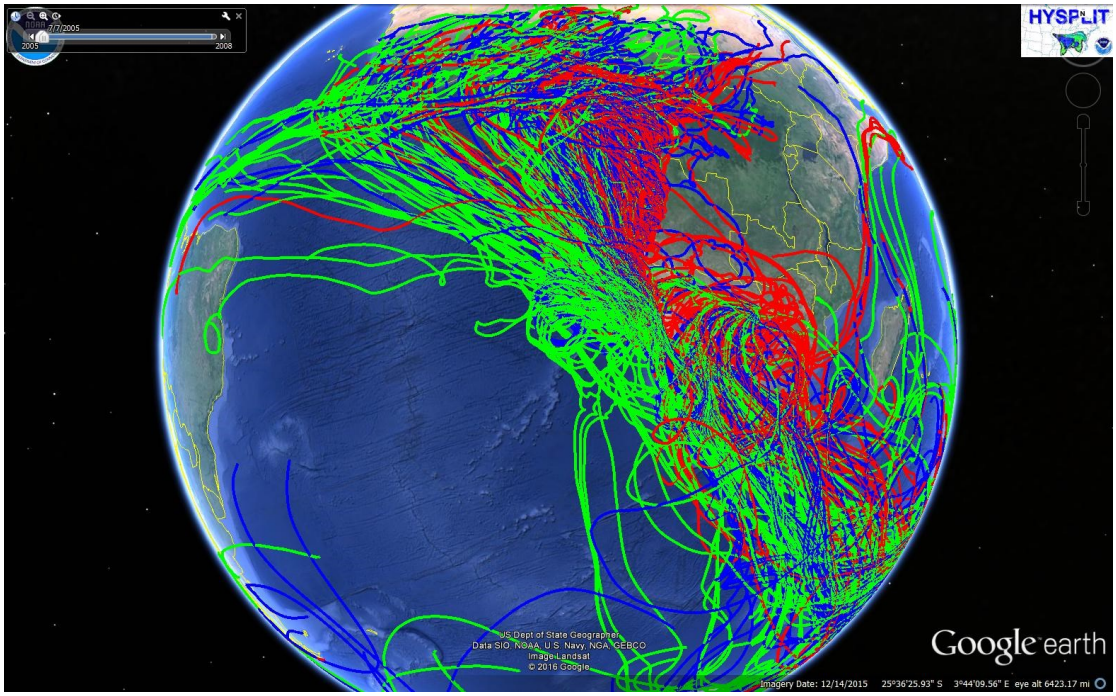

Winter trajectories map showing the different heights.

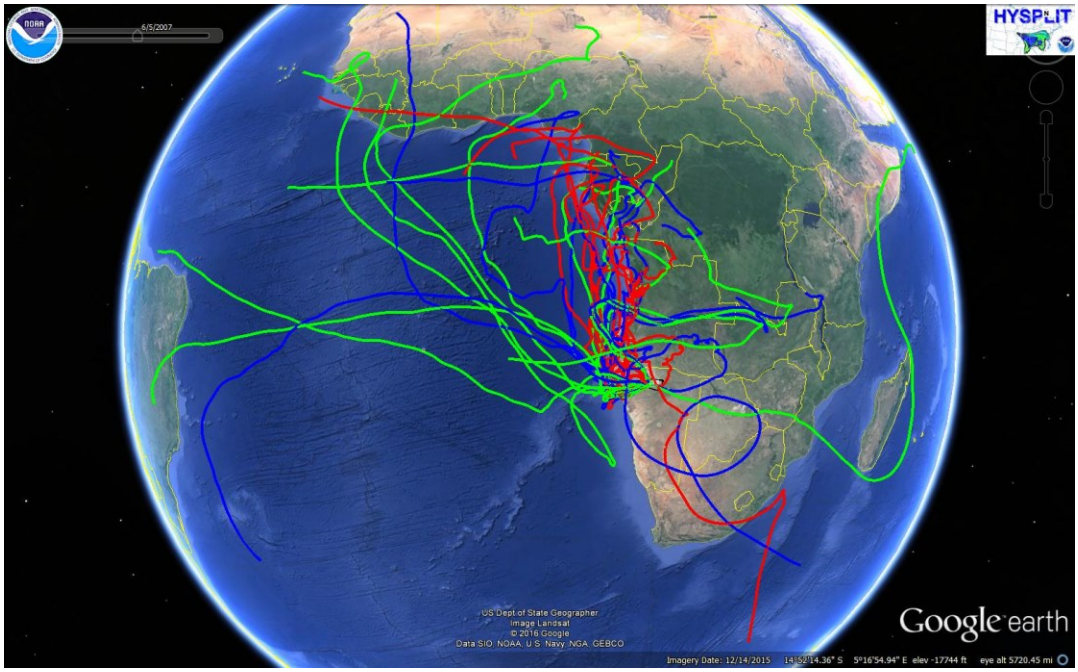

Omaruru River trajectories map showing the different heights.

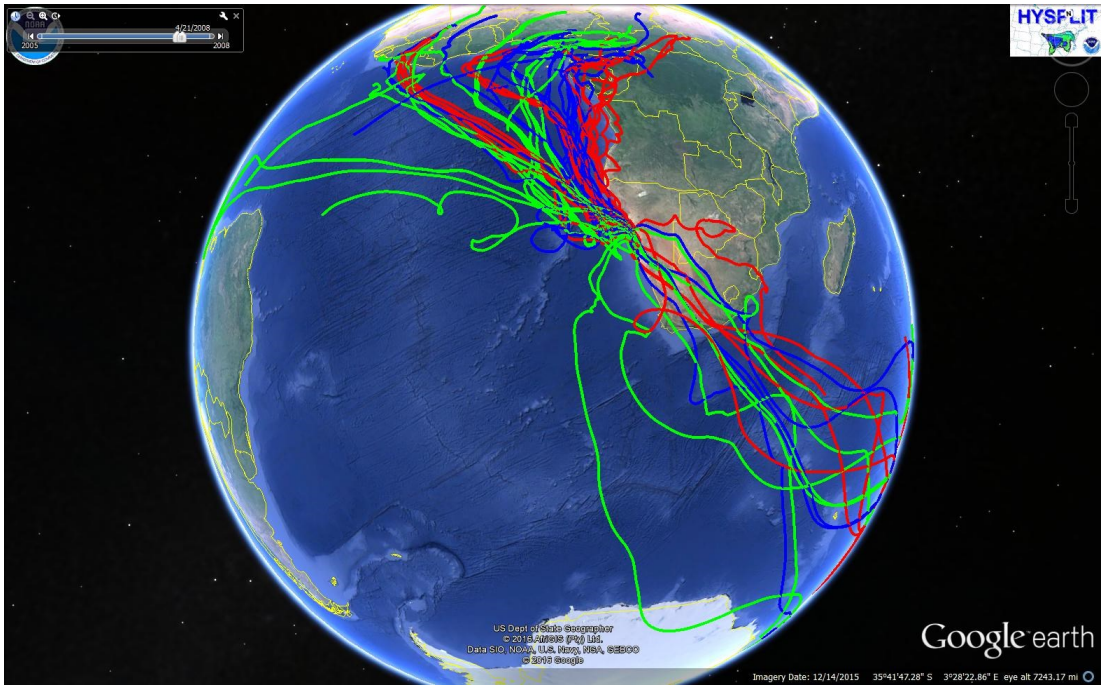

Kuiseb River trajectories map showing the different heights.

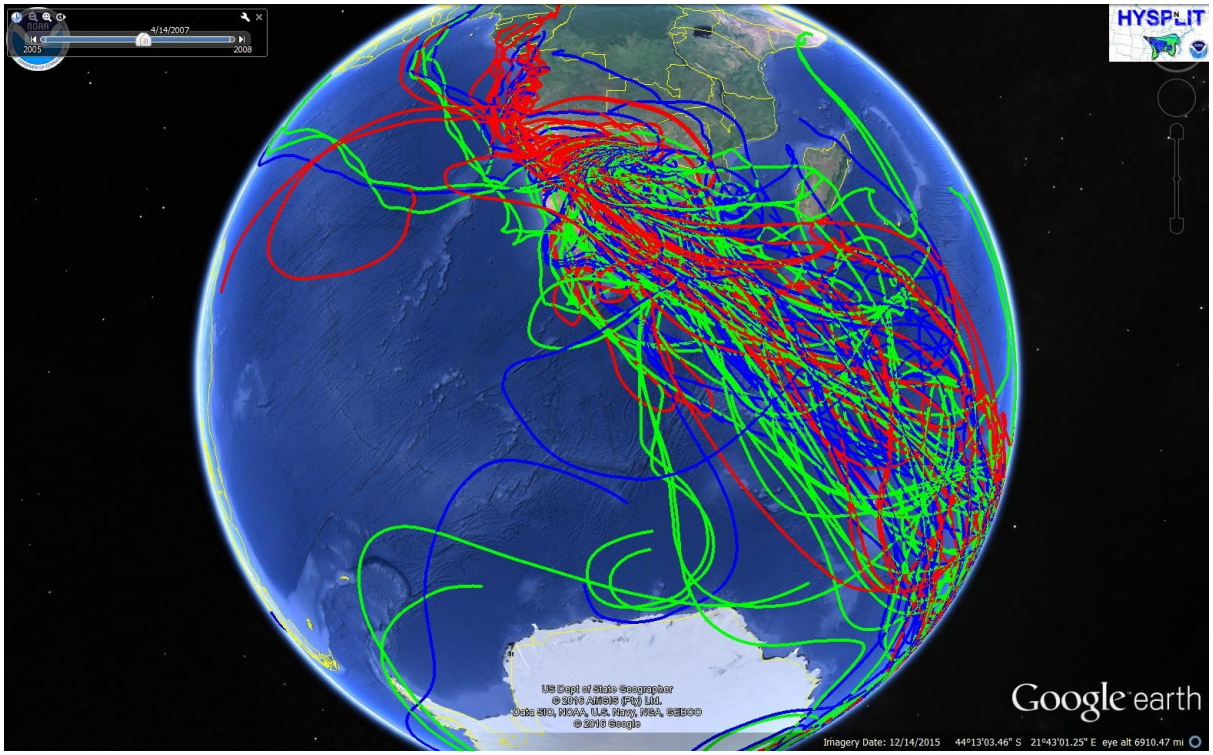

Makgadikgadi Pan trajectories map showing the different heights.

APPENDIX C: Description of XRD Analysis

The mineralogical composition of mineral dust samples is predominantly analysed by X-ray diffractrometry (XRD) and has been used for more than 40 years for the characterization of mineral dust samples and their possible source sediments (Knippertz & Stuut 2014). The mineralogical composition of dust plays an essential role that affects the solubility (bioavailability) of elements in the sediments. X-ray powder diffraction (XRD) is a rapid analytical technique primarily used for phase identification of a crystalline material and can provide information on unit cell dimensions. Usually the analysed material is finely ground, homogenized, and average bulk composition determined. Measurements using XRD can provide mineralogical compositions which will help to better understand the variation of the bioavailability in the samples of this study.

APPENDIX D: XRD analysis result for the Etosha Pan

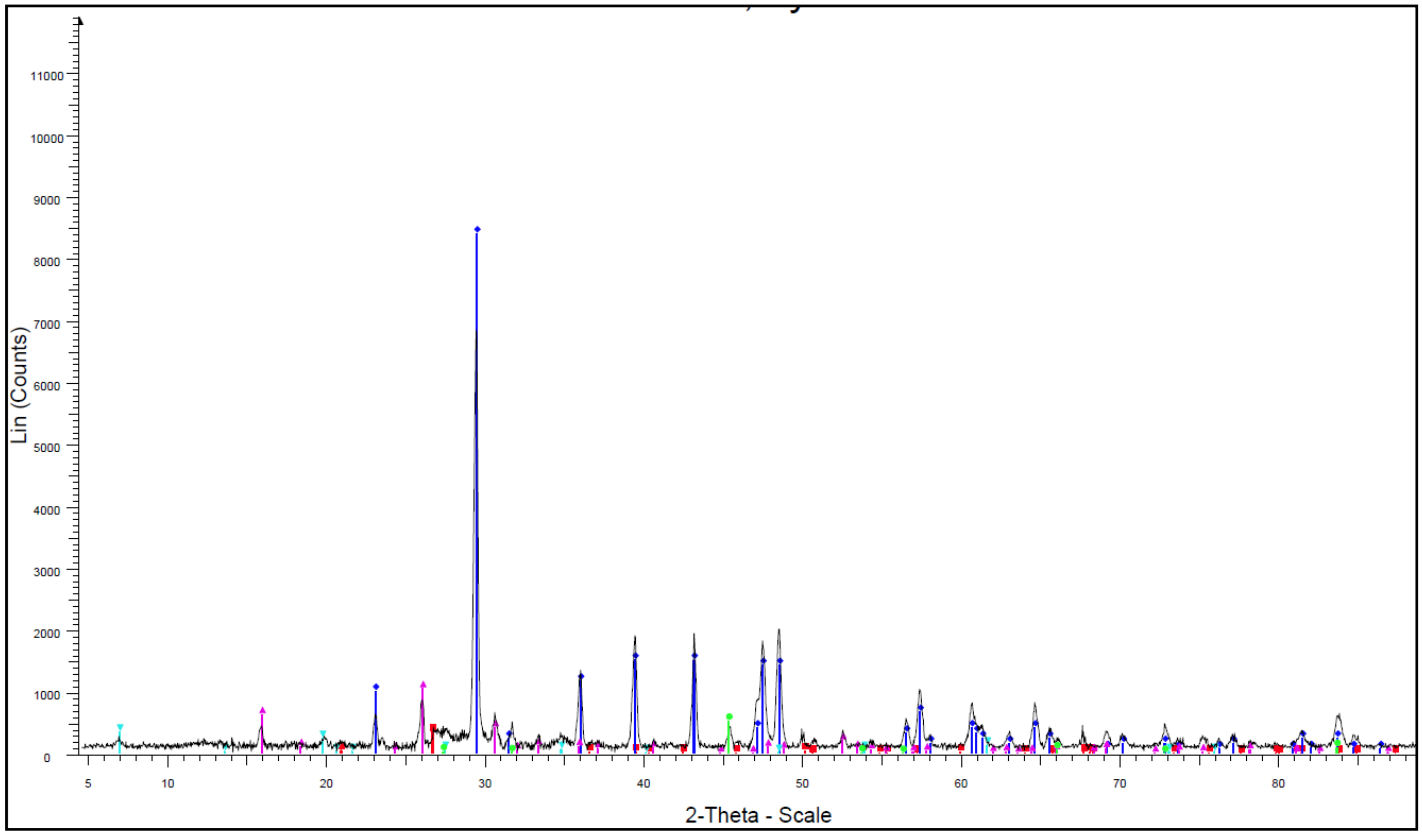

File: S7.raw - Type: 2Th/Th locked - Start: 4.500 ° - End: 90.049 ° - Step: 0.034 ° - Step time: 96. s - Temp.: 25 °C (Room) - Time Started: 7 s - 2-Theta: 4.500 ° - Theta: 2.250 ° - Chi: 0.00 ° - Phi: 0.00 ° - X: 0.0 mm - Y: 0.0 mm - Z:
Operations: Y Scale Add -875 | Y Scale Add 1000 | Background 4.571,1.000 | Import

00-046-1045 (*) - Quartz, syn - SiO2 - Y: 2.08 % - d x by: 1. - WL: 1.5406 - 0 - I/Ic PDF n.a. - I/Ic User n.a. - S-Q n.a. - F30=539(0.0018,31)

00-005-0586 (*) - Calcite, syn - CaCO3 - Y: 50.00 % - d x by: 1. - WL: 1.5406 - 0 - I/Ic PDF n.a. - I/Ic User n.a. - S-Q n.a. - F30= 57(0.0159,33)

00-045-1207 (C) - Iron Silicon - Fe3Si - Y: 3.12 % - d x by: 1. - WL: 1.5406 - 0 - I/Ic PDF n.a. - I/Ic User n.a. - S-Q n.a. - F11=218(0.0030,17)

00-041-1478 (*) - Analcime-C - Na(Si2Al)O6·H2O - Y: 6.25 % - d x by: 1. - WL: 1.5406 - 0 - I/Ic PDF n.a. - I/Ic User n.a. - S-Q n.a. - F30= 46(0.0151,43)

00-012-0204 (D) - Montmorillonite - Nax(Al,Mg)2Si4O10(OH)2·zH2O - Y: 2.08 % - d x by: 1. - WL: 1.5406 - 0 - I/Ic PDF n.a. - I/Ic User n.a. - S-Q n.a. -

APPENDIX E: XRD analysis result for the Makgadigadi Pan

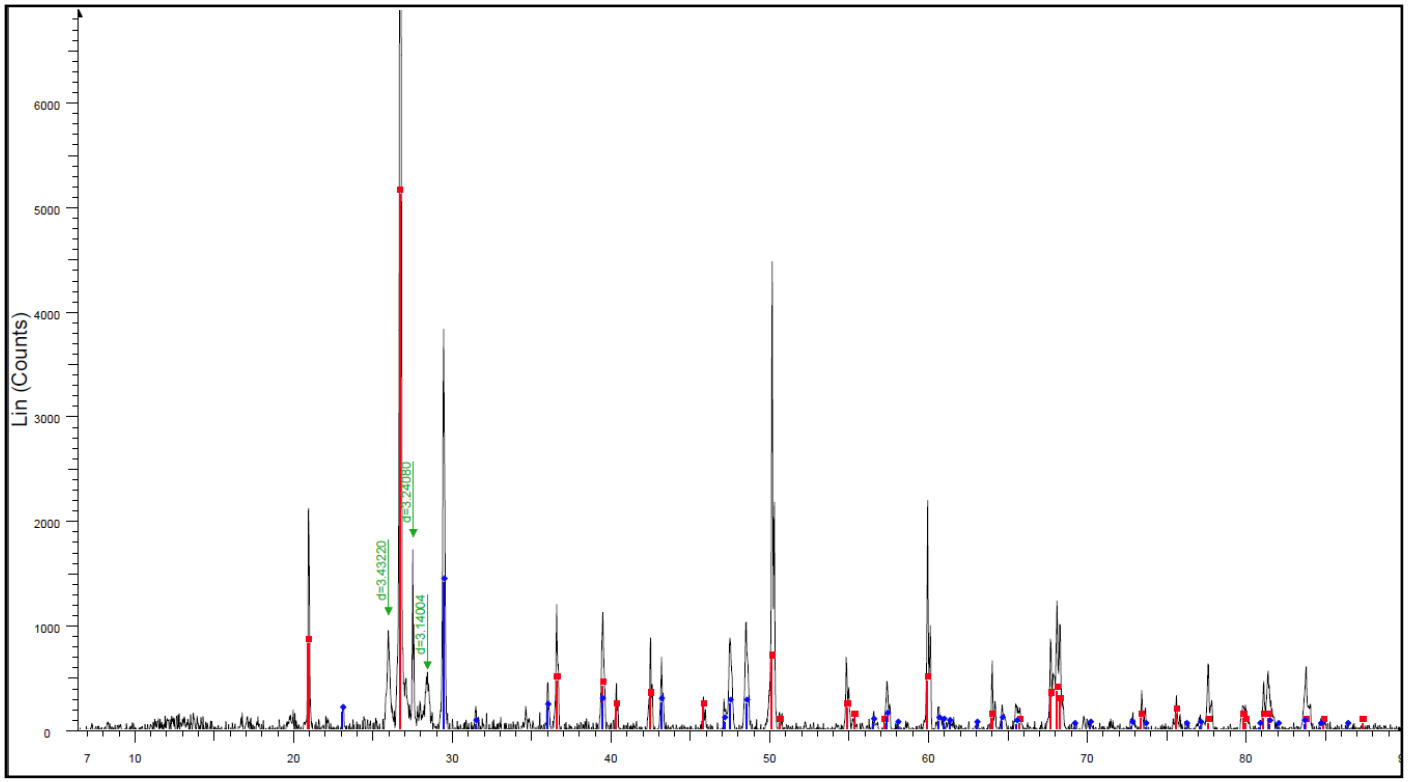

File: S4.raw - Type: 2Th/Th locked - Start: 4.500 ° - End: 90.049 ° - Step: 0.034 ° - Step time: 96. s - Temp.: 25 °C (Room) - Time Started: 19 s - 2-Theta: 4.500 ° - Theta: 2.250 ° - Chi: 0.00 ° - Phi: 0.00 ° - X: 0.0 mm - Y: 0.0 mm - Z:
Operations: X Offset 0.086 | Background 6.761,1.000 | Import

00-046-1045 (*) - Quartz, syn - SiO2 - Y: 39.34 % - d x by: 1. - WL: 1.5406 - 0 - I/Ic PDF n.a. - I/Ic User n.a. - S-Q n.a. - F30=539(0.0018,31)

00-005-0586 (*) - Calcite, syn - CaCO3 - Y: 10.75 % - d x by: 1. - WL: 1.5406 - 0 - I/Ic PDF n.a. - I/Ic User n.a. - S-Q n.a. - F30= 57(0.0159,33)

APPENDIX F: XRD analysis result for the Kuiseb River

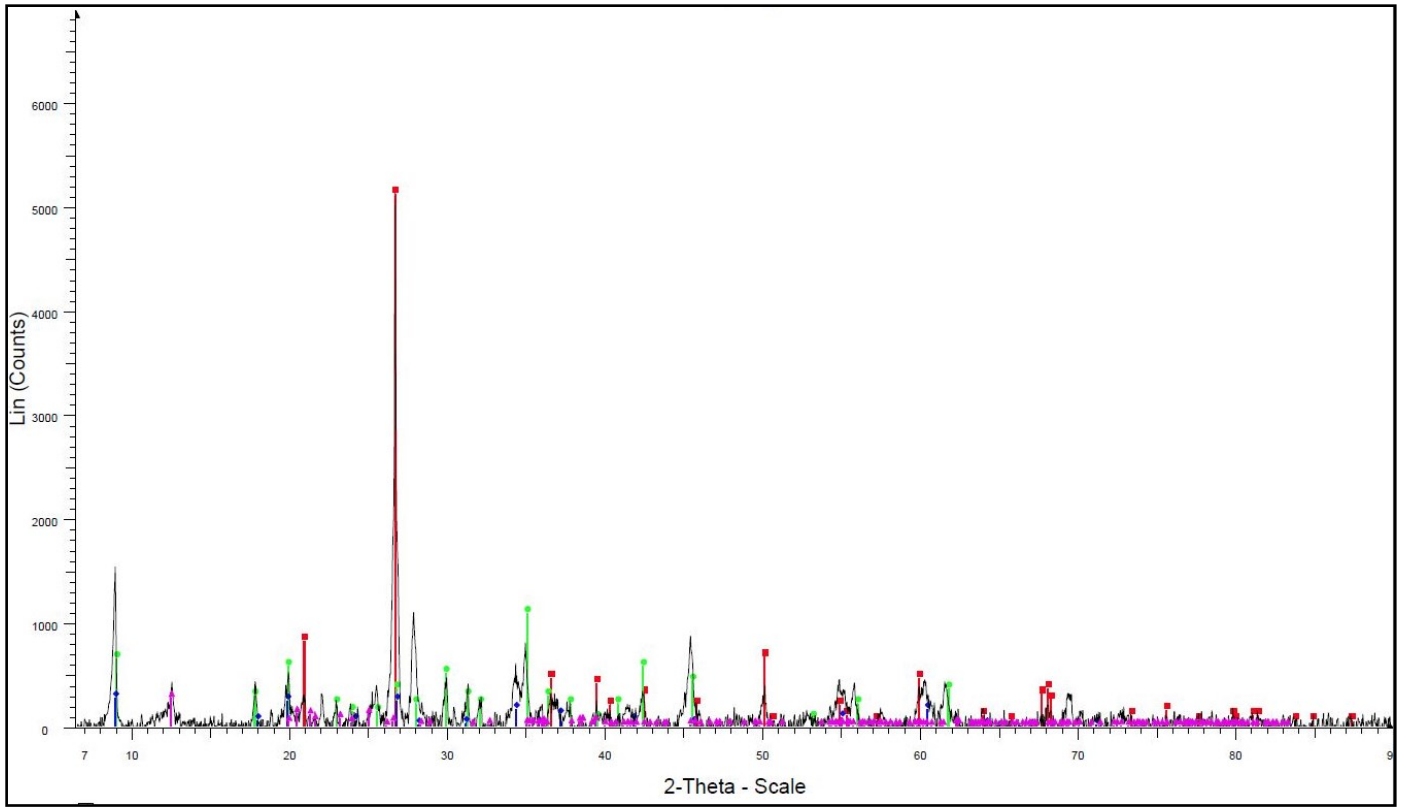

File: S2.raw - Type: 2Th/Th locked - Start: 4.500 ° - End: 90.049 ° - Step: 0.034 ° - Step time: 96. s - Temp.: 25 °C (Room) - Time Started: 7 s - 2-Theta: 4.500 ° - Theta: 2.250 ° - Chi: 0.00 ° - Phi: 0.00 ° - X: 0.0 mm - Y: 0.0 mm - Z:
Operations: Background 2.570,1.000 | Import

00-046-1045 (*) - Quartz, syn - SiO2 - Y: 39.34 % - d x by: 1. - WL: 1.5406 - 0 - I/Ic PDF n.a. - I/Ic User n.a. - S-Q n.a. - F30=539(0.0018,31)

00-001-1098 (D) - Muscovite - H2KAl3(SiO4)3 - Y: 8.33 % - d x by: 1. - WL: 1.5406 - 0 - I/Ic PDF n.a. - I/Ic User n.a. - S-Q n.a. - F21= 4(0.0340,148)

00-009-0343 (D) - Illite, trioctahedral - K0.5(Al,Fe,Mg)3(Si,Al)4O10(OH)2 - Y: 2.08 % - d x by: 1. - WL: 1.5406 - 0 - I/Ic PDF n.a. - I/Ic User n.a. - S-Q n.a. - F16= 1(0.0680,290)

01-083-0971 (C) - Kaolinite - from Keokuk, Iowa, USA - Al2(Si2O5)(OH)4 - Y: 2.08 % - d x by: 1. - WL: 1.5406 - 0 - I/Ic PDF n.a. - I/Ic User n.a. - S-Q n.a. - F30=185(0.0048,34)

APPENDIX G: XRD analysis result for the Omaruru River

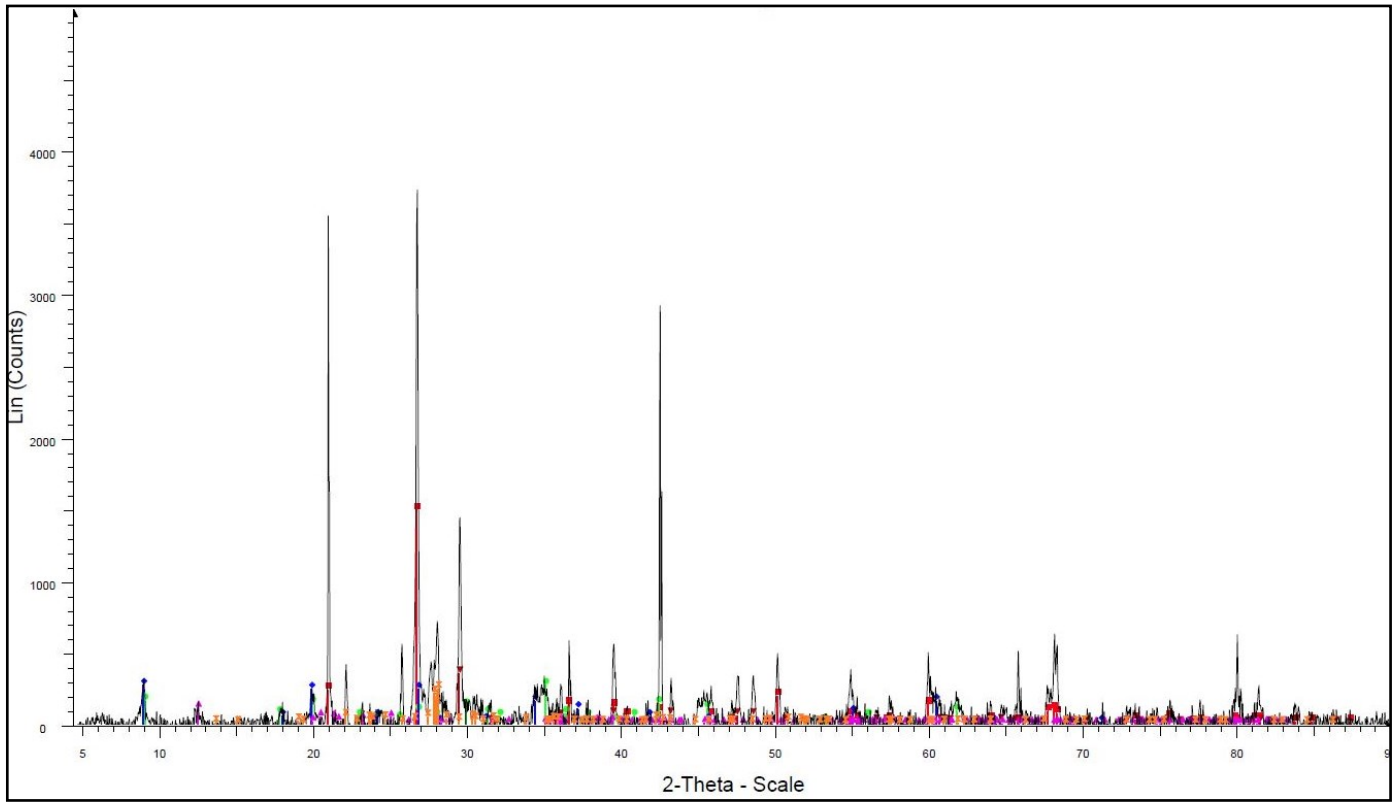

00-046-1045 (*) - Quartz, syn - SiO2 - Y: 11.47 % - d x by: 1. - WL: 1.5406 - 0 - I/Ic PDF n.a. - I/Ic User n.a. - S-Q n.a. - F30=539(0.0018,31)
00-005-0586 (*) - Calcite, syn - CaCO3 - Y: 2.69 % - d x by: 1. - WL: 1.5406 - 0 - I/Ic PDF n.a. - I/Ic User n.a. - S-Q n.a. - F30= 57(0.0159,33)
00-041-1486 (*) - Anorthite, ordered - CaAl2Si2O8 - Y: 1.89 % - d x by: 1. - WL: 1.5406 - 0 - I/Ic PDF n.a. - I/Ic User n.a. - S-Q n.a. - F30= 9(0.0157,212)
00-001-1098 (D) - Muscovite - H2KAl3(SiO4)3 - Y: 2.08 % - d x by: 1. - WL: 1.5406 - 0 - I/Ic PDF n.a. - I/Ic User n.a. - S-Q n.a. - F21= 4(0.0340,148)
00-009-0343 (D) - Illite, trioctahedral - K0.5(Al,Fe,Mg)3(Si,Al)4O10(OH)2 - Y: 2.08 % - d x by: 1. - WL: 1.5406 - 0 - I/Ic PDF n.a. - I/Ic User n.a. - S-Q n.a. - F16= 1(0.0680,290)
01-083-0971 (C) - Kaolinite - from Keokuk, Iowa, USA - Al2(Si2O5)(OH)4 - Y: 0.87 % - d x by: 1. - WL: 1.5406 - 0 - I/Ic PDF n.a. - I/Ic User n.a. - S-Q n.a. - F30=185(0.0048,34)

APPENDIX H: Particle Size Method Description

A Standard Operating Procedure or SOP was set up using quartz (silica) as a base refractive constituent of the sample with a refractive index of 1.544. The SOP was used for both the dry and wet sample. According to the Malvern Instruments Limited (2012), knowledge of the refractive index of the sample and the dispersant are essential as they affect the associated absorption of the laser beam and polarised light and therefore define the optical model used for detection. For all sampling, an obscuration value of between 10% and 20 % was obtained, which allowed results from multiple runs, using various dispersants to be comparable. An obscuration value refers to the suspension density within the dispersant, meaning it is dependent on the grain size and therefore the sample mass required for analysis varied.

Three readings were taken with a 10 second time interval between readings for each sample. The results of each reading as well as an average of the three were recorded for all the samples. For the Hydro 2000SM, a manual sample stirrer speed of 1400 rpm was set as this was determined to be the point at which particle size detection reached a plateau, below this speed the particles were too low suggesting that the pump rate was not fast enough to suspend the larger particles (Vickery 2014). Mastersizer output, providing results between user sizes from 0.012 µm and 2000 µm, was extracted for all samples.

The laser diffraction method (LDM) measures particle size distributions by measuring the angular variation in intensity of light scattered as a laser beam passes through a dispersed particulate sample (Instruments, 2016). Laser diffraction uses Mie theory of light scattering to calculate the particle size distribution, assuming a volume equivalent sphere model. Large particles scatter light at small angles relative to the laser beam and small particles scatter light at large angles. The scattering intensity data is then analysed to calculate the size of the particles responsible for creating the scattering pattern. The particle size reported as a volume equivalent sphere diameter. The particle size analyses lower limit can extend to 0.045 µm, while the upper limit is reached at 2000 µm. In order to reduce the bias of grain morphology on detection, the size distribution is measured while the suspension is continuously being pumped around (Vickery 2014). This was reported to ensure random orientation of most particles relative to the laser beam. LDM has a great advantage of being able to allow a range of processing environments, both dry and wet.

APPENDIX I: Particle Size Method Results

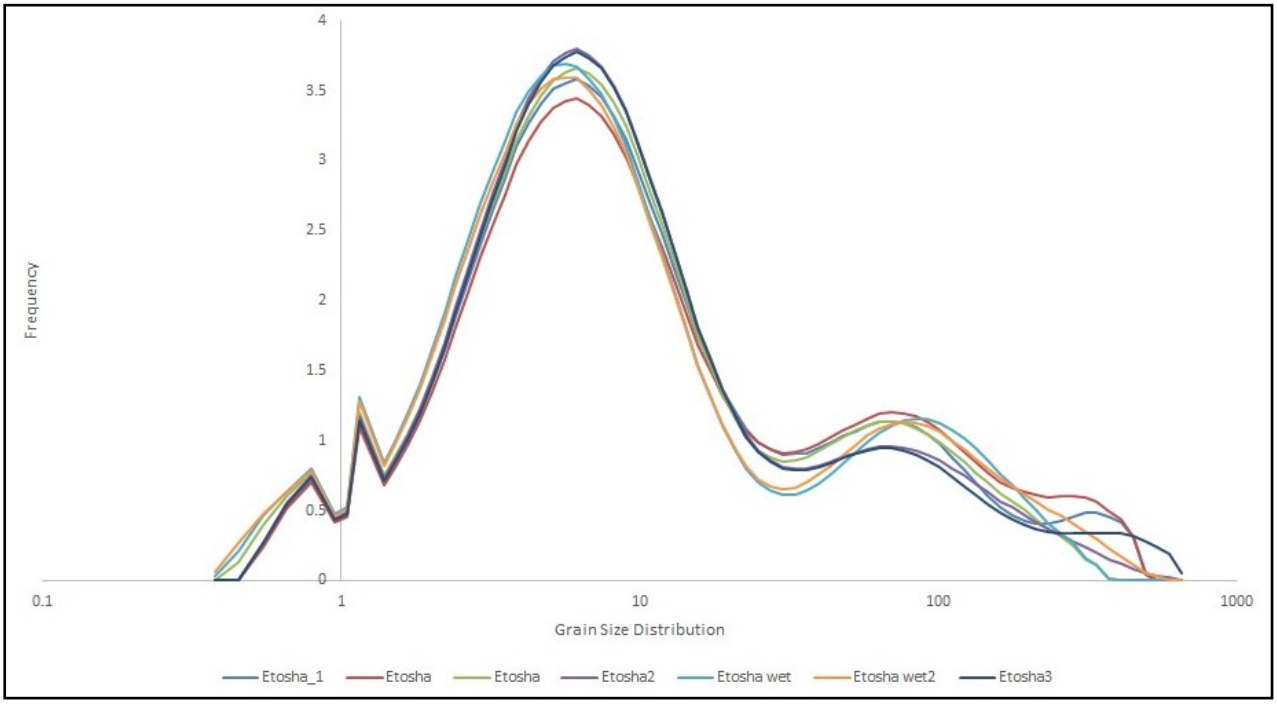

Etosha Pan particle size distribution for all analysed samples.

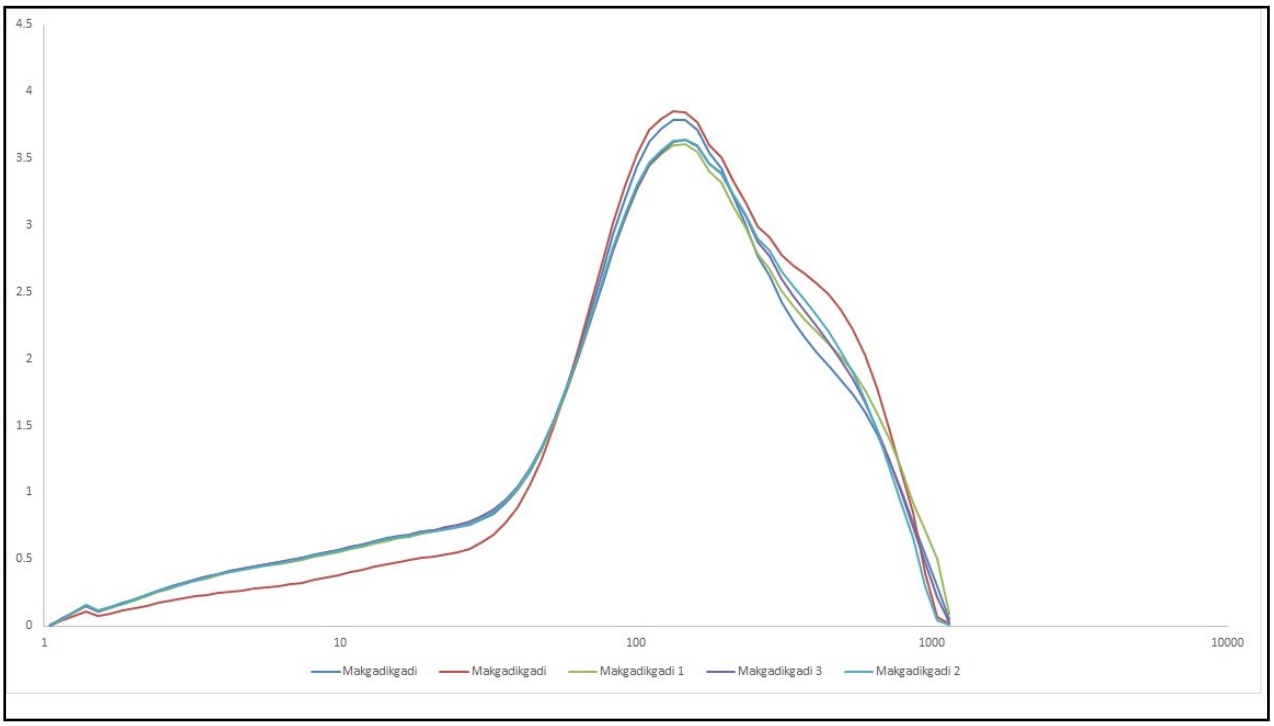

Makgadikgadi Pan particle size distribution for all analysed samples.

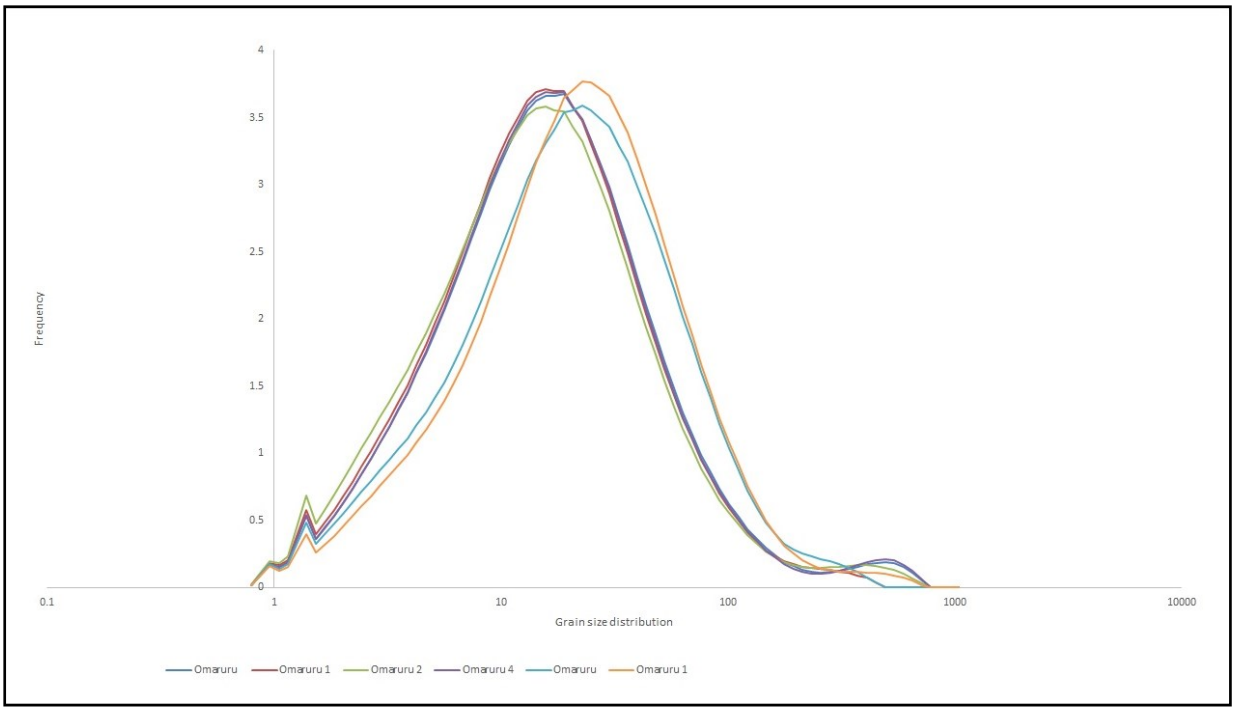

Omaruru River particle size distribution for all the analysed samples.

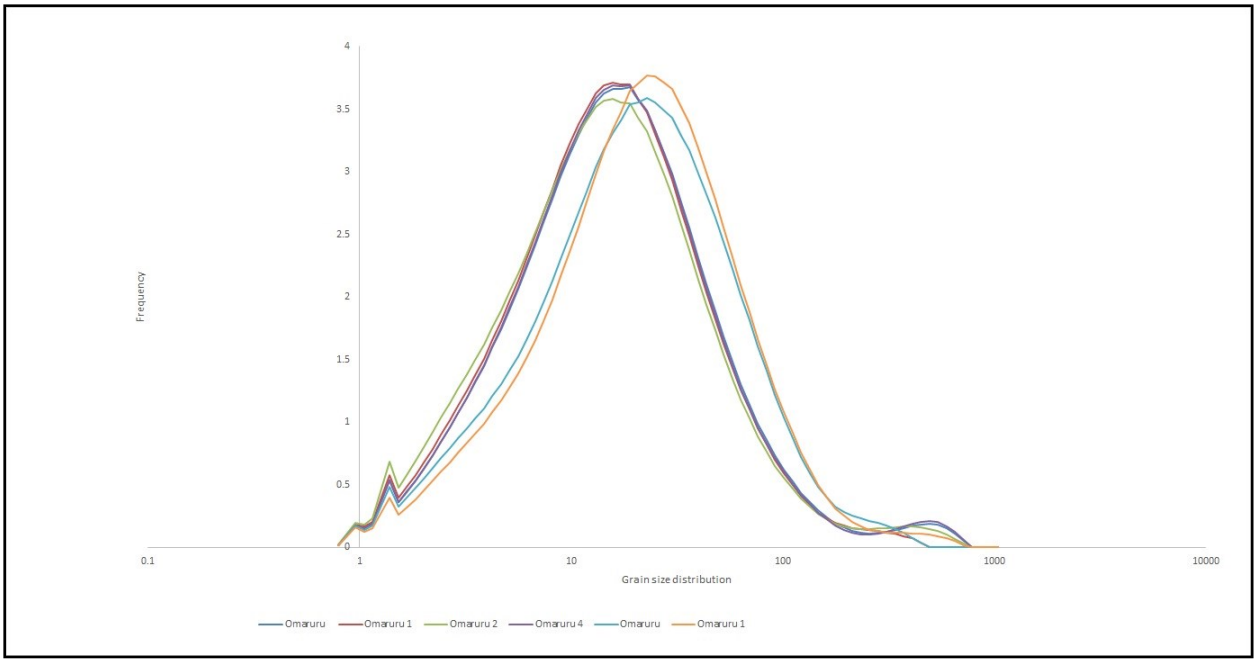

Kuiseb river particle size distribution for all analyzed samples